ELSEVIER

Linear organic π-conjugated systems featuring the heavy Group 14 and 15 elements

Muriel Hissler [a], Philip W. Dyer [b,*], Régis Réau [a,*]

[a] *Phosphore et Matériaux Moléculaires, UMR 6509, CNRS-Université de Rennes 1, Institut de Chimie, Campus de Beaulieu, 35042 Rennes Cedex, France*
[b] *Department of Chemistry, University of Leicester, University Road, Leicester LE1 7RH, UK*

Contents

Abstract

An overview of the synthesis and properties of linear organic π-conjugated systems featuring Group 14 and 15 moieties is presented and comparisons made with their better-known hydrocarbon, and nitrogen- and sulfur-containing analogues. The major focus of this review is π-conjugated systems based on heteroles. The unique electronic structure and nature of siloles and phospholes is examined, highlighting the influence of both the ring substituents and the character of the heteroatom on their photophysical properties. The synthesis of a variety of Group 14 and 15 heterole building blocks suitable for the construction of π-conjugated systems is presented. The preparation and physical properties of poly- and oligo-(1,1-silole)s and -(2,5-silole)s, oligo-(2,5-phosphole)s and co-oligomers of silole and phosphole blocks with other electron-rich monomer units, all with extended π-conjugation, are discussed. A brief resume of linear π-conjugated materials that possess heavy Group 15 elements in the polymer backbone is also presented.
© 2003 Elsevier B.V. All rights reserved.

Keywords: π-Conjugated polymers; Heteroelements; Electronic structure; Metalloles

* Corresponding authors.
  E-mail addresses: p.dyer@le.ac.uk (P.W. Dyer), regis.reau@univ-rennes1.fr (R. Réau).

1. Introduction

Almost by definition, organic polymers with all-carbon backbones are regarded as insulators. However, in 1977, Heeger and co-workers [1] discovered that conjugated organic polymers with alternating single and double bonds along their backbones [polyacetylene (**A**) (Fig. 1)] define a new class of electrically conducting material. Since this seminal discovery, recognised by the award of the *Nobel Prize in Chemistry 2000*, linear organic π-conjugated systems have been shown to exhibit a broad spectrum of extremely desirable electrical, optical, and photoelectrical properties [2,3]. These compounds have found applications as organic semiconductors (when doped), optical storage and nonlinear optical (NLO) devices, sensors, liquid crystals and photo- and electro-chromic materials, to name but a few. As a result, they have attracted and continue to attract huge interest from both academia and industry, where the development of new materials and applications continues apace.

Interest in these types of conjugated materials began in 1937 when theoretical investigations were undertaken to establish whether extended linear CH-polymers, the simplest being the as then unknown polyacetylene, would display bond alternation or delocalisation [4]. This was followed, some years later, by the discovery that near-linear *trans-anti*-polyacetylene (**A**) (Fig. 1) could be prepared from acetylene using a hexane solution of the polymerisation initiator system Et₃Al/Ti(Oi-Pr)₄ [5]. The polymer was isolated as a crystalline, black, air-sensitive, intractable solid. Compressed pellets (690 MPa) of this material were found to display semiconductor behaviour on exposure to donor or acceptor molecules [6].

Subsequently, Shirakawa and Ikeda demonstrated that strong, self-supporting, well-defined films of polyacetylene could be prepared via polymerisation of acetylene at the interface with an unstirred, highly concentrated hydrocarbon solution of a 'classical' Ziegler–Natta polymerisation initiator. Copper-coloured *cis-anti*-polyacetylene (>95% *cis*, Fig. 1) was obtained at −78 °C while silvery *trans-anti*-polyacetylene (the thermodynamically most stable form at room temperature) was isolated at 150 °C. These new materi-

als displayed conductivities of 10^{-8}–10^{-7} and 10^{-3}–10^{-2} S m^{-1} [7], respectively, which were attenuated on lowering the temperature, as would be expected for a true semiconductor [8]. Subsequently, it was shown that doping samples of the so-called '*cis*- and *trans*-Shirakawa polyacetylenes' with iodine afforded new materials that had dramatically enhanced conductivities of 50 S m^{-1} and ca. 3000 S m^{-1}, respectively [1]. Remarkably, using a modification of Shirakawa's high-temperature polymerisation methodology, it is possible to prepare a polymer which, once doped, demonstrates a conductivity of 10^7 S m^{-1}, which is comparable to that of copper, 10^8 S m^{-1} [9,10]!

At this point it is important to relate the physical properties of these materials to their structure, something for which simple band theory pictures can be used. In this approach, when atoms or molecules aggregate in the solid state, the outer atomic orbitals containing the valence electrons divide into filled bonding and vacant antibonding orbitals, forming two energy levels. These are usually called the valence and the conduction bands, respectively. The difference in energy between these levels is defined as the *bandgap* and is the crucial parameter controlling the properties of semiconductor π-conjugated systems [11]. Experimentally, the bandgap is usually estimated from the lowest energy absorption edge (λ_{onset}) in the electronic spectrum of the material or from the difference between its oxidation and reduction potentials [12]. For linear polyenes {CH}$_n$ such as polyacetylene, MOs can be constructed that are delocalised throughout the structure [13]. This simple Hückel approach shows that the bandgap for such materials should theoretically be zero [14,15]. Indeed, the wavelength of absorption lengthens with increasing chain length, i.e. the bandgap ΔE decreases when double bonds are added to the structure. However, it has been demonstrated that there appears to be an upper limit above which the addition of double bonds to an infinite linear polyene has no further effect [4,16]. This arises because coupling of phonons and electrons with lattice vibrations occurs, resulting in a localisation of some single and double bonds that removes their degeneracy widening the bandgap (typically > 1.50 eV) [the so-called Peierls distortion]. Put simply, this means that not all the bonds in polyacetylene are equal and there
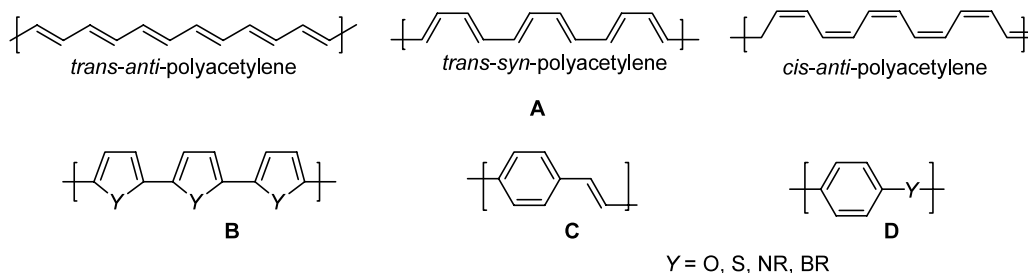

Fig. 1. Organic π-conjugated polymers.

are regions where there is distinct single–double bond alternation. As a consequence of the significant bandgap and filled valence orbitals, polyacetylene would not be predicted to be a conductor, clearly making it necessary to dope polyacetylene in order to prepare a conductive material. The application of simple band theory to organic polymers is further complicated by the fact that each chain is subjected to weak intermolecular interactions [12]. Thus, macroscopic conduction will necessitate electron movement both along and between chains.

Intensive work has been undertaken with a view to preparing new linear-conjugated frameworks of enhanced stability and performance. A commonly employed approach involves the incorporation of heteroatoms into the backbone of π-conjugated systems [2]. Compound **B** (Fig. 1), based on heterocyclopentadiene building blocks (pyrrole, furan, thiophene, etc.), can simply be regarded as *trans*-*syn*-polyacetylene in which the dienic moieties are bridged by heteroatomic groups **Y** (Fig. 1). These polymers offer several advantages compared to their all-carbon analogues **A**. Due to the aromatic character of the heterocyclopentadiene subunits, the stability of these π-conjugated systems is considerably increased and substituents can easily be introduced via electrophilic substitution reactions. Furthermore, their electrical and optical properties are directly related to the nature of the heteroatomic moiety **Y**. Thus, modification of the substituents at **Y** and the nature of **Y** itself allow the properties of derivatives **B** to be fine-tuned by chemical engineering at the molecular level. Aromatic aryl building blocks have also been widely used and *p*-phenylenevinylenes (PPVs) **C** (Fig. 1) are probably the most studied conjugated π-systems [17a,17b]. In compound **D** (Fig. 1), the vinylene bridges of PPV **B** are replaced by a heteroatom possessing either a vacant orbital or a lone pair that can participate in the π-conjugation. Here also, the electrical and optical properties of derivatives **D** can be tuned by varying the nature of the heteroatomic moiety **Y**.

In this review, we present from '*a chemist's point of view*' the synthesis and physical properties of organic π-conjugated systems featuring heavy Group 14 and 15 element moieties. These new π-conjugated systems can be divided into two families. The first includes derivatives based on heteroles that are closely related to compounds of type **B** (Fig. 1). Compounds of the second family feature unsaturated carbon moieties bridged by a heteroatom, which possess either a vacant orbital or a lone pair. Although the development of derivatives featuring heavy Group 14 and 15 elements is still in its infancy, they seem to be particularly attractive since they exhibit novel electronic properties that differ vastly from those of well-studied polypyrrole, polythiophene or polyaniline [2]. This review covers work reported in the literature up to June 2002.
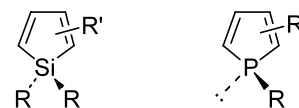

Fig. 2. Silole and phosphole rings.

2. π-Conjugated systems incorporating heavy Group 14 and 15 heteroles

Siloles and phospholes (Fig. 2) are the most common heterocyclopentadienes featuring the heavier Group 14 and 15 elements. They are now readily prepared on a large-scale and are known with a vast range of both R and R′ substituents. Their history shares common roots: the first silole [18] and phosphole [18,19] were described in the same year (1959) and were prepared using the same synthetic methodology, both being isolated fully substituted by phenyl rings.

Siloles and phospholes can formally be regarded as a *cis*-butadiene moiety bridged by a SiR$_2$ (silylene) or a PR (phosphinidene) unit. At first glance, they are just heavier analogues of cyclopentadiene and pyrrole, respectively. However, these metalloles exhibit electronic structures that differ dramatically from those of their corresponding second-row counterparts, making them very attractive building blocks for the engineering of π-conjugated systems. The electronic nature of both the silole [20] and the phosphole [21] ring frameworks was recently discussed in a number of excellent reviews, hence only the more important features will be recalled herein.

2.1. The electronic structure of siloles and related metalloles

Theoretical calculations at the HF//B3LYP level of theory revealed that the HOMO energy levels of the parent silole and cyclopentadiene are comparable, whereas the LUMO level of silole is about 0.3 eV lower in energy than that of cyclopentadiene [22]. Thus, siloles exhibit an unusually high electron affinity as illustrated by the ease with which they are reduced by alkali metals [23]. This feature has been ascribed to an interaction between the butadiene π*(b$_1$) orbital and the silylene σ*(b$_1$) orbital resulting in a significant lowering in the energy of the LUMO of the silole ring (Fig. 3) [20]. This interaction is possibly due to the tetrahedral geometry of the silicon atom, which forces a parallel arrangement of the π*(b$_1$) and σ*(b$_1$) orbitals, and to the weakness (i.e. energetically low-lying σ* orbital) of the Si–R bonds. It is important to note that the interaction depicted in Fig. 3 cannot occur with cyclopentadiene because of the much higher energy of the σ*(C–H) orbitals [20].

The heavier silole congeners, namely the germoles and stannoles, exhibit comparable low-lying LUMO energy levels [22]. This is due to the fact that the energies of the
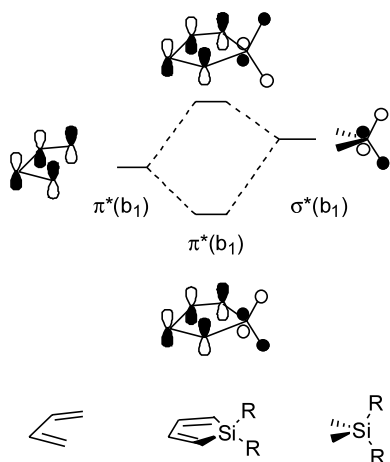
Fig. 3. Partial HO description of silole.

$\sigma^*(Si-R)$ and $\sigma^*(Ge-R)$ orbitals are similar. In contrast, the $\sigma^*(Sn-R)$ level is much lower in energy; however, the efficiency of the $\sigma^*-\pi^*$ conjugation is probably hampered by a less efficient orbital interaction and elongated bond distances for this fourth-row element [22]. This combination of non-aromatic character, along with their unusually high-electron-accepting properties, makes the heavier Group 14 metalloles very interesting subunits for the construction of highly conjugated π-systems.

2.2. The electronic nature of phospholes

The highly aromatic character of pyrrole is well established. In contrast, the evaluation of the degree of aromaticity of its P-analogue has been the subject of numerous experimental and theoretical studies [21,24–30]. Their conclusions, based on energetic, structural and magnetic criteria, are that the aromaticity of phosphole is very low, being only slightly superior to that of cyclopentadiene [26,27,30]. This feature is due to the non-planar conformation of the phosphorus atom that prevents efficient interaction of the phosphorus lone pair with the endocyclic dienic system. Calculations have shown that planar phosphole would be more aromatic than pyrrole; however, this stabilisation would not be sufficient to overcome the high barrier to planarity associated with the P-atom [21]. The fact that phosphole is slightly more aromatic than cyclopentadiene has been attributed to hyperconjugation involving the exocyclic P–R bond and the π-system of the dienic moiety [28]. This interaction is possible since the phosphorus atom adopts a tetrahedral geometry and the P–R bonds are relatively weak. The significant impact of this hyperconjugation on the electronic properties of phosphole has recently been highlighted [29]. It is noteworthy that the aromaticity of phospholes is strongly influenced by the nature of the ring substituents, especially those linked to the P-atom [24,25,30].

The effects are subtle, but allow a fine-tuning of the phospholes' reactivity. For example, phospholes bearing bulky substituents at phosphorus are flattened and show rather high aromaticity indices as well as electrophilic substitution reactivity [31]. In marked contrast, P-alkoxy- and P-halogenophospholes have lost most of the cyclic delocalisation and readily undergo [4+2]-cycloadditions with dienophiles [29,32].

Calculations at the HF/6-61+G*//B3LYP/6-31+G* level of theory have shown that the LUMO level of the parent phosphole ring is of similar energy to that of the corresponding silole (LUMO: phosphole, 1.50 eV; silole, 1.39 eV) [33]. It is very likely that an interaction between the butadiene π^* orbital and the low-lying $\sigma^*(P-R)$ orbital, similar to that observed for silole (Fig. 3), takes place in the phosphole ring. It is noteworthy that the P-α carbon atoms bear a significant negative charge, higher than that calculated for pyrrole [21,34]. This feature is particularly important for the engineering of linear polymeric systems since the linkages between the subunits involve these carbon centres.

With regard to their potential use as building blocks for the preparation of π-conjugated systems, the most important property of phospholes is their very weak aromatic character. This feature should favour delocalisation of the endocyclic π-system along a conjugated chain and allow the P-atom to retain its versatile reactivity. The electronic properties of the phosphole ring are strongly influenced by the nature of its substituents and depend on hyperconjugation, a rather subtle phenomenon. Thus, electronically at least, phospholes can be regarded as somewhat 'chameleon-like' monomer units.

2.3. Theoretical studies on π-systems based on silole or phosphole rings

Polypyrrole (PPy) (F) and polythiophene (PTh) (I) (Fig. 4) are among the most widely studied π-conjugated organic polymers. This is due to their high conductivity upon doping, their linear and nonlinear optical properties and their possible transparency in the visible region, which makes them attractive for the fabrication of devices [12a,17a,17b]. These materials are also very popular because of their high stability, their straightfor-
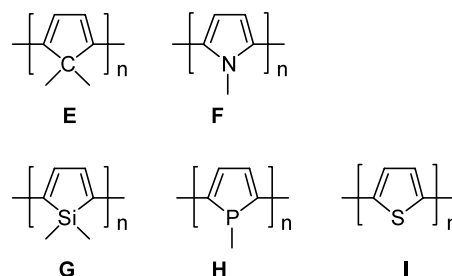

Fig. 4. Polycyclopentadiene and polyheterocyclopentadienes.

ward preparation via either electropolymerisation or metal-catalysed cross-coupling reactions [2,35], combined with the rich chemistry of the underlying monomers that allows for the preparation of numerous structural variants. Theoretical studies on polysilole (PSi) (**G**) [36] and polyphosphole (PPh) (**H**) [37–39] materials (Fig. 4) have been performed in order to investigate the influence of the heteroatom on the bandgap. Calculations at different levels of theory are not comparable and only general trends obtained at a uniform level of theory can be assessed. Thus, the following discussion is mainly based on recent papers presenting a comparative study of polymers **E**–**I** [37,38].

The properties of the high molecular weight polymers can be estimated from calculations on oligomers of increasing length ($n = 2–10$) and subsequent extrapolation to infinite chain length (the *oligomer extrapolation technique*). The bandgaps of polymers **E**–**I** have been evaluated by this method on the basis of calculated HOMO and LUMO levels (DFT study) by Lagowski and co-workers [37] and on vertical energies (TDDFT study) by Ma et al. [38]. Both theoretical studies revealed the same general trends. The first important piece of information is that polymers including the heavier elements have much narrower bandgaps than their corresponding second-row analogues (Table 1: **G** versus **E**, **H** versus **F**). This effect is particularly prominent for the Group 15 derivatives with the estimated bandgap for poly(phosphole) **H** being half of that for poly(pyrrole) **F**. Thus, as Lagowski and co-workers [37] pointed out, "*polypyrrole and polythiophene, the systems which are the most common in the search for conducting polymers because of their chemical stability, are about the worst possible choice as far as bandgap is concerned*".

It would appear that the bandgaps of polysilole **G** and polyphosphole **H** lie in the same range (Table 1) as a result of the high polarisability of the endocyclic dienic system that arises due to the lack of aromaticity of the silole and phosphole subunits. The vertical ionisation potentials and the electron affinities of polymers **G** and **H** are predicted to be similar, making them both potentially *n*- and *p*-dopable. Another useful parameter in understanding the properties of a homologous series

Table 1
Theoretical bandgaps E_g (eV), vertical ionisation potentials I_P (eV) and electron affinities E_A (eV) for polycyclopentadiene (**E**), polypyrrole (**F**), polysilole (**G**), polyphosphole (**H**), and polythiophene (**I**)

	E_g [37]	E_g [38]	I_P [37]	E_A [37]
E	1.58	0.98	4.61	2.97
F	3.16	1.95	4.77	1.61
G	1.39	0.86	5.14	3.75
H	1.49	1.08	5.23	3.73
I	2.30	1.52	5.50	3.20

Table 2
Calculated energy gap (eV) for oligo(cyclopentadiene)s (Cp)$_n$, oligo(silole)s (Si)$_n$, oligo(pyrrole)s (Py)$_n$, oligo(phosphole)s (Ph)$_n$, and oligo(thiophene)s (Th)$_n$ [38]

n	1	2	3	4	5	6
(Cp)$_n$	5.37	3.59	2.82	2.39	2.11	
(Si)$_n$	4.80	3.30	2.58	2.17	1.90	–
(Py)$_n$	5.83	4.75	4.24	3.65	3.40	–
(Ph)$_n$ [39]	5.2	3.6	2.8	2.4	2.2	2.0
(Ph)$_n$	5.16	3.57	2.85	2.44	2.18	–
(Th)$_n$	5.99	4.13	3.49	3.06	2.18	–

of linear polymers is the effective conjugation length (ECL), i.e. the number of monomer units at which saturation of conjugation occurs [12a,12b]. The ECLs are comparable for the two polymers (**H**, 21; **G**, 22) and are slightly lower than those calculated for the corresponding second-row derivatives (**E**, 23; **F**, 24) and polythiophene (**I**, 23) [38]. These theoretical studies revealed a certain analogy between polysilole **G** and polyphosphole **H**, and show that heterocyclopentadienes featuring heavy Group 14 and 15 elements are promising building blocks for the design of low bandgap π-conjugated systems.

In the 'oligomer extrapolation technique', oligomers are used to establish structure–property relationships to rationalise or predict the properties of the corresponding π-conjugated polymers. However, it is now recognised that well-defined π-conjugated oligomers are more than simple model compounds [12a,12b,40]. They exhibit very interesting optical and electronic properties in their own right, making them very promising components for a range of applications (e.g. LEDs, organic transistors, nonlinear optical chromophores, etc.) [12a,12b,17a,17b,40].

The bandgaps calculated for oligo(silole)s decrease in a regular fashion upon addition of monomer units, but are only slightly lower than those of the corresponding oligo(cyclopentadiene) (Table 2) [38]. The energy gaps of oligo(phosphole)s also decrease regularly with increasing chain length; however, they are significantly lower than those predicted for the corresponding oligo(pyrrole)s or oligo(thiophene)s (Table 2) [38,39,41].

It is noteworthy that the phosphorus atoms of oligo(phospholes) are chirogenic centres, thus the number of possible diastereoisomers rapidly increases on lengthening the chain [42]. Quaterphosphole has been the subject of several theoretical investigations with this
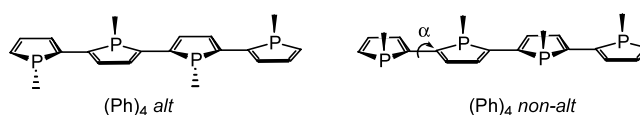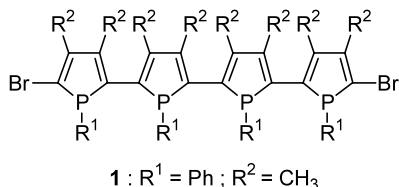

Fig. 5. Conformations of quaterphosphole.

respect since derivative **1** was prepared and structurally characterised by Mathey and co-workers in 1994 [43].

1 : R^1 = Ph ; R^2 = CH$_3$

Calculations have predicted that an *anti*-conformation of the P-ring is preferential (Fig. 5) [38,39]. Quite surprisingly, the (Ph)$_4$ *non-alt* oligomer is predicted to be slightly more stable than its (Ph)$_4$ *alt* counterpart [38]; however, their bandgaps and vertical ionisation energies are almost comparable [38,39]. The (Ph)$_4$ *alt* is planar while the (Ph)$_4$ *non-alt* suffers from a rotational disorder with torsion angles of 15–20° [39]. However, this distortion does not prevent the delocalisation of the π-system over the entire molecule since the energy gap is not significantly altered for torsion angles below 30° [12,39].

These theoretical studies revealed that oligo(phosphole)s should exhibit different properties to those of well-studied oligo(thiophene)s in terms of (i) electronic delocalisation, due to the weak aromatic character of the phosphole ring and (ii) organisation in the solid state, due to the tetrahedral geometry about the P-atom. This makes oligo(phosphole)s important synthetic target molecules.

Theoretical studies have also suggested that phospholes can be useful building blocks for the engineering of chromophores with nonlinear optical (NLO) properties. The archetypical molecular NLOphores can be represented as D-(π-bridge)-A where D and A are donor and acceptor groups, respectively [44]. The modification of the π-bridge is an efficient way to optimise the NLO response of such a chromophore; therefore, phospholes **2** and **3** bearing donor and acceptor groups at the 2- and 5-positions were investigated in this regard [30,34] (Fig. 6).

Donor/acceptor-substituted phosphole **2** exhibits classical properties; the phosphorus atom has a pyramidal shape and its aromatic character is similar to that of cyclopentadiene [30]. Due to the push–pull substitution pattern, significant delocalisation of the endocyclic π-electron density over the entire system was indicated by a combination of structural (Julg index [45]) and magnetic (nucleus-independent chemical shift method [27]) criteria [30]. These studies show that the π-electrons of the phosphole ring are easily polarisable, a feature crucial in achieving a high NLO response. The NLO responses of push–pull phospholes **3** as well as a comparison with the corresponding chromophores based on other five-membered rings were computed [34]. The NLO response of chromophore **3** ($\beta_x = 6.17 \times 10^{-30}$ esu) is significantly greater than those of related derivatives featuring a pyrrole ($\beta_x = 5.59 \times 10^{-30}$ esu), a thiophene ($\beta_x = 5.49 \times 10^{-30}$ esu) or a cyclopentadiene ($\beta_x = 6.04 \times 10^{-30}$ esu) central ring. A comparison of the aromatic character of the five-membered bridges can explain why **3** gives a large NLO response compared to chromophores incorporating pyrrole or thiophene rings. However, the electronic density (i.e. the excess/deficiency of electrons) of the π-bridge also plays a crucial role. As expected from the quite high electronic density found on the α-P carbon atoms [21], phosphole **4** with an electron-acceptor group exhibits a much higher NLO response ($\beta_x = 5.66 \times 10^{-30}$ esu) than phosphole **5** bearing an electron-donating substituent ($\beta_x = 0.63 \times 10^{-30}$ esu). Chromophores **6** and **7**, having stilbene-like bridges in which one phenyl is replaced by a phosphole ring, also exhibit good NLO responses. The highest NLO activity is observed for derivative **7** having a donor NH$_2$ substituent on the phosphole ring, showing that the electron-rich P-ring acts as an auxiliary donor [34].

2.4. Homo-oligomers and -polymers based on Group 14 heteroles

Somewhat surprisingly, oligo- or poly-2,5-(stannole)s remain unknown, while only one report of an oligo-2,5-(germole) is documented; thus this section will focus largely on derivatives **G** featuring silole subunits (Fig. 7). However, it is noteworthy that another class of Homo-polymers based on siloles, i.e. the silicon-catenated 1,1-siloles **H** (Fig. 7), is also known [46].
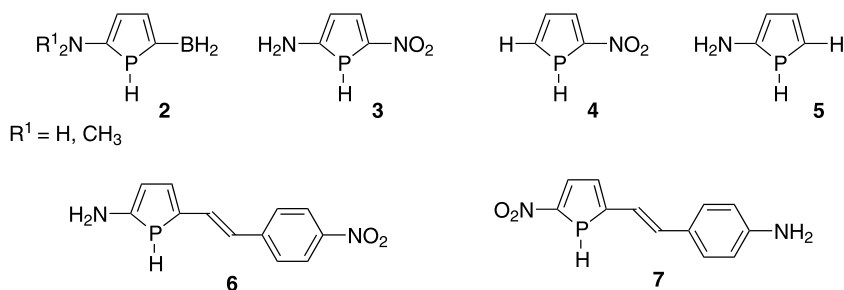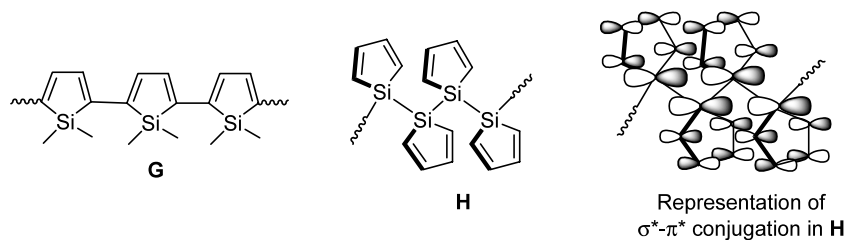

2   R^1 = H, CH$_3$

Fig. 6. Push-Pull dipoles based on phosphole rings.

Fig. 7. Poly-2,5- and 1,1-siloles.

Derivatives **H** can be regarded as a new class of polysilane $[-Si(R)(R')-]_n$ (R,R' = H, alkyl, aryl), compounds that have attracted considerable attention over the last two decades as a result of their unique physical and structural properties [46]. Polysilanes possess an extended σ-conjugated Si–Si backbone, these derivatives are thus beyond the scope of this review. However, 1,1-siloles (**H**) possess very different properties to classical polysilanes as a result of σ*–π* conjugation that arises from the interaction between the σ*-orbital, delocalised along the polymeric Si–Si backbone, with the π*-orbital of the *cis*-butadiene fragment (Fig. 7) [47–50]. Significantly, this type of orbital overlap is only possible with siloles since for simple aryl-substituted polysilanes σ*–π* interactions are prevented as a consequence of orbital symmetry. Thus, derivatives **H** with their unique electronic properties will also be included in this review.

The synthesis of derivatives **G** and **H** requires the preparation of similar monomeric 1*H*-silole building blocks. Thus, a number of key syntheses leading to these common synthons, and their related heavier Group 14 derivatives, is described in the following section. Note that Dubac et al. [23a,51] and Armitage [52] have comprehensively described the syntheses of siloles, in addition to reporting some of their physical and chemical properties.

2.4.1. Synthesis of silole and related ring systems

The first successful preparation and isolation of a discrete silole and its stannyl analogue dates back to the work of Bray and Hübel in the late 1950s who prepared 1,1,2,3,4,5-hexaphenyl-1*H*-metalloles (**8**) through the reaction of 1,4-dilithiotetraphenylbutadiene with Ph_2MCl_2 (M = Si, Ge, Sn, Pb) (Scheme 1a) [18,19]. More recently, this methodology has been extended by the groups of Jutzi and Mitzel [53,54]. In a similar fashion, 1-haloheteroles (**9**) (Scheme 1), that are useful intermediates for the preparation of many other heteroles via nucleophilic substitution at M, can be prepared from the trihalo-silanes and -germanes $R'MX_3$ (R' = H, alkyl, aryl) (Scheme 1b) [23]. Disappointingly, this synthetic methodology has limitations since the use of tetrahalides MX_4 (M = Si, Ge) leads to low yielding mixtures of spiro compounds **10** and the desired heteroles (Scheme 1c) [23]. Notably, all these syntheses are applicable only to heavily substituted derivatives since less sterically encumbered species tend to undergo a Diels–Alder dimerisation process, although this can
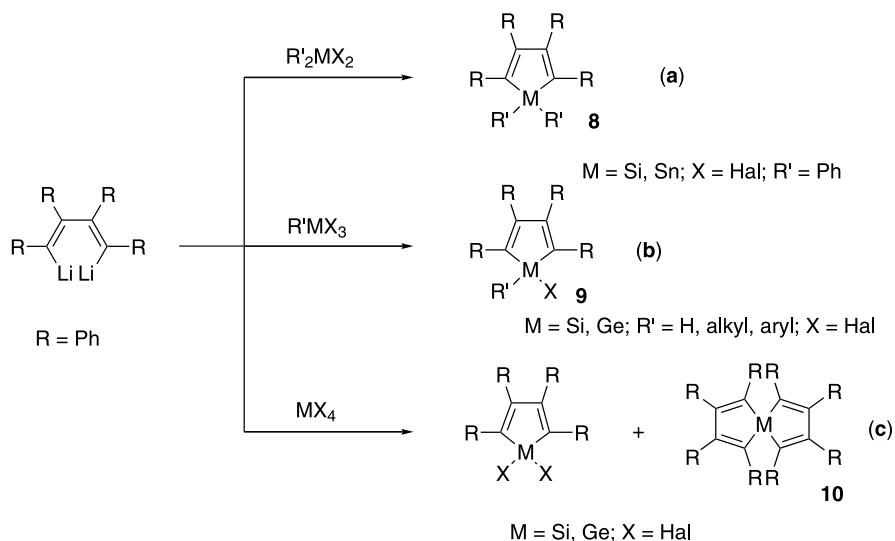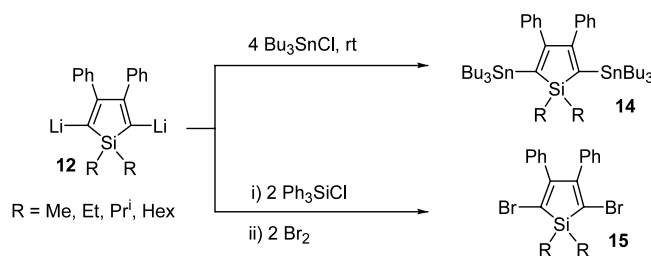

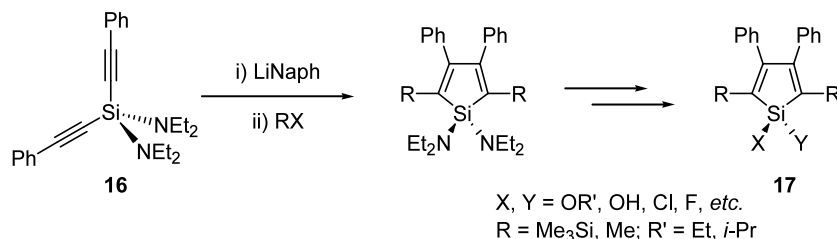Scheme 1.
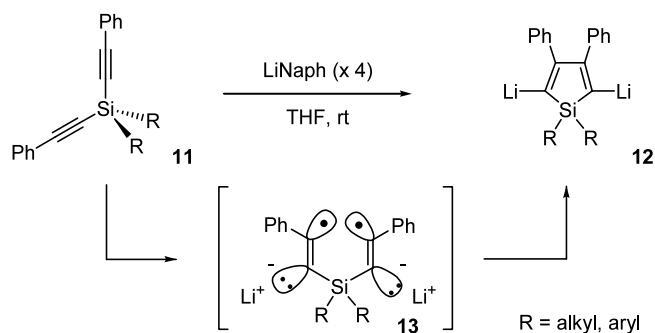
Scheme 2.

Scheme 5.

be suppressed if alkyl groups are incorporated at the 3- and 4-positions [55,56].

Perhaps one of the most versatile methods for the isolation of siloles functionalised both at Si and in the 2,5-positions was developed by Tamao et al. [57]. Their approach involves the initial preparation of an appropriate di(phenylethynyl)silane (**11**) which is subsequently added to an excess (4 mol amounts) of lithium dihydronaphthylide in THF. This leads to the formation of a stable 2,5-lithiosilole (**12**) via an intramolecular reductive cyclisation, which proceeds through formation of an intermediate bis(anion) radical **13** (Scheme 2). This methodology is unique in that it gives a product that results formally from an *endo–endo* diyne cyclisation whereas other metal-mediated cyclisations generally afford *exo–exo* products [58]. However, one limitation here is that it is essential to employ a phenyl-terminated acetylene in order to generate **12**, other substituents (e.g. R_3Si, alkyl) afford complex mixtures of products.
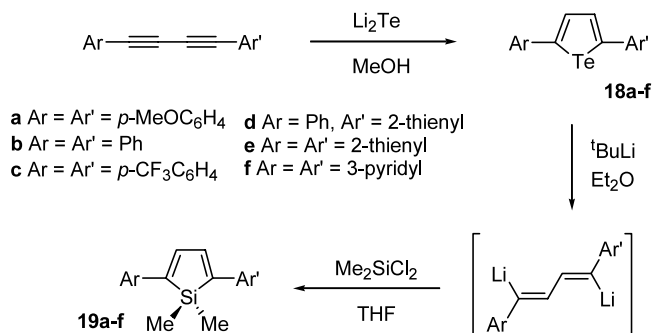
This versatile dilithio species **12** is a key building block for the synthesis of silole containing π-conjugated systems since it is the direct precursor of 2,5-difunctio-

nalised stannyl- and dihalo-siloles (**14** and **15**), respectively (Scheme 3) [57].

This methodology is also applicable to the preparation of 1,1-difunctional siloles (**17**), including dihalogeno derivatives which are precursors to silicon-catenated 1,1-siloles (**P**), from amino-substituted diaminosilanes (**16**) (Scheme 4) [59].

Despite the versatility of Tamao's initial synthetic approach (Schemes 3 and 4), it is only effective for the preparation of 3,4-diphenyl derivatives. Thus, this group have developed further methods to prepare new target 2,5-functionalised silole building blocks. The first employs intermediate tellurophenes (**18a–18f**) which can be regarded as stable 1,4-dilithio-buta-1,3-diene mimics (Scheme 5) [60]. This methodology has allowed a variety of variously 2,5-disubstituted siloles (**19a–19f**) (Scheme 5) to be synthesised in yields of ca. 50% based upon the starting 1,4-diaryl-buta-1,3-diyne [61].

A second methodology for the preparation of 2,5-difunctionalised 3,4-dialkylsiloles (**21**) has been established and is based upon the halodesilylation of 2,5-disilylsiloles (**20**) (Scheme 6) [62]. These materials are attractive precursors for the synthesis of 2,2′-disiloles (vide infra).

Thirdly, siloles can be isolated through the synthesis and subsequent reactions of intermediate 1,4-diiodobutadienes (**23**), prepared through halogenation of the corresponding diisopropoxytitanacyclopentadienes (**22**) (Scheme 7) [63]. This well-established methodology for the preparation of a range of metalloles [64] can be employed to access a number of different 3,4-dialkyl and 3,4-unsubstituted mono- and bi-cyclic siloles (**24**) (Scheme 7).
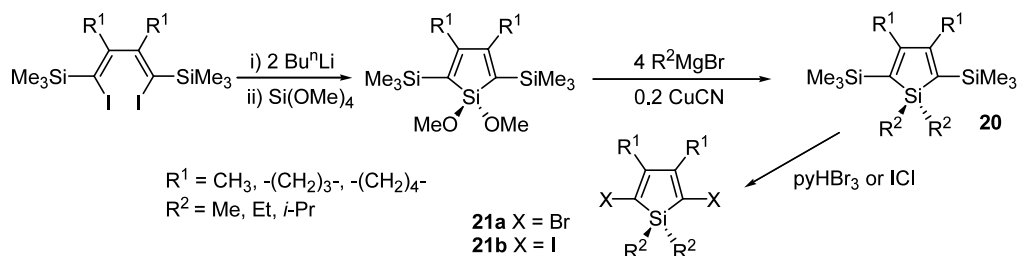
Scheme 3.

Scheme 4.

Scheme 6.

A variation on this transition metal-mediated approach utilises a zirconacyclopentadiene coupling methodology, something that has been used for the preparation of variously substituted siloles (**25**) (Scheme 8). This technique has met with somewhat limited success since the transmetallation step has been shown to be extremely sensitive to both the steric bulk of the zirconacycle and the halosilanes, in addition to being susceptible to significant solvent effects [65]. However, it is interesting to note that this zirconocene-mediated route proceeds extremely efficiently with a range of germanium and tin halides, affording the corresponding heteroles in excellent yields [65–69].

Siloles can also be prepared in moderate yields by nickel-catalysed intramolecular cyclisation of 1,6-diynes with hydrodisilanes (Scheme 9). This route is of great interest for the preparation of well-defined silole-thiophene co-oligomers and other 2,5-difunctional siloles (vide infra) [70].
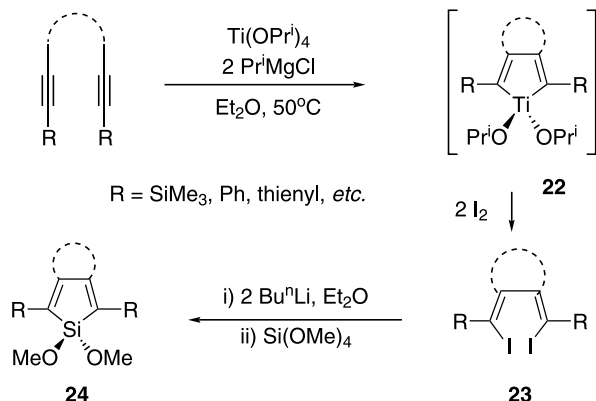
2.4.2. Oligo- and poly-1,1-Group 14 heteroles

The preparation of silicon-catenated oligo- and polymeric materials has proved to be a significant challenge. Indeed, there are extremely few true homo(1,1-polysiloles) known. The methoxy-capped oligosilole (**26**) was isolated (ca. 30%) by West and co-workers [71] following reaction of 1,1-dichlorotetraphenylsilole with 2 equiv. of lithium, sodium or potassium in THF, followed by quenching with methanol (Scheme 10). It is noteworthy that the material formed contains mono-
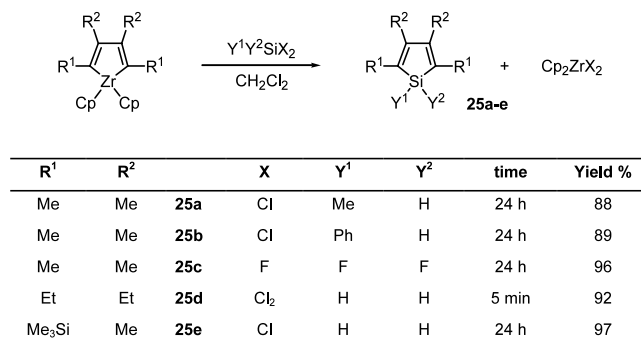
disperse oligomers ($M_n \approx 5500$, $M_w/M_n = 1.1$). Despite the comparatively low degree of polymerisation (DP = 15), **26** does exhibit polymer-like properties and can readily be cast into self-supporting films from solution.

In contrast, the same reaction performed with a lower alkali metal loading (1.2 equiv., THF) gives rise to a mixture of three lower molecular weight derivatives: the dimeric and trimeric dichloro-siloles (**27** and **28**), in addition to what is believed to be a yellow crystalline cyclooligosilole (**29**) (Scheme 10) [71]. The molecular structures of both **27** and **28** were determined by X-ray crystallography. The silole rings of both species were arranged with an all-*gauche* conformation along the Si–Si backbone. The trimer **28** exhibits inter-ring dihedral angles of ca. 60°. These structures differ considerably from those determined for the less hindered tersilole (**30**) and quatersilole (**32**) prepared by Tamao and co-workers [72] and the permethyl-tersilole (**31a**) of Kira and co-workers [73] (Scheme 11), which adopt *gauche–anti*, *gauche–anti–gauche* and *trans–trans* conformations, respectively.
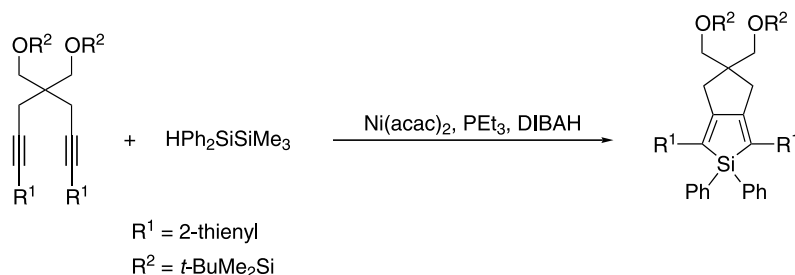
West's compounds (**26**–**28**) (Scheme 10) exhibit bands near 300 and 370 nm in their UV–Vis spectra and the fluorescence of each differs significantly. 1,1-Dichloro-2,3,4,5-tetraphenyl-1*H*-silole and dimer **27** emit at ca. 380 nm, while both trimer **28** and oligomer **26** show strongly Stokes-shifted emissions at ca. 520 nm. Furthermore, **26** is highly electroluminescent with an emission at 520 nm. Indeed, this oligomeric material has been demonstrated to behave as a single-component LED with an external quantum efficiency of 3×10^{-2}% at a current density of 0.3 mA cm^{-2} [71], which is

R = SiMe₃, Ph, thienyl, *etc.*

Scheme 7.

R¹	R²	X	Y¹	Y²	time	Yield %
Me	Me	**25a**	Cl	Me	H	24 h	88
Me	Me	**25b**	Cl	Ph	H	24 h	89
Me	Me	**25c**	F	F	F	24 h	96
Et	Et	**25d**	Cl₂	H	H	5 min	92
Me₃Si	Me	**25e**	Cl	H	H	24 h	97

Scheme 8.

Scheme 9.

comparable to that of other single-layer organic LEDs such as poly(p-phenylenevinylene) [74]. This unusual emission phenomenon is believed to result from either excimer formation or a twisted intramolecular charge-transfer (TICT) state in solution. Recently, the oligotetraphenylsilole $(C_4Ph_4Si)_n$ has become the subject of renewed interest since Yang and Swager [75] successfully demonstrated that highly π-conjugated, porous organic polymers could be used to detect vapours of electron-deficient chemicals. This behaviour is believed to be dependent upon electron delocalisation, which provides a means of amplification; interaction with an analyte molecule anywhere along the chain is readily 'communicated' throughout the rest of the material [76]. This has led to the search for new 'sensor' materials, with photoluminescent polysiloles being an attractive choice [77].

It is interesting to compare the optical data for related oligo(1,1-silole)s of increasing length (Table 3). The monosilole 33 exhibits a band at 307 nm that has been assigned to the silole group. The absorptions of the silole moieties of dimer 34 are hidden by broad phenyl bands while those of oligomers 30 and 32 are recorded at 279 and 289 nm, respectively [72]. A bathochromic shift of the value of λ_{max}, i.e. a decrease of the HOMO–LUMO gap, is observed upon increasing the number of repeat units from 2 to 3. However, further increase of the chain length has only a modest effect on the value of λ_{max}.

Kira and co-workers [73] prepared another series of oligo-1,1,2,3,4,5-tetramethylsiloles (31a–31c) of increasing chain length in low yields according to the synthe-

tically methodology outlined in Scheme 12. The tersilole 31a was characterised in the solid state by X-ray diffraction. The study revealed a near all-*trans* pentasilane chain, the slight distortion observed occurring presumably as a result of inter-silole ring steric repulsions (Si–Si–Si–Si torsion angles of $166.90°$ and $173.74°$). Interestingly, the terminal silole rings are aligned almost parallel, with a face-to-face separation of ca. 3.7 Å.

Both the groups of Tilley and Hong have reported similar methods for the preparation of 1,1-disoles [78,79]. Treatment of 1,1-dibromo-2,3,4,5-tetramethyl-$1H$-silole (35) with potassium in THF generates an intermediate dianion 36, which can be quenched with Me_3SiCl to give the 1,1′-disilole 37 (Scheme 13). It is noteworthy that addition of excess potassium leads to the formation of a monomeric salt which can be converted to the related aromatic dianion 38 on addition of a crown ether (Scheme 13) [78]. Using the same approach, a trigermole 39 has also been prepared (Scheme 13) [80].

These compounds are of considerable interest since they possess methyl substituents in place of the more usual phenyl groups, something that enables distinct UV absorptions due to σ–$\sigma*$, σ–$\pi*$, and π–$\pi*$ transitions to be observed without interference from pendant aromatic units (Table 4). Two absorption maxima were observed for the monomer 40 with the band at longer wavelength being assigned to a π–$\pi*$ transition of the silole ring, while the other was attributed to an intramolecular charge-transfer σ–$\pi*$ transition from the oligosilane σ-HOMO to the diene $\pi*$ LUMO. Conse-
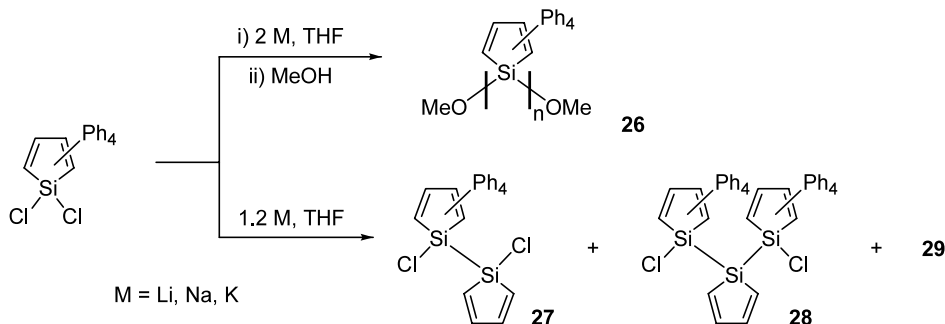
Scheme 10.
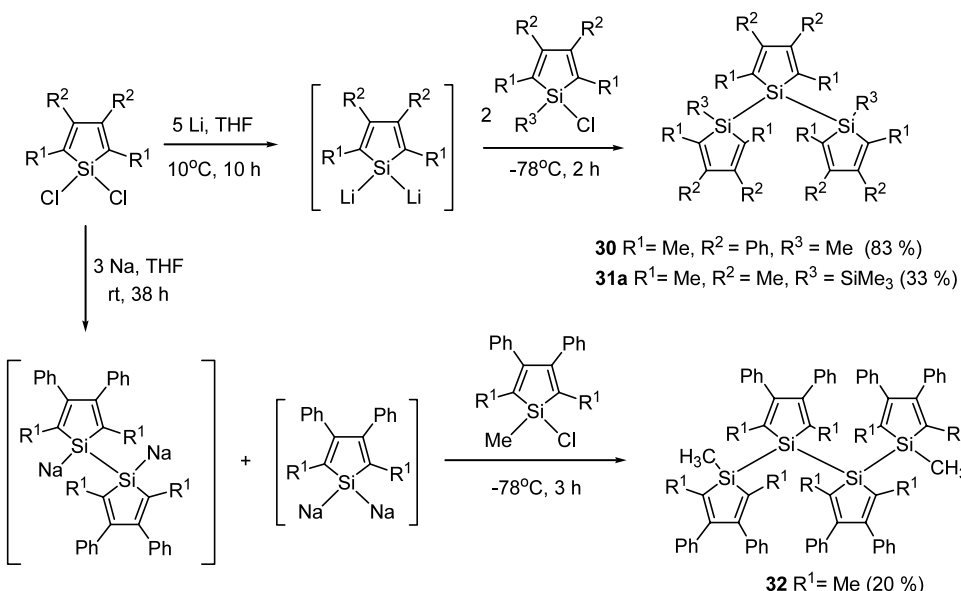
Scheme 11.

quently, the absorption bands centred around 280 nm for **31a**–**31c** and **37** have been assigned to overlapping σ−π* and π−π* bands [73]. The wavelengths at which absorption occurs vary only slightly with chain length, while the absorption coefficients increase with increasing numbers of monomer units. These data are consistent with there being little, if any, through-space interaction between silole rings, as may have been expected from the molecular structure of **31a** [73].

Note that this reductive coupling approach has also been applied to Si and Ge 1-haloheteroles (**41**) for the synthesis of dimeric 1,1′-biheteroles (**42** and **43**), the simplest of oligomeric 1,1-heteroles (Scheme 14) [23a].

It is clear that the nature of the substituents in the 2,5-positions of 1,1-dichlorosiloles have a pronounced influence on the outcome of the Wurtz-like coupling reactions. Thus, it was desirable to develop a generally applicable synthesis of 1,1-dichlorosiloles. To this end,

Tamao et al. [57,59] exploited the intramolecular reductive cyclisation of bis(phenylethynyl)silanes (see Schemes 2–4) to prepare a range of the desired dichloro compounds. With the latter in hand, lithium-mediated coupling of the sterically less hindered silole **44** in THF at low temperatures affords only two products (Scheme 15): a Si-catenated polysilole **45** (61%), analogous to **26** (Scheme 10), and trace amounts of the hexameric cyclic silole **46** (6%) [81]. The polymer **45** was isolated following SEC and was determined to have an $M_w = 7200$, $M_n = 6300$ and, again, a narrow polydispersity ($M_w/M_n = 1.14$). In contrast, reaction of 2,5-bis(trimethylsilyl)-3,4-diphenyl-1,1-dichlorosilole under the same conditions afforded only the corresponding 1,1′-dichloro-2,5,2′,5′-tetramethyl-3,4,3′,4′-tetraphenyl-1H,1′H-[1,1′]bisilole, the analogue of **27** (Scheme 10).

The isolation and structural characterisation of the cyclic hexamer **46** is of interest in its own right. This compound is soluble in i-PrOH and could be recrystallised from ethylacetate (mp > 400 °C) [81]. A study by

Table 3
UV−Vis spectral data for methyl-capped oligo(1,1-silole)s

Compound	λ_{max}	log ε
33	307	3.22
34	255	4.42
tersilole **30**	279	4.60
quatersilole **32**	289	4.59
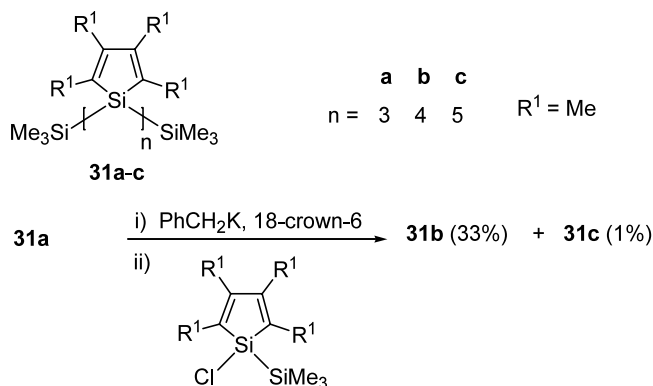
Scheme 12.
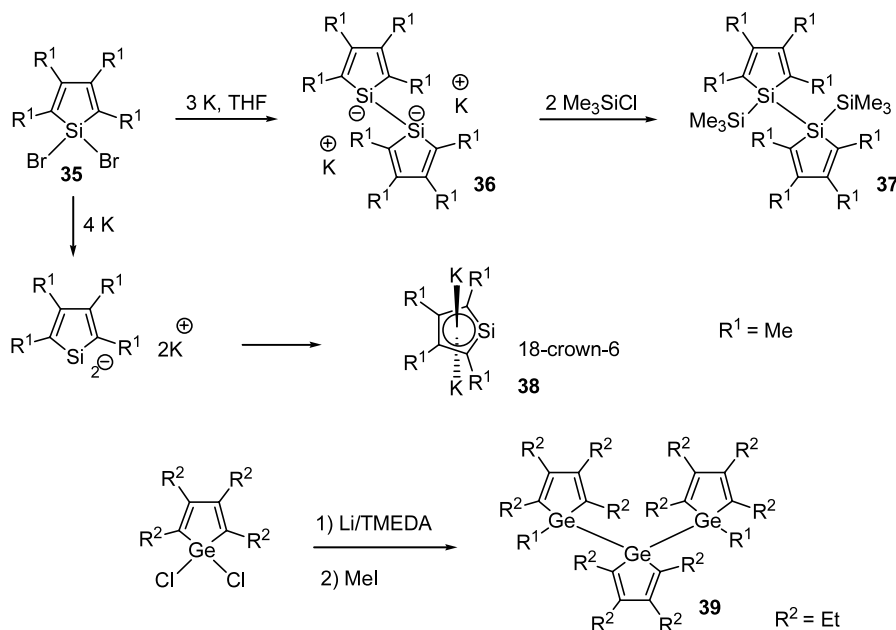
Scheme 13.

X-ray diffraction revealed that the Si–Si bond distances lie within the normal range and that the central cyclic silane skeleton adopts a considerably flattened chair conformation. The average Si–Si–Si–Si dihedral and
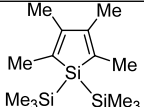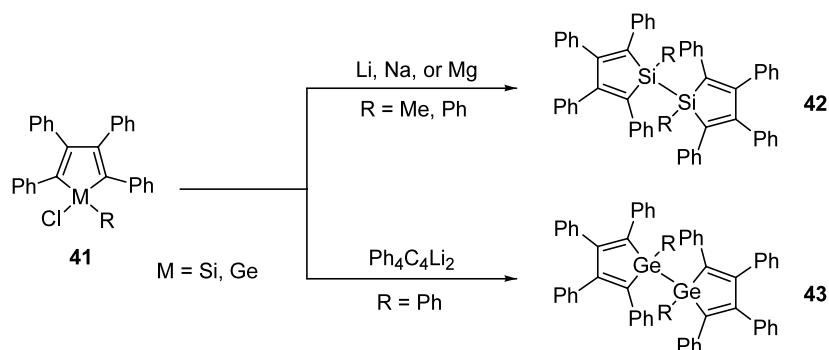
Table 4
UV absorption spectral data for trimethylsilyl-capped 1,1-oligosiloles

	Absorbance maxima (nm)			
	λ_1	$\log \varepsilon$	λ_2	$\log \varepsilon$
40	257	3.85	299	3.30
37	222	4.51	282	4.04
31a	235	4.56	278	4.20
31b	242	4.62	276	4.38
31c	247	4.63	275	4.51

the averaged Si–Si–Si bond angles are 37.5° and 116.3°, respectively. These metric parameters differ significantly from those of other cyclohexasilanes that have been structurally characterised. Typically, the latter adopt Si–Si–Si–Si torsion angles that lie in the range 53–57° [81]. The unusually flat geometry associated with the *cyclo*-Si$_6$ core is thought to result from the tight angular constraints imposed by the C–Si–C angles of the silole rings (avg. 93.3°), which induce a widening of the Si–Si–Si bond angles.

An alternative methodology for the preparation of this type of 1,1-polysilole through polycondensation of a silole dianion **47** (itself prepared from reaction of **44** with Li in THF [82]) and trimer **48** has been probed (Scheme 16) [81]. The composition of the polymeric material obtained, **49**, is identical to that of **45**, however both the yield (48%) and the molecular weight ($M_{\mathrm{w}} = 3000$, $M_{\mathrm{n}} = 2400$, $M_{\mathrm{w}}/M_{\mathrm{n}} = 1.25$) were found to be somewhat lower. Notably, this latter approach afforded none of the cyclic hexamer **46**.

Scheme 14.
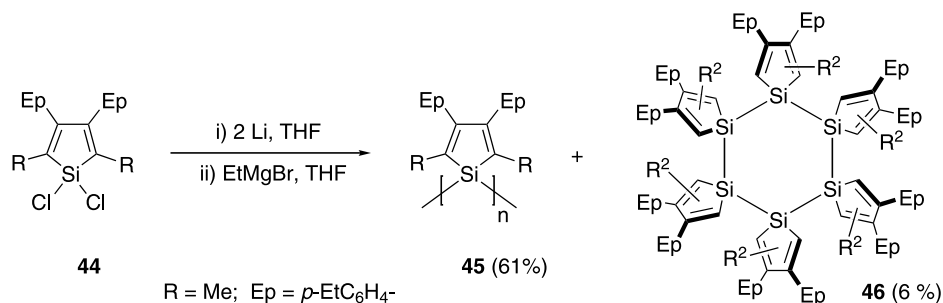
Scheme 15.

Both the p-EtC$_6$H$_4$– derivatives described in Schemes 15 and 16 exhibited interesting photophysical behaviour (Table 5) [72,81]. As reference, the monosilole shows two absorption bands around 250 and 310 nm, assignable to the $\pi-\pi^*$ transitions of the phenyl and silole moieties, respectively. Polymer **45** exhibits broadened absorption bands with a shoulder at 320 nm, which is red-shifted by ca. 30–40 nm relative to the trimer and tetramer (see Table 3). Note that the value of λ_{max} of the cyclic hexamer **46** is comparable to that of the oligomers. The emission bands of both the polymer and hexamer are broad and centred around 460 nm, low quantum yields are recorded (Table 5). There is a small but distinct shift to longer wavelengths in the emission spectra on going from monosilole to polymer, possibly as a result of increased orbital mixing of the Si–Si backbone and the dienic moieties.

From the studies of 1,1-oligo-siloles, it is evident that small changes in the makeup of the silole monomers can have a profound effect upon both the ease and outcome of attempted polymerisation reactions. Of particular interest, there is an intense intramolecular $\sigma-\pi^*$ charge-transfer absorption associated with these types of compound that is likely to have an impact on their unique optoelectronic properties.

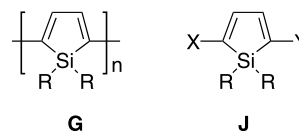### 2.4.3. Oligo- and poly-2,5-siloles

From a viewpoint of potential applications, poly(2,5-silole)s (**G**) (Fig. 8) are perhaps the most interesting silole-containing polymers because of their a priori structural similarity with polyacetylene. Although only one true polymeric 2,5-silole has been isolated, a wealth of information has been obtained for an assortment of oligomeric derivatives, prepared using a number of different synthetic strategies [83]. It is still very much

Table 5
UV absorption and fluorescence spectral data for linear and cyclic 1,1-oligosiloles

|	UV absorption		Fluorescence	
	λ_{max} (nm)	log ε	λ_{max} (nm)	$\Phi_f \times 10^3$
45	320 (sh)	4.02	460	0.314
46	285	5.07	467	0.353

sh = shoulder.

R = alkyl, aryl, H; X, Y = Li, Br, I, B(OH)$_2$, SnR'$_3$, *etc.*

Fig. 8. Poly(2,5-silole)s and their precursors.

the case that despite the explosion of interest in oligo- and poly-siloles, the development of generic, reproducible synthetic methodologies for their preparation (and that of their heavier congeners) has been somewhat slow [84–86].

Barton was among the first to attempt the direct preparation of a poly(2,5-silole)s (**G**) from diethynylsilane employing both catalytic and thermolytic approaches [36a]. However, later studies revealed that rather than the desired polysilole material, this methodology led instead to the formation of a polymer with a methylenesilacyclobutene-based skeleton [87]. Since then, there has been considerable interest in the conceptually straightforward metal-catalysed coupling for the preparation of conjugated poly(2,5-silole)s. Unfortunately, as outlined in Section 2.4.1, the synthesis of the
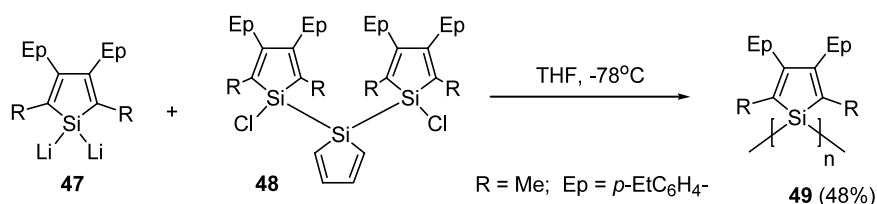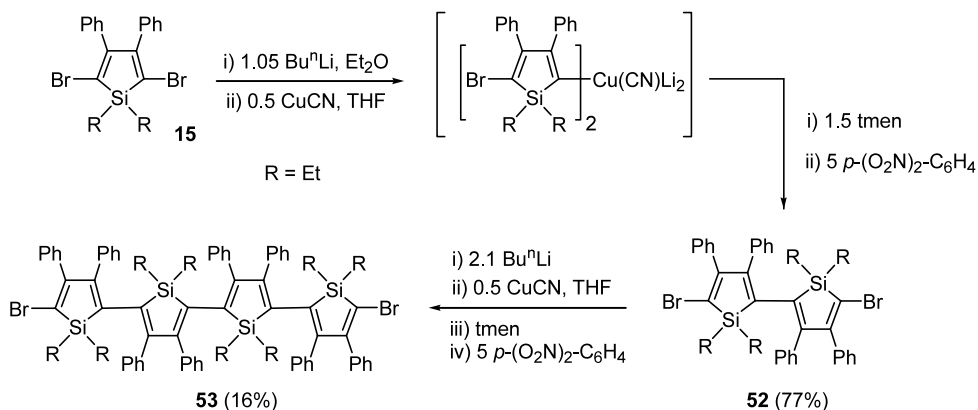

Scheme 16.
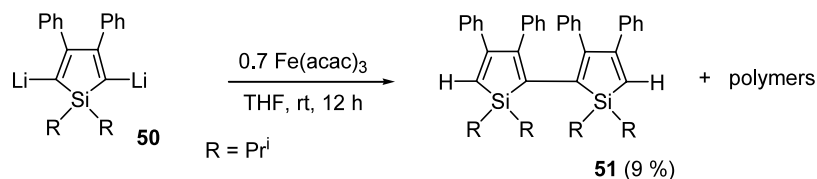
Scheme 17.

necessary 2,5-difunctionalised monomers **J** (Fig. 8) have proved problematic [23a]. Note that Wrackmeyer et al. [88] have prepared a number of 3-boryl-2,5-distannylsiloles form bis(stannalkynyl)silanes, but this approach is rather substituent-specific.

Once a range of functionalised 2,5-disilole compounds (**J**) had been prepared (Section 2.4.1), a number of approaches for their conversion to polymers were investigated, the most direct being the homocoupling of the 2,5-dilithio derivatives. However, despite screening a range of metallic reagents, none afforded isolable polymeric materials [57]. This is believed to be due to the steric hindrance imposed by the substituents in the 3,4-positions and also due to the low inherent reactivity at the 2,5-positions. In contrast, oligosiloles were produced in low isolated yield by oxidative coupling of 2,5-dilithiosilole **50** with tris(acac)iron(III) (Scheme 17) [57]. The bisilole **51** was isolated in low yield as a yellow crystalline solid along with a number of uncharacterisable polymeric materials.
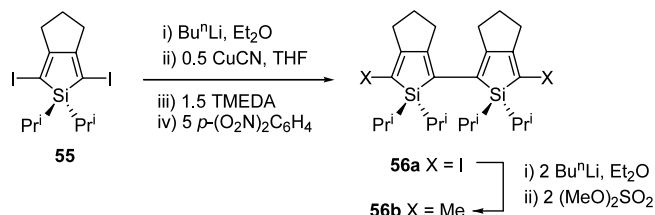
A highly attractive route to oligo(silole)s has been developed starting from 2,5-dibromo-3,4-diphenyl-1*H*-silole (**15**) (Scheme 18). This derivative is readily converted into the corresponding 5,5′-dibromo-3,4,3′,4′-tetraphenyl-1*H*,1′*H*-[2,2′]bisilolyl (**52**) (77%) in a two-step reaction: (i) selective lithiation followed by (ii) a copper-mediated oxidative coupling (Scheme 18) [57]. The scope of this approach is such that the corresponding quatersilole **53** (Scheme 18) could be isolated in reasonable yield (16%) following column chromatography.

Both 2,2′-bisiloles **51** and **52** have been characterised by X-ray diffraction studies [57]. The most interesting feature is the non-coplanar arrangement of the two silole rings with torsion angles of 62.3° and 63.7° for compounds **51** and **52**, respectively. However, UV–Vis spectroscopic investigations clearly showed that these compounds possess an extended π-conjugated system. A significant red-shift is observed upon increasing the number of monomeric 2,5-silole subunits, indicating a decrease in the HOMO–LUMO gap (Table 6). It is noteworthy that the UV–Vis absorptions for derivatives **51**–**53** appear at relatively long wavelengths compared with those of other conjugated oligomers such as 2,2′-bithiophene (302 nm) or quaterthiophene (391 nm). It is also interesting to note that bicyclopentadiene derivative **54** (Fig. 9), an analogue of bisilole **51**, is colourless and exhibits a λ_{max} of 340 nm (log $\varepsilon = 3.43$) [89]. Thus, in spite of large torsion angles revealed by X-ray diffraction studies, oligo(2,5-silole)s exhibit an extended π-conjugated system. In fact, theoretical calculations carried out at the CIS/6-31G* level revealed that the effect of the twist angle θ on the HOMO–LUMO gap is less pronounced for bisilole compared with its all-carbon counterparts (Fig. 9) [48]. These data clearly show that siloles are attractive building blocks for the engineering of highly delocalised π-conjugated systems, in line with the theoretical calculations reported previously (see Section 2.3).

Using the 'higher-order cyanocuprate', 2,2′-bisiloles **56a** were prepared from the 2,5-difunctionalised 3,4-dialkylsilole precursors **55** (Scheme 19) [62]. Derivatisation of **56a** afforded **56b** in high yield.
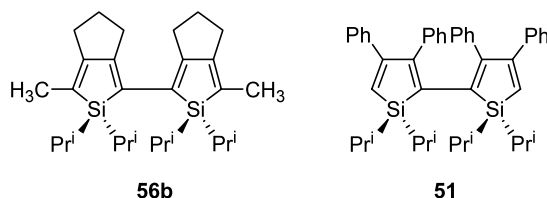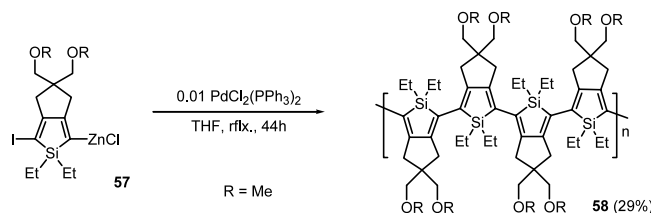

Scheme 18.

Scheme 19.

Table 6
UV absorption of oligo-(2,5-silole)s depicted in Schemes 17 and 18

	λ_{max} (nm)	log ε
Monosilole **15**	326	3.64
Bisilole **51**	398	3.71
Bisilole **52**	417	4.05
Quatersilole **53**	443	4.21

The 5,5′-dimethyl-1*H*,1′*H*-[2,2′]bisilolyl (**56b**) was characterised in the solid state by X-ray diffraction and found to adopt a highly twisted *syn* conformation of the two silole rings (dihedral angle of 52.2°). In contrast, the previously reported 3,4,3′,4′-tetraphenyl-1*H*,1′*H*-[2,2′]bisilolyl derivative **51** takes up an *anti* conformation with a dihedral angle of 62.3° [57]. However, derivative **56b** exhibits an absorption maximum ($\lambda_{max} = 343$ nm, log $\varepsilon = 3.88$) at a wavelength that is ca. 50 nm shorter than that for the analogous phenyl compound **51** ($\lambda_{max} = 396$ nm, log $\varepsilon = 3.75$), something that highlights the effect of the nature of the 3,4-substituents on the optical properties of the silole moieties.

The only true poly-2,5-silole **58** was isolated as a red powder from reaction of the mono-organozinc derivative **57** using a Pd(0)-catalysed cross-coupling reaction (Scheme 20) [83]. The structure of **58** was elucidated from a combination of NMR spectroscopy and MALDI-TOFF mass spectrometry, the latter giving an M_n of 3730 which is in good agreement with that obtained by GPC ($M_w = 4560$, $M_n = 3440$). Remarkably, polymer **58** is essentially monodisperse ($M_w/M_n = 1.33$). This new material has a UV–Vis absorption band at 482 nm (2-Me-THF, 293 K), which is at a wavelength that is ca. 140 nm longer than for the silole dimer **56b**, something consistent with extended π-conjugation. Significantly, this absorption band was found to be temperature-dependent, λ_{max} shifting to longer wavelengths of up to 542 nm at 153 K. This bathochromic

shift is presumed to arise from variation in the extent of conjugation caused by temperature-induced conformational changes.

2.5. Co-oligomers and -polymers based on Group 14 heteroles

A commonly adopted approach for tuning the properties of organic π-conjugated systems involves the incorporation of electronically disparate heterocycles into the carbon backbone [12a,12b,17]. Heterocyclopentadienes have been extensively used for such purposes as their electronic nature differs significantly from that of the carbon framework, something that allows for a degree of engineering at the molecular level. This idea inspired the design of two families of novel π-conjugated systems. The first group is made up from co-
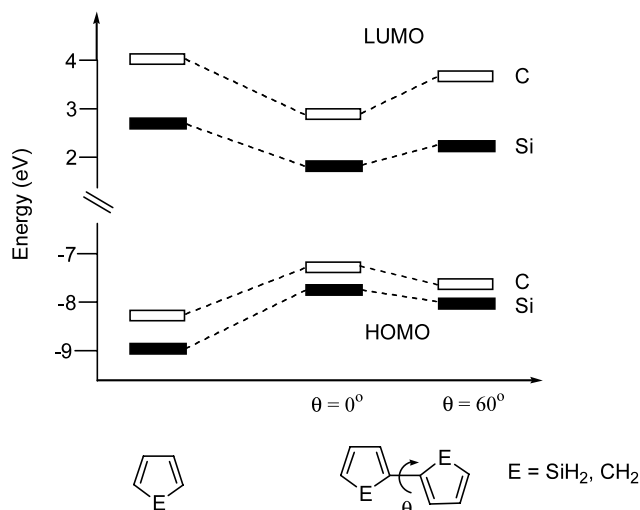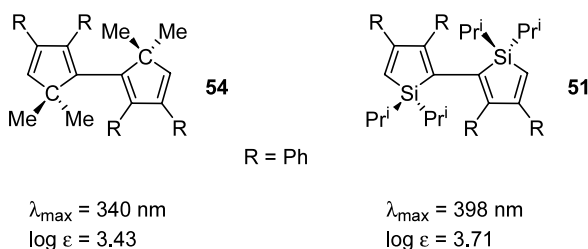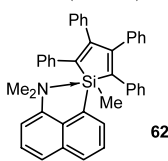

Scheme 20.

Fig. 9. Influence of rotational disorder on the HOMO-LUMO gap for Group 14 derivatives.

Table 7
Comparison of UV–Vis absorption data for some 2,3,4,5-tetraphenyl-siloles and germoles

	λ_{max} (nm)		λ_{max} (nm)
$Ph_4C_4SiH(ONMe_2)$ **59**	375	$Ph_4C_4SiCl_2$	378
$Ph_4C_4Si(ONMe_2)_2$ **60**	372	$Ph_4C_4SiMe_2$	351
$Ph_4C_4Ge(ONMe_2)_2$ **61**	367	$Ph_4C_4SiPh_2$	365
		$Ph_4C_4GeMe_2$	348
		$Ph_4C_4GePh_2$	354
62	365		

oligomers of alternating heteroles and aromatic rings such as phenyl, thiophene, or pyridine. The second consists of compounds in which heterole rings are substituted or linked by alkylene moieties.

2.5.1. [Silole]-[aromatic heterocycle] systems

The simplest π-conjugated silole-aromatic ring co-oligomers possible are the 2,5-diphenyl heteroles. Structurally, all the 2,3,4,5-tetraphenyl Group 14 heteroles are similar: (i) they are essentially planar, (ii) the geometry around the heteroatom is distorted tetrahedral, with an endocyclic bond angle of ca. 83–94°, (iii) the phenyl substituents about the ring are arranged in a *propeller*-like manner, and (iv) the bond lengths associated with the ring show distinct single/double bond character [23a]. These observations are in good agreement with molecular orbital calculations that have been described recently [90].

It has been shown that the electronic properties of these heavier heteroles are intimately linked to the environment about the Group 14 atom and to the nature of any coordinated substituents. Losehund and Mitzel [54] have recently undertaken a study into the effect of introducing aminoxy substituents at Si and Ge in some simple 2,3,4,5-tetraphenyl heteroles prepared through treatment of the appropriate 1-chloro-siloles

with $LiONMe_2$. UV–Vis spectroscopy was used to probe the perturbation of the heterole core, the data being reported in Table 7. The absorption maxima for heteroles **59** and **60** (assigned to the HOMO–LUMO transition, π–π*) are shifted to longer wavelengths relative to those of the simple 1,1-dimethyl derivative and hexaphenylsilole [90]. A small effect is observed that parallels the changes in electronegativity of the substituents at Si. A similar red-shift is also observed for the analogous germole **61**. Thus, it seems that partial hypercoordination with an N-donor in the β-position, relative to the metal centre, exerts little observable effect on the π-system of these heteroles, something that is also apparent from Tamao's study of the partially hyper-coordinate silole **62** [91]. Similarly, there is little impact structurally as a consequence of hypercoordination at silicon, the metric parameters associated with the silole core being consistent with those observed for the 1,1-dimethyl-silole, $Ph_4C_4SiMe_2$ [92].

A comparative study of the electronic properties and electrochemistry of the 1,1-dimethyl- and 1,1-diphenyl-2,3,4,5-tetraphenyl-1H-metalloles has been reported (Table 8) [90]. The results obtained can be used to explain the activation and deactivation of the various metallole rings. Absorption causes an electronic transition in the chromophore which is unaffected by heteroatom substitution, implying that the absorption arises from transitions between diene- and phenyl-based MOs. The excited state decays to an intermediate state which, in the case of the phenyl-substituted compounds, undergoes radiative decay to the ground state emitting a photon at ca. 490 nm, a process showing little dependence on the nature of the heteroatom itself (Table 8). For the dimethyl derivatives, the heteroatom evidently perturbs the electronic/vibrational structure of the emissive state, inducing a higher emission energy for the $GeMe_2$ compound and causing a lack of luminescence for the $SnMe_2$ analogue.

Much of the continued interest in silole materials rests upon the early observation that the hexaphenyl derivatives displayed distinct blue fluorescence [18b,93]. Today the availability of red, green and blue electrolumines-

Table 8
Photophysical and electrochemical data of 1,1-dimethyl- and 1,1-diphenyl-2,3,4,5-tetraphenyl-1H-metalloles

	UV–Vis absorption band maxima (nm)[a]		Luminescence band maxima (nm)[a,b]		Anodic and cathodic peak potentials (mV)[a,c]			
					Oxidation		Reduction	
	Me_2	Ph_2	Me_2	Ph_2	Me_2	Ph_2	Me_2	Ph_2
$Ph_4C_4SiR_2$	351	360	480	496	1482	1527	−2174	−1943
$Ph_4C_4GeR_2$	348	354	466	486	1496	1495	−2482	−1962
$Ph_4C_4SnR_2$	350	355	None	494	1191	1539	−2197	−2142

[a] MeCN.
[b] Excitations at UV–Vis band maxima.
[c] irreversible oxidation and reduction in solution.

cent, emitting materials is of paramount importance for the development of full-colour displays [17a,17b]. Crucially, strong, stable blue-emitters remain rare, despite many examples of well-established red and green OLEDs. Thus, it is somewhat surprising therefore, that few systematic studies of silole luminescence have been undertaken.

Zhu and co-workers [94] prepared a family of air-stable, substituted 1,1′-disubstituted tetraphenylsiloles **63–66** using a simple one-pot procedure starting from diphenyl acetylene (Scheme 21). All the compounds isolated displayed two peaks in their UV–Vis spectra at ca. 250 and 360 nm, the former being assigned to a π–π* transition of the phenyl substituents and the latter to the π–π* transition associated with the silole ring. Little difference in the absorption wavelength is observed upon changing the substituents at Si. For all, a small but discernible red-shift of the silole transitions could be detected on replacing alkyl with phenyl groups. All their bandgaps (E_g) were estimated from the onset positions of the absorption bands to be ca. 2.96 eV which are of significantly lower energy than that of acyclic **67** (3.35 eV) (Scheme 21) as a result of electronic transitions associated with the ring. All the siloles displayed emission in the blue region of the spectrum (emission max. ~490 nm) whose brightness and quantum efficiencies were attenuated dramatically when alkyl substituents, rather than phenyl groups were present in the ring. It is notable that the luminescence and quantum efficiency of the 1-methyl,1′-phenyl-silole (**65**) is 2–3 orders of magnitude greater than that displayed by a related silane–silole copolymer [95–97]. In contrast to the general trend that aggregation of chromophores quenches the light emission, light emission of derivative **65** is considerably increased (two orders of magnitude) by aggregation [98]. This derivative has been used as a light-emitting material to prepare LEDs with external quantum yields (number of photons emitted/number of electrons injected) reaching 8% for a low turn-on voltage (3.4 V) [98].

To try and further increase the potential degree of conjugation, the synthesis of simple 2,5-diaryl- and 2,5-distyryl-siloles has been addressed [97]. A range of these

types of functionalised siloles (**69a–69l**) have been prepared using an extension to the intramolecular cyclisation of divinylsilanes developed by Tamao et al. This versatile method involves the preparation of 2,5-dilithiosilole **12** that is subsequently converted to the desired diaryl- or distyryl-siloles via a palladium-catalysed coupling of a 2,5-dizinc intermediate **68** (Scheme 22, Table 9) [57,97].

As expected, the UV–Vis absorption spectra and luminescence spectra show distinct differences depending on the nature of the aryl or styryl substituents. Similar variation is found with the fluorescence spectra, the emission maxima moving from the blue-green to the red-orange regions. The effect of further π-conjugation on these 2,5-diarylsiloles is clearly evident on comparing 2,5-diphenyl silole **69d** with compounds **69j–69l**. The π–π* absorption band for the dinaphthyl compound **69j** lies to lower wavelength by ca. 20 nm. The bis(biphenyl) compound **69l** exhibits an absorption shift of only 17 nm to higher wavelength despite the presence of two additional aromatic rings. In contrast, the 2,5-distyryl compound **69k** gives rise to an absorption maxima and emission that are both bathochromically shifted by ca. 50–70 nm. An electrochemical study on **69k** implies that the additional conjugation has an impact on the HOMO rather than the LUMO. These results indicate that the optical and electrochemical properties of 2,5-diarylsiloles can be tuned over a wide range by varying the nature of the substituents in the 2,5-positions.

Co-polymers containing one of the heavier Group 14 metalloles, namely poly(2,5-diphenylgermole)s have only very recently been described [99]. Using a modification of Fagan and Nugent's [66] zirconium-mediated coupling of diynes, 2,5-bis-*p*-halophenylgermoles (**70a–70c**) (Scheme 23) have been prepared. Subsequently, nickel(0)-mediated homo-coupling was utilised to prepare the yellow polymeric species (**71a–71c**) (Scheme 23), whose precise molecular weights are intimately linked to the nature of the nickel source and the dihalo-germole employed. The reaction between **70b** and NiCl$_2$/Zn produces a of mixture of **71a** (75%; $M_n = 1900$, $M_w/M_n = 1.2$) and **71b** (25%; $M_n = 4700$, $M_w/M_n = 1.9$), while that between **70c** and Ni(cod)$_2$ affords

	R	R′
63	CH$_3$	CH$_3$
64	CH$_3$	(CH$_2$)$_3$Cl
65	CH$_3$	C$_6$H$_5$
66	C$_6$H$_5$	C$_6$H$_5$
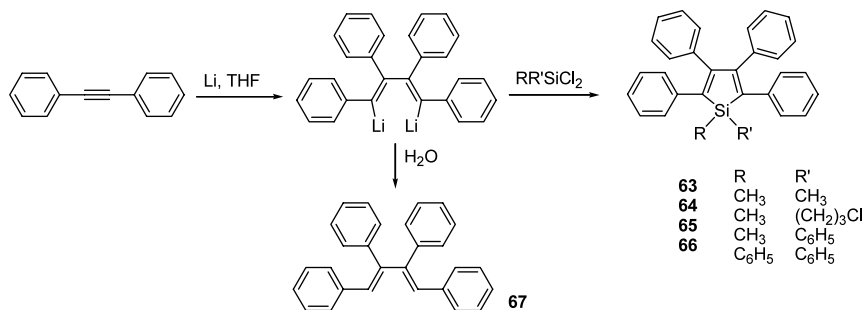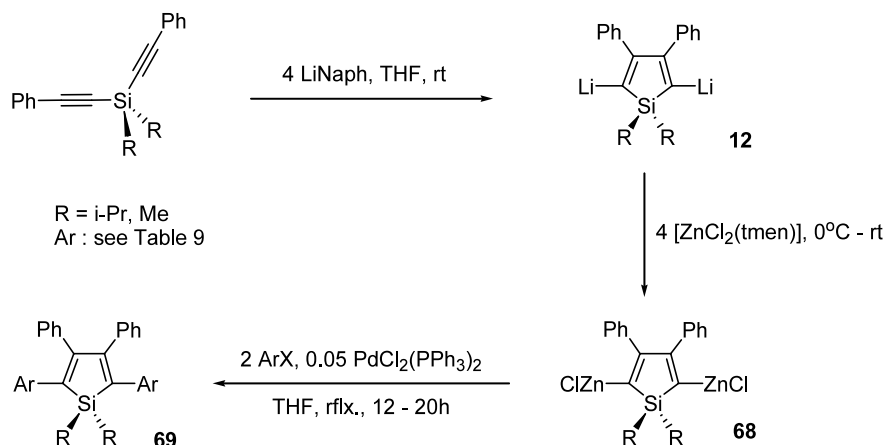
Scheme 21.

Scheme 22.

the higher molecular weight material **71c** (88%; $M_n = 20\,000$, PDI = 2.9). All the polymers **71a–71c** exhibit values of λ_{max} in their UV–Vis absorption spectra that are significantly red-shifted with respect to poly(*p*-phenylene) [100] as well as lower LUMO energies. There is a significant shift in the absorption values of each of the polymers relative to that of the corresponding monomer **70**, the absorption maxima moving to longer wavelength with increasing chain length (Table 10). Taken as a whole, these data are consistent with the extended electron delocalisation for polymers **71**, with a conjugation length of greater than about 7 monomer units (or 21 rings) [100].

To further probe the fundamental behaviour and to extend the potential utility of these types of polymeric material, there has been a considerable drive to prepare π-conjugated materials incorporating other electronically distinct ring systems. In particular, significant emphasis has been placed upon combining electron-accepting silole moieties with π-electron-rich heterocycles such as thiophene and pyrrole.

Polythiophenes have long been established as important conducting materials for molecular electronics, something that makes the silole–thiophene combination particularly attractive targets [12a,40,101]. Thus, a range of such co-oligomers (**72–74**) have been prepared via an intramolecular diyne coupling approach or using the 2,5-dilithioderivative **12** (Scheme 24) [70,96,102] while the Sn and Ge derivatives **75** were obtained via the Fagan–Nugent route [22] (Scheme 24).

Perhaps surprisingly, the absorption maxima of derivatives **72**, **74**, **75a**, and **75b** were found to be similar (Table 11) [20,22]. This trend was rationalised by a theoretical study that revealed that Si, Ge, and Sn influence the LUMO energy of these metalloles by σ*–π* conjugation to a similar extent. It is noteworthy that the λ_{max} of Group 14 containing compounds **72**, **74**, **75a**, and **75b** are considerably red-shifted in comparison to the corresponding ter-thiophene (356 nm) and cyclopentadiene **76** derivatives [22] (Table 11). Significantly, therefore, it is the nature of the substituents at the 3,4-positions rather than the nature of the Group 14 element

Table 9
2,5-Diaryl and 2,5-distyryl siloles (**69a–69l**) (R = Me) prepared via a palladium-catalysed Zn-halide coupling (Scheme 22) with UV–Vis absorption and electrochemical data

Ar		Yield (%)	UV–Vis absorption		Fluorescence		Electrochemical data	
			λ_{max} (nm)	log ε	λ_{max} (nm)	$\Phi_f \times 10^{-3}$	E_{pa} (V)	E_{pc} (V)
p-(Me$_2$N)C$_6$H$_4$	**69a**	53	423	4.33	529	2.51	+0.11	−2.43
p-MeOC$_6$H$_4$	**69b**	68	379	4.11	493	2.40	+0.66	−2.30
p-MeC$_6$H$_4$	**69c**	75	367	4.11	475	1.96	+0.94	−2.36
C$_6$H$_5$	**69d**	70	359	3.97	467	1.43	+1.02	−2.27
p-CF$_3$C$_6$H$_4$	**69e**	67	358	4.02	469	8.78	+1.18	−1.93
p-(O$_2$N)C$_6$H$_4$	**69f**	87	399	4.35	522	2.66	+1.28	−1.44
m-MeC$_6$H$_4$	**69g**	82	364	3.78	471	2.78	+1.12	−2.30
m-FC$_6$H$_4$	**69h**	81	358	4.00	466	4.38	+1.24	−2.15
m-CF$_3$C$_6$H$_4$	**69i**	67	358	3.99	468	1.09	+1.30	−2.09
1-Napthyl	**69j**	42	340	3.96	435	4.71	+1.10	−2.36
2-Styryl	**69k**	82	435	4.04	527	4.70	+0.64	−2.02
Biphenyl	**69l**	74	381	4.32	497	5.13	+0.99	−2.16
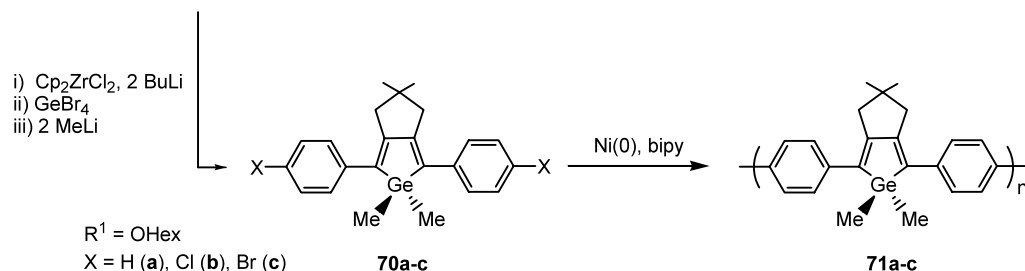
Scheme 23.

Table 10
UV–Vis absorption and emission spectral data for monomers **70a**–**70c** and poly(2,5-diphenylgermole)s (**71a**–**71c**)

	$M_n{}^a$	Absorption λ_{max} (nm)	Emission λ_{max} (nm)	Φ^{350}
70a	–	364	452	0.018
70b	–	368	457	0.084
70c	–	376	464	0.12
71a	1900	404	486	0.059
71b	4700	430	498	0.14
71c	20000	442	500	0.21

[a] GPC data relative to polystyrene standards.

that have a primary influence upon the emission wavelengths of such compounds (Table 11). Once again, these data clearly show that siloles are remarkable building block for the synthesis of low bandgap π-conjugated systems.
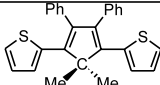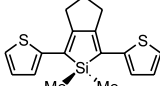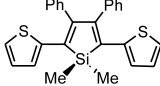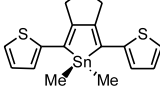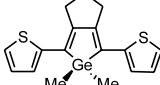
Well-defined regular alternating 1:1 silole–thiophene compounds were prepared according to the general routes depicted in Scheme 25 [70,102,103] whereas the corresponding polymers have been prepared via Pd-catalysed cross-coupling reactions from **77** (Scheme 25) [103–105]. Polymer **78** was characterised by NMR spectroscopy. GPC analysis revealed that it had $M_w = 487\,000$, $M_n = 184\,000$, and $M_w/M_n = 2.6$ (versus polystyrene standards), which equates to a structure in which there are ca. 80 consecutive 5-membered rings. In contrast, direct coupling of **77** with 2,5-dibromothiophene led, under the same conditions, to the formation of a lower molecular weight material **79** ($M_w = 9000$, $M_n = 4600$, and $M_w/M_n = 2.0$, $n \approx 11$, ca. 22 consecutive rings). Bronze-coloured solid (**78**) was found to be remarkably stable to atmospheric conditions (no apparent change after 1 year) and dissolves in both THF or CHCl$_3$ to give dark blue-coloured solutions. The UV–Vis absorption spectra exhibit comparable values of λ_{max} for **78** (648 nm) and the shorter chain **79** (640 nm), both values being at considerably longer wavelengths than the starting dithienyl dihalide **80** (λ_{max} at 418 nm, Scheme 25). This is suggestive of considerable π-conjugation along the backbone of **78** (over greater than 22 rings). The bandgap determined for **78**, 1.55 eV,
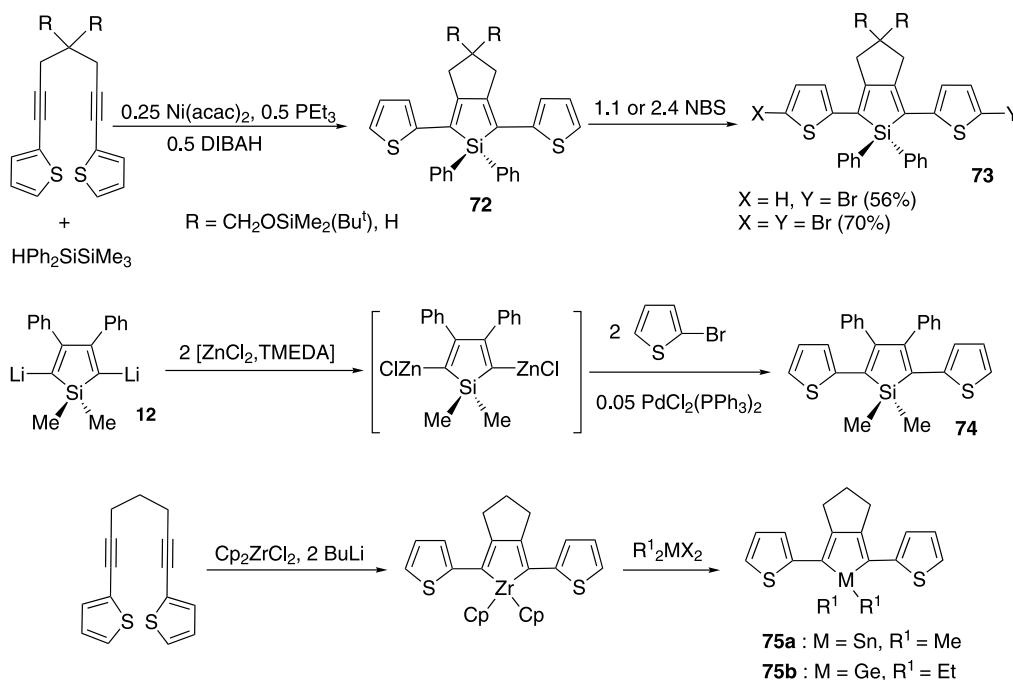
Scheme 24.

Table 11
UV–Vis absorption and fluorescence data for related 2,5-dithienyl Group 14 heteroles

		UV-vis absorption		Fluorescence	
		λ_{max}/nm	log ε	λ_{max}/nm	$\Phi_f \times 10^2$
(structure)	**76**	368	4.10	461	0.996
(structure)	**72**	409	4.38	492	5.44
(structure)	**74**	418	4.28	515	0.141
(structure)	**75a**	406	4.36	479	0.495
(structure)	**75b**	405	4.37	479	8.72

is small compared with other linear π-conjugated polymers, but is in good agreement with a value determined theoretically by Hong and Song ($E_g = 1.55$ eV) [106].

Co-oligomers and -polymers with a variety of structures based on silole and thiophene monomers were prepared via Pd-catalysed cross-coupling reactions using the intermediate key building block **81** (Scheme 26) [70,102,107].

Representative examples of these derivatives are illustrated in Fig. 10 along with their UV–Vis spectroscopic data. The absorption maxima for these compounds tend to shift to longer wavelengths as the number of 2,5-dithienyldilole units is increased suggesting a decrease in the bandgap. The absorption maxima are also considerably red-shifted in comparison to all the thiophene oligomers (Fig. 10) due to the presence of silole rings with comparatively low-lying LUMO levels allowing intramolecular charge transfer. All oligomers described here show remarkably good solubility characteristics, with even the longer chain polymers being sparingly soluble in $CHCl_3$; all are stable in air for prolonged periods of time.

A related Stille-type coupling has been utilised to prepare the functionalised 2,5-disilole **82**, which incorporates the extremely electron-rich 3,4-ethylenedioxythiophene unit (EDOT) (Scheme 27) [109]. This new compound displays a λ_{max} at 437 nm (π–π*) in its UV–Vis absorption spectrum, which is somewhat red-shifted compared with other bis(2-thienyl)-siloles, as a result of the combination of the low-lying silole LUMO level and the electron-rich character of the 3,4-ethylene-dioxythio-

phene unit [22]. Following an oxidative electrochemical polymerisation of **82** in the presence of $LiClO_4$, polymer **83a** was obtained (Scheme 27). Spectroelectrochemistry of this material revealed that the neutral blue polymer **83a** has a narrow bandgap (1.3–1.4 eV). Gradually increasing the potential applied to the polymer induces oxidation and subsequent formation of the yellowish-green doped material **83b**, which exhibits a broad absorption band starting at 830 nm [109].

Attempts have been made to study the effect of combining a yet more π-electron-rich heterocyclic fragment, namely pyrrole, with silole moieties [110]. Once again, these materials **84**–**86** (Fig. 11) were prepared using extensions to the previously described palladium-catalysed tin coupling reaction. A molecular structure determination of **84** revealed that the 2,5-dipyrrolylsilole favours a significantly twisted structure, with torsion angles of 51.7° and 55.7°, something presumed to result from steric repulsion. However, the value of λ_{max} for **84** (406 nm) is much longer than that for the parent terpyrrole ($\lambda_{max} = 271$ nm) [111] and only slightly inferior to that of 2,5-dithienylsilole **74** (418 nm). Calculations on **84** by Tamao et al. revealed that, as might be predicted, it possesses a high-lying HOMO (delocalised over three rings) and a low-lying LUMO, based largely on the silole ring. Notably, the degree of red-shift observed for the longer chain co-oligo-pyrrole–silole compounds is considerably smaller than that observed for 2,5-dithienylsilole-based oligomers (Fig. 10).

A tin coupling has been employed to prepare longer chain silole/pyrrole oligomers, as outlined in Scheme 28 [110]. The two oligomers **87** and **88** were separated using preparative GPC as orange and red powders, respectively. Significantly, the UV–Vis absorption data (**87**: $\lambda_{max} = 436$ nm {log ε = 4.24}; **88**: $\lambda_{max} = 447$ nm {log ε = 4.53}) indicate only a small bathochromic shifts compared with pyrrole-substituted **84**, possibly as a result of twisting along the backbone due to steric constraints preventing efficient π-delocalisation along the longer chains.

The potential to tune the optical and electronic properties of siloles by varying the nature of the 2,5-aryl substituents is of particular importance for the optimisation of organic LEDs based on these materials. Indeed, aryl-silole oligomers **69g**, **74**, **89**, and **90** (Fig. 12) have been shown to behave as emissive electron-transporting (ET) materials in multilayer LEDs [96]. It is noteworthy that the emission wavelength observed for a device based on **90** (585 nm) is red-shifted by 100 nm compared to that obtained using **69g** (488 nm), showing that emission colours can indeed be tuned by modification of the 2,5-aryl silole substituents.

However, in the field of silole-based organic LEDs, the most promising results have been obtained using derivatives **91**–**96** that are substituted by electron-
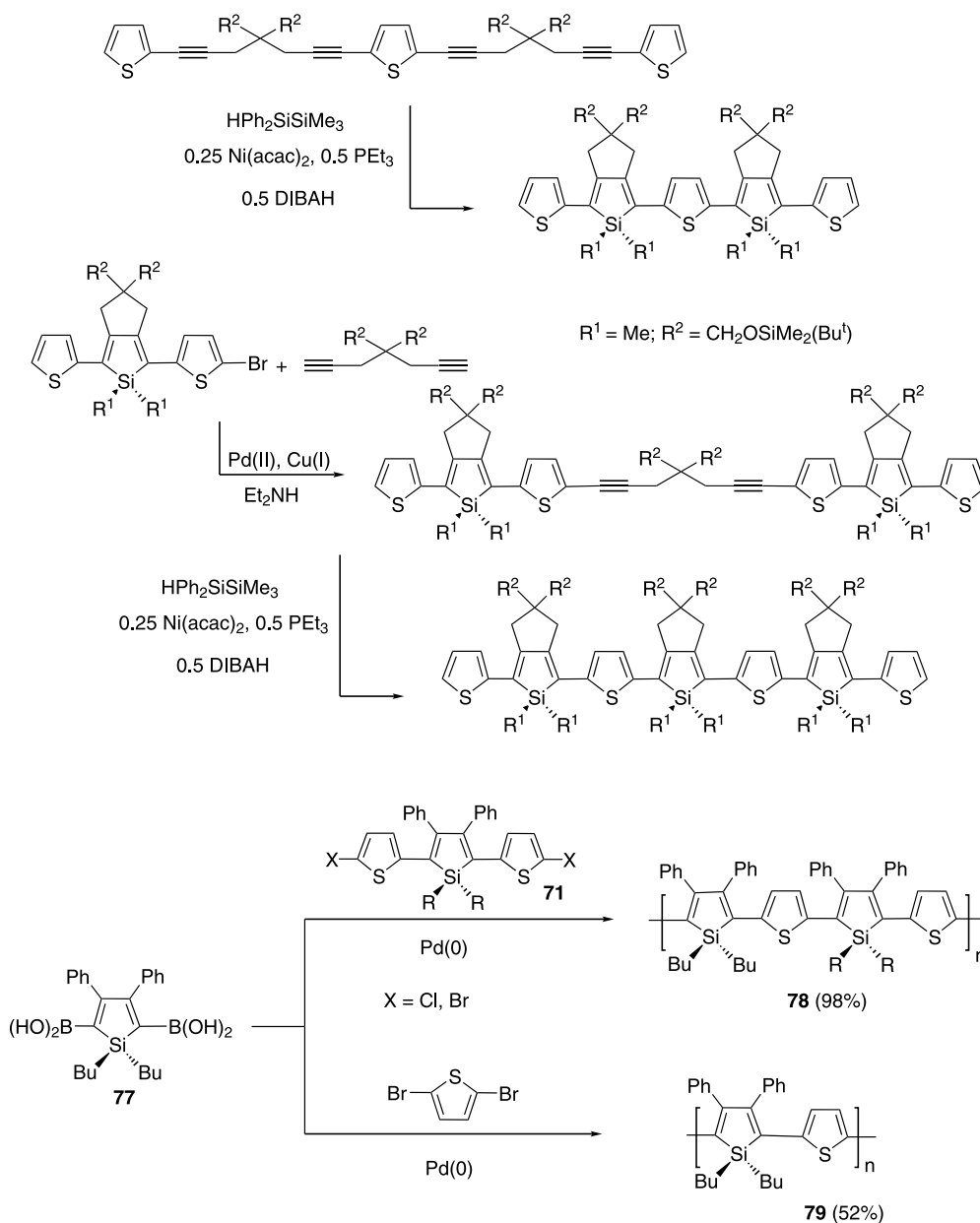
Scheme 25.

deficient heterocycles, as ET materials (Fig. 13). These derivatives were prepared according to the general strategy depicted in Scheme 22. The inherent high electron affinity of the silole ring is considerably enhanced by the presence of electron-withdrawing aromatic substituents at the 2- and 5-positions [96,97]. For example, the thiaozyl-substituted derivative **93** exhibits a very low reduction potential close to that of poly(quinoxaline-2,6-diyl), one of the most π-electron-deficient systems [112]. Indeed, derivative **91** is a very efficient ET material in devices with an indium tin oxide (ITO)/ triphenylamine dimer (TPD)/tris(8-quinolinolato)aluminium (Alq)/**91**/Mg:Ag composition, where TDP and Alq are employed as hole transporting and emissive materi-als, respectively. Derivative **91** showed an ET perfor-mance that exceeded that of tris(8-quinolinolato)aluminium, one of the most widely used ET materials [20,96,103]. Tailoring the 2,5-substituents afforded derivatives **94–96** with improved properties [113]. Indeed, high-performance organic LEDs based on compound **96** as the ET material and di(tetraphenylsi-lole) **97** (Fig. 14) as the emissive layer have been recently reported [113c]. They showed very interesting perfor-mance with high durability and an external quantum efficiency reaching 4.8%. This efficiency is the best yet achieved for LEDs using undoped emissive and carrier transport layers and is close to the theoretical limit for a device using a fluorescent emitter [113c].
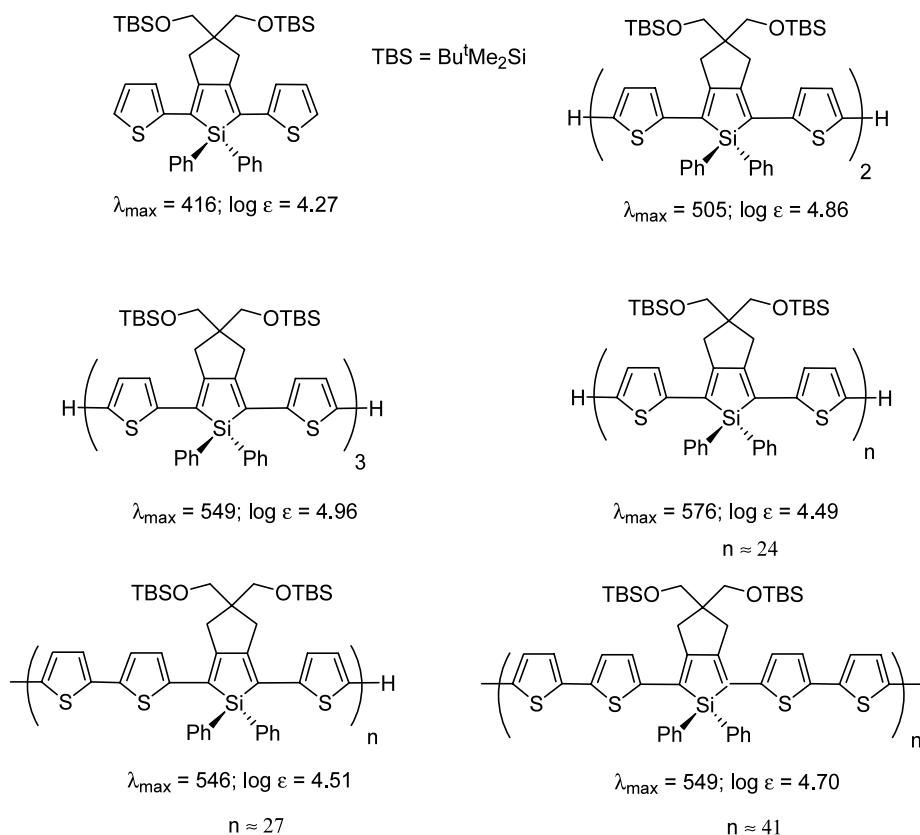
Scheme 26.

TBS = Bu^{t}Me$_2$Si

$\lambda_{max} = 416$; log ε = 4.27

$\lambda_{max} = 505$; log ε = 4.86

$\lambda_{max} = 549$; log ε = 4.96

$\lambda_{max} = 576$; log ε = 4.49

n ≈ 24

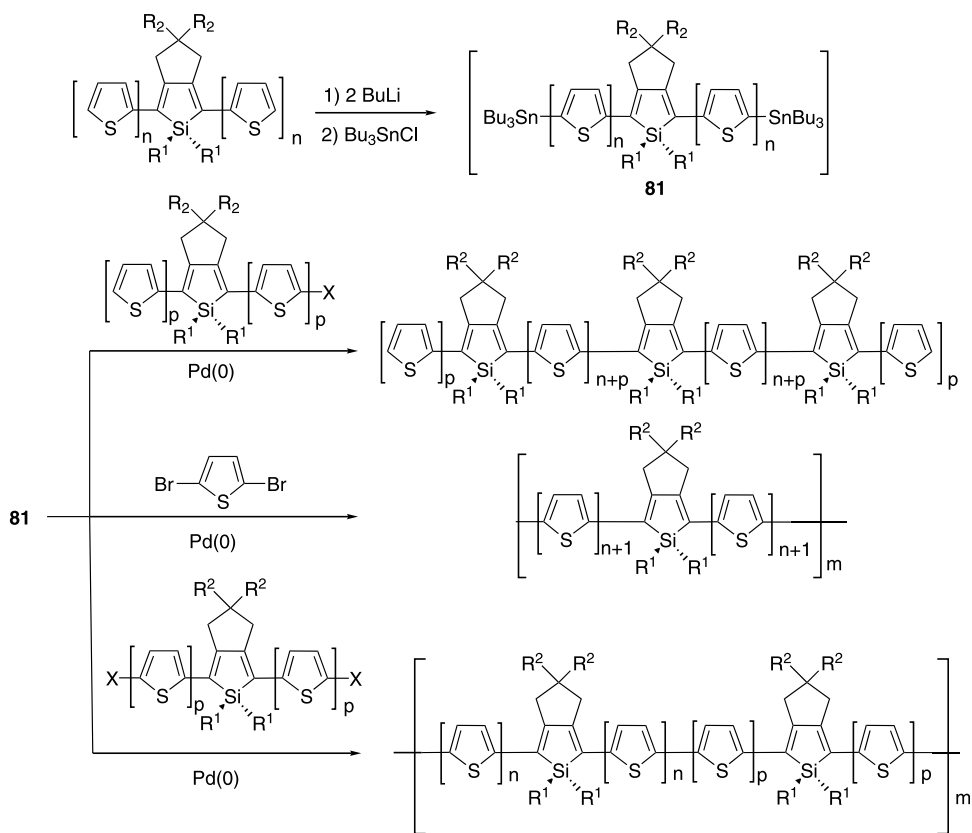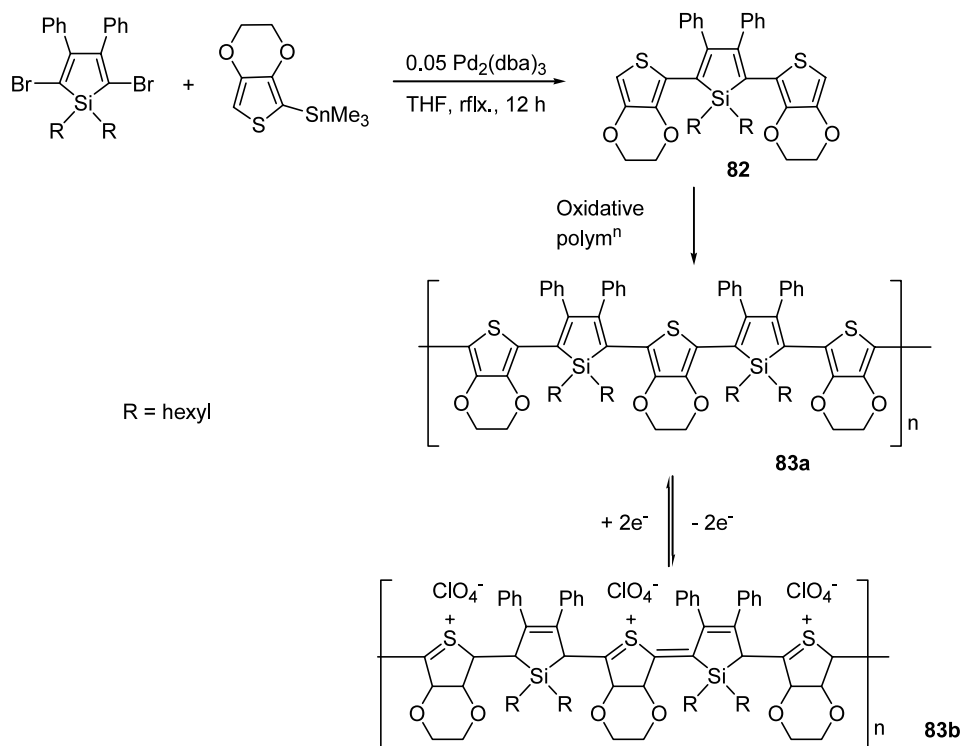$\lambda_{max} = 546$; log ε = 4.51

n ≈ 27

$\lambda_{max} = 549$; log ε = 4.70

n ≈ 41

Fig. 10. For comparison, terthiophene has a $\lambda_{max} = 353$ nm, while poly(3-hexylthiophene) exhibits $\lambda_{max} = 442$ nm [108].

Scheme 27.

Finally, more elaborate derivatives **98a** and **98b** (Fig. 14) incorporating both triphenylamine and silole moieties have been prepared and used as components for single-layer organic LEDs, emitting yellow light with a high luminescence efficiency [114].

2.5.2. [Silole]-[ethynyl] systems

Co-oligomeric siloles **99–101** (Fig. 15) incorporating acetylene moieties were prepared independently by the groups of Tamao and Barton [115,116]. Derivative **99b** was characterised by an X-ray diffraction study [115]. Oligomers **99a–99e** exhibit absorption in the visible region, with the highest λ_{max} being recorded for the thienyl-capped derivative **99e** ($\lambda_{max} = 452$ nm). Polymers

100 ($M_w = 63\,000$, $M_n = 13\,000$) and **101** ($M_w = 64\,000$, $M_n = 9000$) display long-wavelength absorption bands in their UV–Vis spectra, and have estimated optical bandgaps of 1.77 and 2.07 eV, respectively. These latter values are much narrower than those usually observed for conjugated acetylenic polymers [117].

Note that other types of silole-containing oligomers or polymers exist including, for example, **102** [118], **103** [119] and **104a** and **104b** [120] (Fig. 16). However, these compounds are not covered by this review since they do not possess pure extended π-conjugated systems.

In conclusion, a wide spectrum of silole-based π-conjugated systems is available today. These derivatives usually display very attractive properties such as low
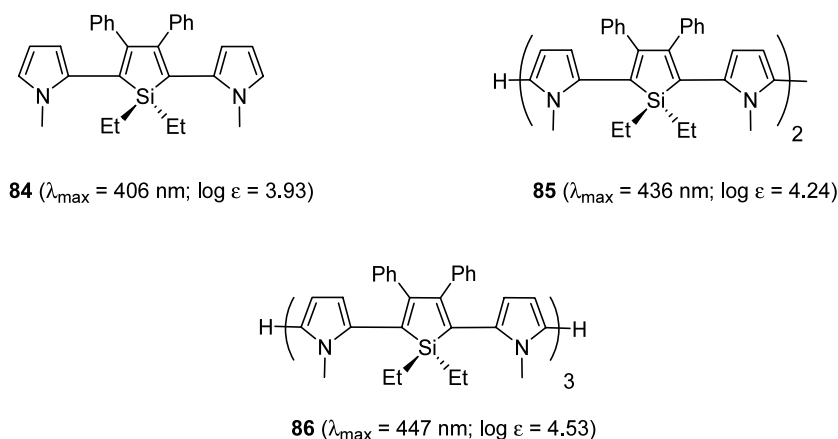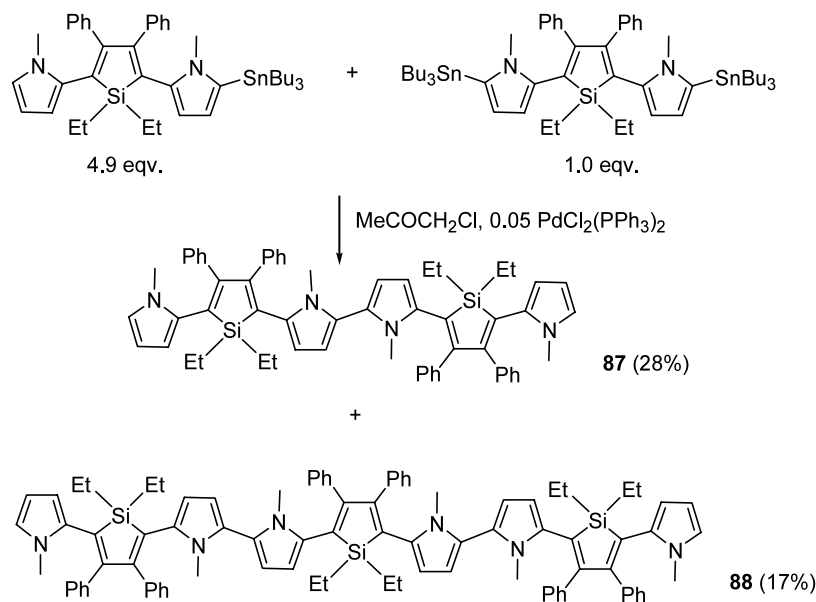

84 ($\lambda_{max} = 406$ nm; log ε = 3.93)

85 ($\lambda_{max} = 436$ nm; log ε = 4.24)

86 ($\lambda_{max} = 447$ nm; log ε = 4.53)

Fig. 11. Optical data for pyrrole-silole oligomers.

Scheme 28.

bandgaps and high electron affinities. The possibility to tune the electronic and optical properties of oligomers by varying the nature of the silole substitution pattern has led to the discovery of versatile and very attractive derivatives for the preparation of tailor-made molecular organic LEDs.

2.6. Homo-oligomers incorporating Group 15 heteroles

To the best of our knowledge, extended linear π-conjugated systems incorporating Group 15 heteroles are restricted to phosphole-containing derivatives. The synthesis of oligo(phosphole)s is a real synthetic challenge since: (i) phospholes are not accessible via the classical routes used for the preparation of pyrroles and thiophenes such as the Paal–Knorr condensations and (ii) the functionalisation of the dienic moiety is difficult to achieve due to the low aromatic character of phosphole that prevents electrophilic substitution [24,25,121]. These difficulties probably explain why no poly(phosphole)s have yet been reported. In contrast, Mathey [24] achieved a breakthrough in the field of oligo(phosphole) chemistry with the discovery of several synthetic routes to bi- and tetra-phospholes starting from 1-phenyl-3,4-dimethylphosphole (105) (Scheme 29) which is readily accessible in multi-gram quantities.

The first method involves the prolonged thermolysis of phosphole 105, which yields the cyclic tetramer 106 via a series of concerted [1,5]-sigmatropic shifts of Ar, H and P plus two dehydrogenation steps (Scheme 29) [122a,122b]. The reductive cleavage of the P–P bonds of 106 gives the 2,2′-biphospholide dianion (107). This compound acts as a bidentate nucleophile towards a wide variety of electrophiles to afford linear and cyclic derivatives featuring 2,2′-biphosphole moieties (Scheme 29) [122]. Biphospholes 108 were obtained as a mixture of diastereoisomers. The major component, with $R^2 =$ CN (Scheme 29) can be isolated by crystallisation. Note that it isomerises in solution at room temperature indicating a low barrier to inversion at phosphorus [122b], as observed for simple phospholes [24,25]. Derivatives 109 are also isolated as a mixture of diastereoisomers. The phosphorus atoms of compounds 108 and 109 exhibit the classical reactivity pattern of monophospholes. They can be oxidised with elemental sulfur and, more importantly, they can act as chelates towards transition metals [122]. Both these reactions suppress the inversion at the phosphorus atoms and allow, in several cases, the isolation of single diastereoisomeric products.

The best and most general route to phospholes is via the dehydrohalogenation of the corresponding 1-halogenophospholium salts [24,25]. This method is broad in
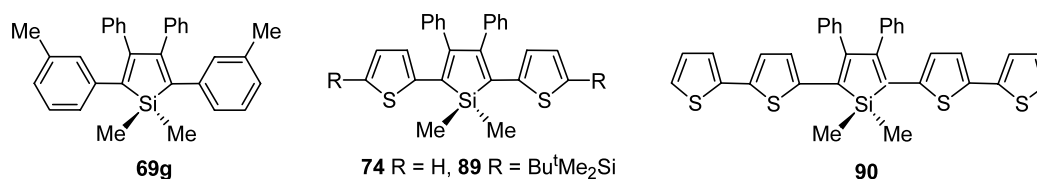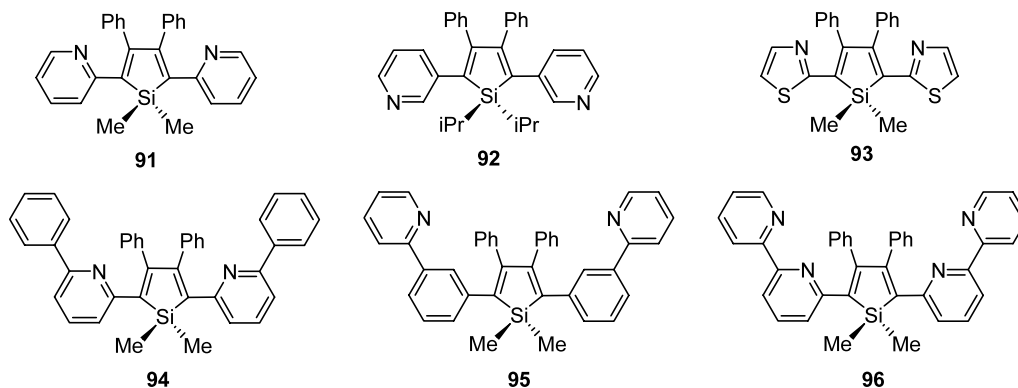

Fig. 12. Aryle-silole oligomers.

Fig. 13.

its scope and has been extended to the synthesis of 2,2′-biphospholes. The Ni(II)-promoted reductive dimerisation of phosphole **105** followed by decomplexation afforded the biphospholene **110** (Scheme 30) [123]. Successive P-bromation and dehydrohalogenation gave rise to the target 2,2′-biphosphole **112** via the di(1-halogenophospholenium) salt **111** (Scheme 30). Compound **112** is stable enough to be purified by column chromatography on silica gel and is isolated in an overall 50% yield from derivative **110** [124]. Biphosphole **112** is obtained as a mixture of interconverting diastereoisomers [124–126], one of which was characterised by an X-ray diffraction study [126].

The inversion at phosphorus is suppressed upon oxidation and the diastereoisomers of oxo- and thiooxo-biphosphole **112a** and **112b** (Scheme 31), respectively, can be separated by crystallisation or column chromatography and were structurally characterised [125,126]. Derivative **112** is a versatile building block for the synthesis of new biphospholes such as **112d** via the readily available 2,2′-biphospholide anion **112c** (Scheme 31). Furthermore, compound **112** exhibits a rich coordination chemistry (Scheme 31) [124,125,127]. The solid-state structures of biphospholes **112** [126] and **112d** [125] are very similar. In both cases, the phosphorus atoms are pyramidalised and the dihedral angles between the two phosphole rings are about 46°.

The discovery of a third route to biphospholes based on the synthesis of 2-lithiophospholes was a landmark in this area. This method provided the first direct means of functionalisation of the phosphole ring and opens the way to a number of phospholes previously inaccessible by other routes. The key intermediates are 2,5-dibromo-2,5-dihydrophosphole oxides **113** (Scheme 32) [128] which are readily accessible from the corresponding phospholes [129,130]. An efficient three-step process (formation of thiooxide, dehydrobromation and reduction) gave rise to 2-bromophospholes (**114**) in 76% yield from **113** [129]. A quantitative bromine–lithium exchange afforded the highly reactive 2-lithiophospholes (**115**), which underwent an oxidative coupling leading to biphospholes **112** upon addition of copper(II) chloride [129]. Note that this reaction sequence can also be performed on thiooxophospholes [130]. This very efficient methodology has been applied to the preparation of the quarter(phosphole) **1** (Scheme 32), the longest oligo(phosphole)s known to date. The 2,5-dibromo-phosphole (**116**) ($R^1 = CH_3$) was obtained via the same reaction sequence that led to **114** with an additional bromination step. This was followed by two consecutive bromine–lithium exchange/oxidative coupling processes that afforded the target oligomer **1** in 55% yield from **116** (Scheme 32) [43].

Linear quaterphosphole **1** was obtained as a mixture of diastereoisomers. According to ^{31}P-NMR spectro-
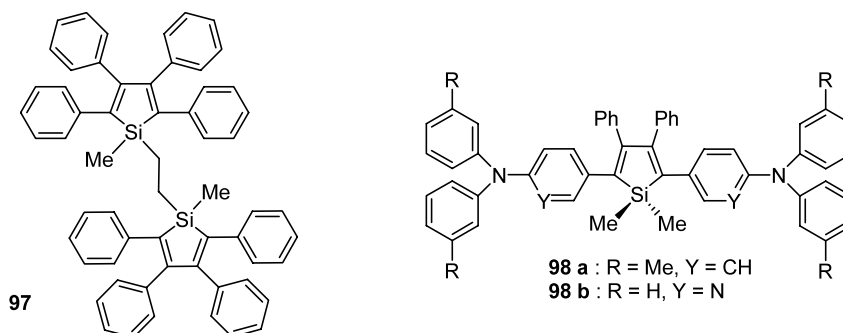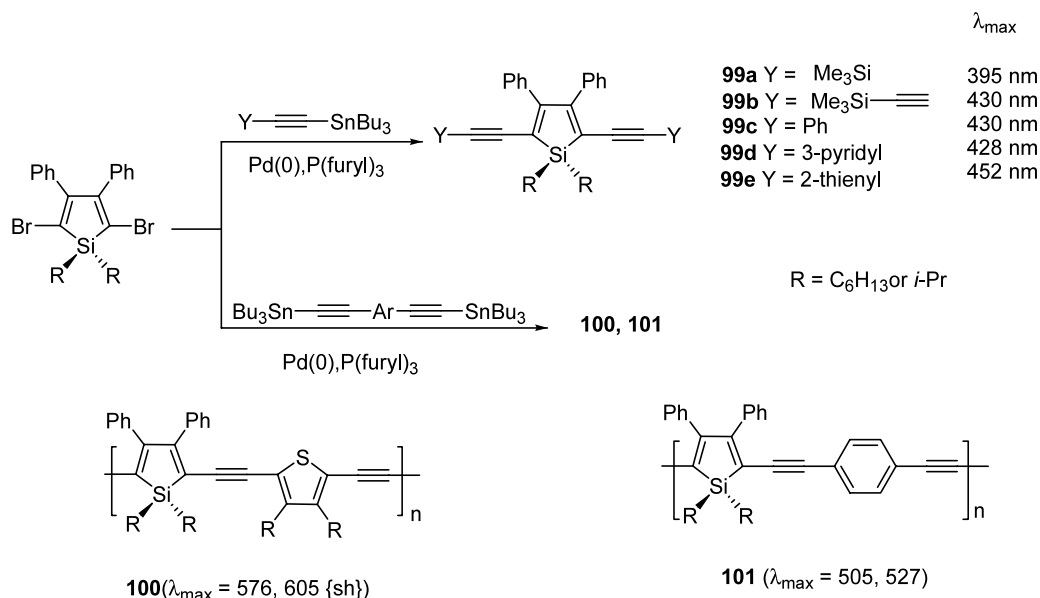

98 a : R = Me, Y = CH
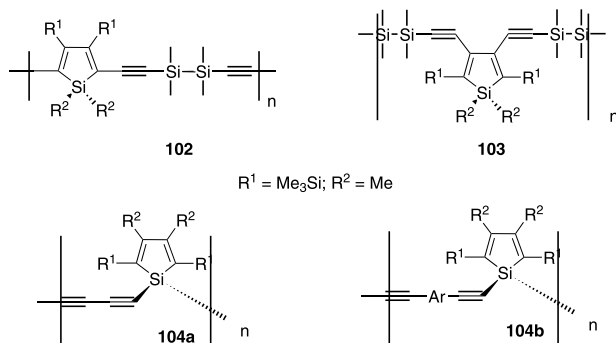98 b : R = H, Y = N

Fig. 14.

Fig. 15.

Fig. 16. Examples of silole-containing oligomers.

scopy, the major isomer possesses a highly symmetric structure as confirmed by an X-ray diffraction study, which revealed the presence of a C_2 symmetry axis [43]. The four phosphorus atoms are mutually *syn*-disposed, despite the *anti*-conformation having been predicted to be the more stable form [38,39]. The phosphorus atoms adopt a pyramidal geometry with the phenyl rings being alternatively up and down with respect to the mean plane of the oligomer. The P–C bond distances are between 1.790(6) and 1.822(6) Å, values which are typical for P–C single bonds (1.8 Å). Overall, these geometric data clearly show that, as observed for monophospholes, the P-lone pair of the σ^3,λ^3-phosphole
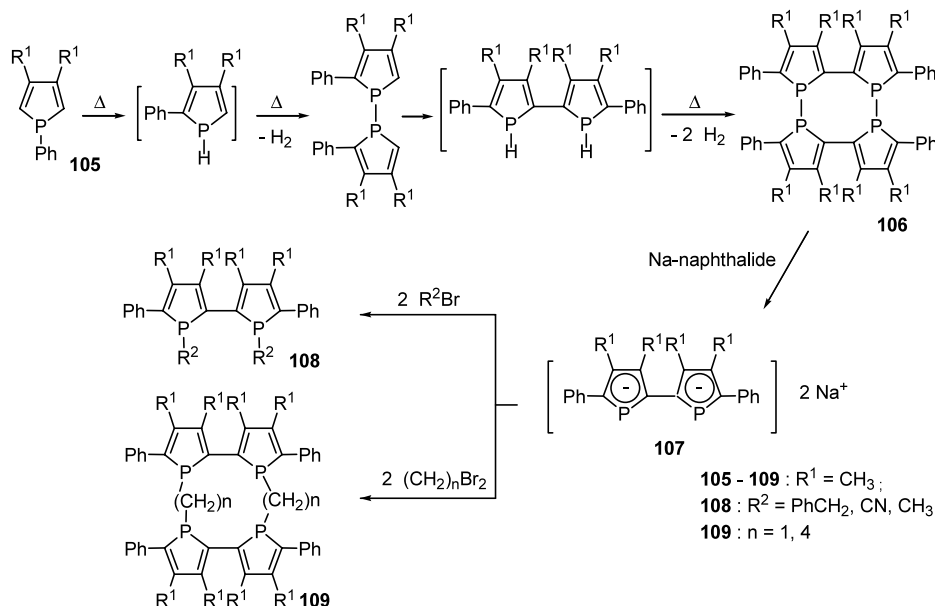
Scheme 29.
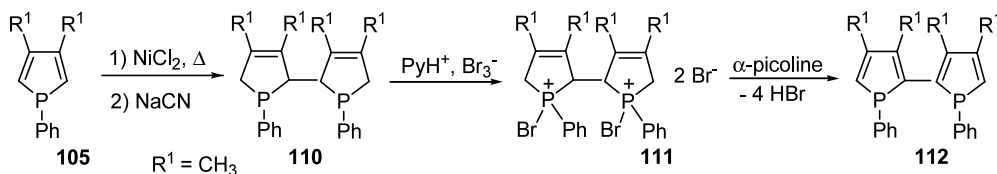
Scheme 30.
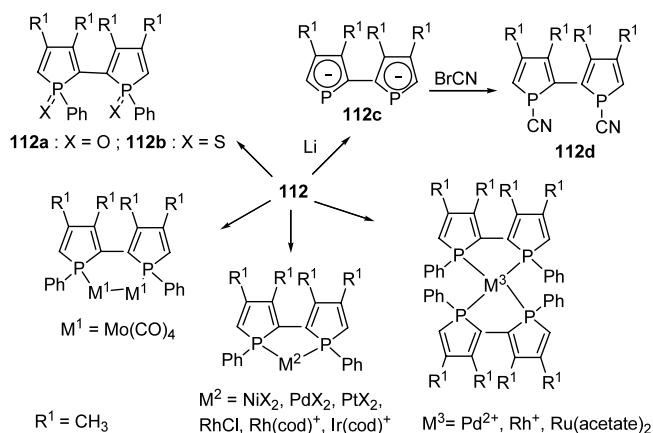
Scheme 31.

subunits is not in conjugation with the endocyclic diene framework.

This study also revealed that the four phosphole rings are not coplanar; the twist angle between the two inner rings is 25.1° while that between the outer pair is 49.7°. This rotational disorder would preclude **1** from being a conjugated system. However, the fact that this significant twist could be due to packing effects in the solid state cannot be discounted. The inter-ring carbon–carbon bond distances are 1.43(1) and 1.451(8) Å. The authors stated that "The C–C bridges are not shortened, and thus, conjugation between the phosphole rings is unlikely" [43]. This conclusion is in marked contrast with the theoretical studies that predicted a significant delocalisation of the π-system over the four rings [37–39]. Lagowski et al. [37] gave the following comment concerning this point "The authors concluded

that there is no conjugation between the phosphole rings because the inter-ring bonds (1.43 and 1.45 Å) are not shortened. This is a surprising conclusion considering that a normal C–C bond is about 1.5 Å long". Unfortunately, the lack of UV–Vis or electrochemical data, which could be used to evaluate the HOMO–LUMO gap of **1**, prevents a definitive answer to this question. Notably, however, quaterphosphole **1** is isolated as deep-orange crystals, a colour suggesting a rather high value of λ_{max} and consequently a low HOMO–LUMO gap!

It is clear that linear oligo(phospholes)s are potentially accessible via the efficient synthetic strategies developed by Mathey et al. as illustrated by the preparation of di- and tetra-phospholes. Until now, these oligomers have not been used for optoelectronic applications but they have proven to be versatile ligands for homogeneous catalysis including asymmetric processes [42b,43,127a,127b].

2.7. Co-oligomers and -polymers based on Group 15 heteroles

Once again, out of all the Group 15 heteroles, only the phosphole ring has been used to prepare extended linear mixed π-conjugated systems. Three different types of these derivatives are known. The first group comprises co-oligomers of alternating phosphole and aromatic heterocycles such as thiophene, furan or pyridine while the second includes compounds based on biphosphole cores. The last set consists of compounds in which two phosphole rings are linked by a vinylene or an alkylene bridge.
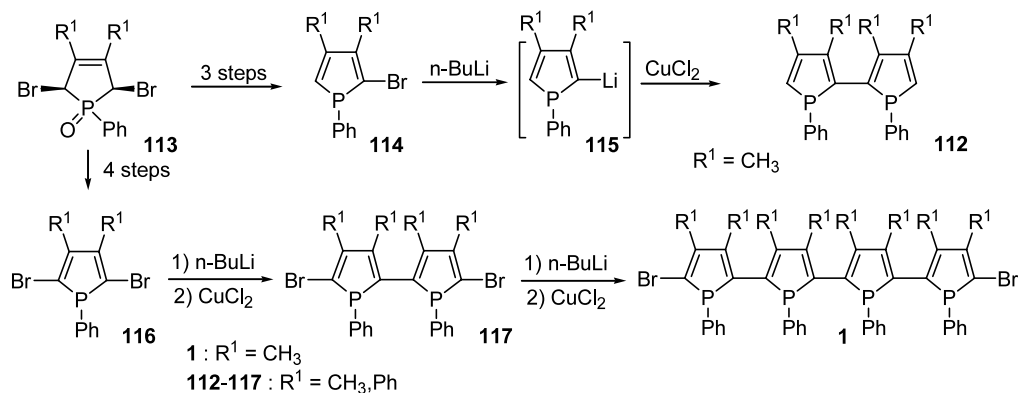
Scheme 32.
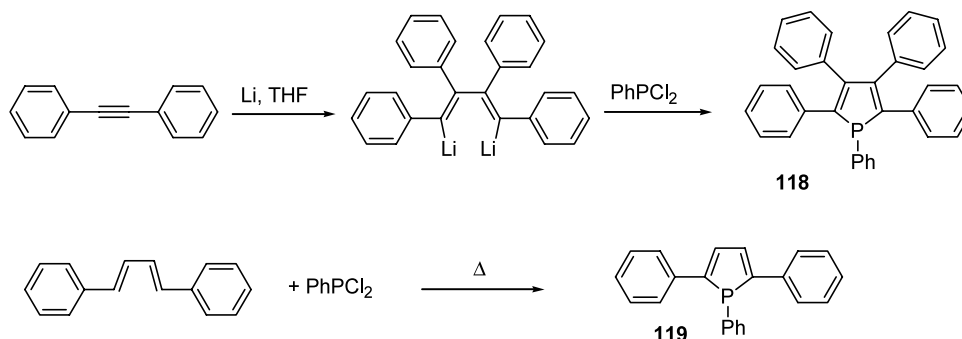
Scheme 33.

2.7.1. [Phosphole]-[aromatic heterocycle] co-oligomers

Historically, the first derivatives of this type are 2,5-diphenylphospholes **118** [18,19] and **119** [131], which are readily accessible on gram scales via the routes depicted in Scheme 33. Note that using the first route, 2,3,4,5-tetraphenyl-arsole and -stilbole have also been prepared this way, a method analogous to that used to prepare the corresponding silole derivatives **63–66** [18,19]. These phosphole derivatives show absorption in the visible region (λ_{max}: **118**, 358 nm; **119**, 374 nm) [132]. Although not recognised at the time, these data strongly suggest the presence of an extended delocalised π-system involving the dienic part of the phosphole ring and the two 2,5-phenyl substituents. This conclusion is reinforced by the X-ray analysis of compound **119** which revealed that the three rings are almost coplanar [133]. These derivatives are fluorescent and exhibit Stoke's shifts varying from 100 nm (**119**) to 120 nm (**118**) [132].

In the 1990s, Mathey et al. [134] prepared a series of 2,5-(diphosphole)-thiophene and -furan oligomers (Scheme 34) via electrophilic substitution. In the presence of AlX$_3$ (X = Cl, Br), complex **120** acts as an electrophile towards electron-rich thiophene or furan rings leading to adducts **121a** and **121b** [135]. These compounds were transformed into the corresponding phosphole derivatives **122a** and **122b** (Scheme 34) through a classical deprotection–bromination–dehydrohalogenation sequence previously detailed for the

synthesis of compound **112** (Scheme 30). Note that oligomer **122**, incorporating the furan ring was not isolated, but was directly transformed into its thio-oxo derivative **123a** (Scheme 34). Compound **123b** was characterised by an X-ray diffraction study [134]. One phosphole ring was found to lie in the plane of the central furan unit while the second P-heterocycle deviates notably from coplanarity with a twist angle of $40.1 \pm 0.1°$. The two inter-ring C–C bond distances [1.452(4) and 1.461(6) Å] lie in between those observed for C–C single and double bonds, a feature that suggests the presence of an extended π-conjugated system. The colour of the crystalline derivatives **122b** (bright yellow) and **123a** (orange) are in favour of relatively high values of λ_{max}.

2,5-Di(heteroaryl)phospholes would constitute a second family of co-oligomers based on the same monomer subunits. However, the synthetic methodology described above has been shown to be inappropriate for the preparation of these derivatives since the second condensation step gave rise to 2,4-dithienylpholene (**124**) (Scheme 35) [134].

In contrast, 2,5-di(heteroaryl)phospholes are accessible via a straightforward, general organometallic route known as the "Fagan–Nugent method" [66] that can be used to prepare a large range of metaloles including phospholes, arsoles, stiboles, stannoles, germoles, etc. as outlined in Section 2.5.1. The intramolecular oxidative
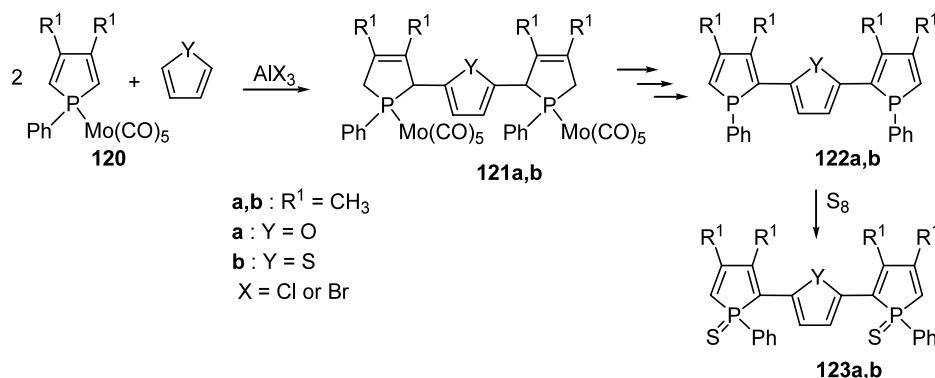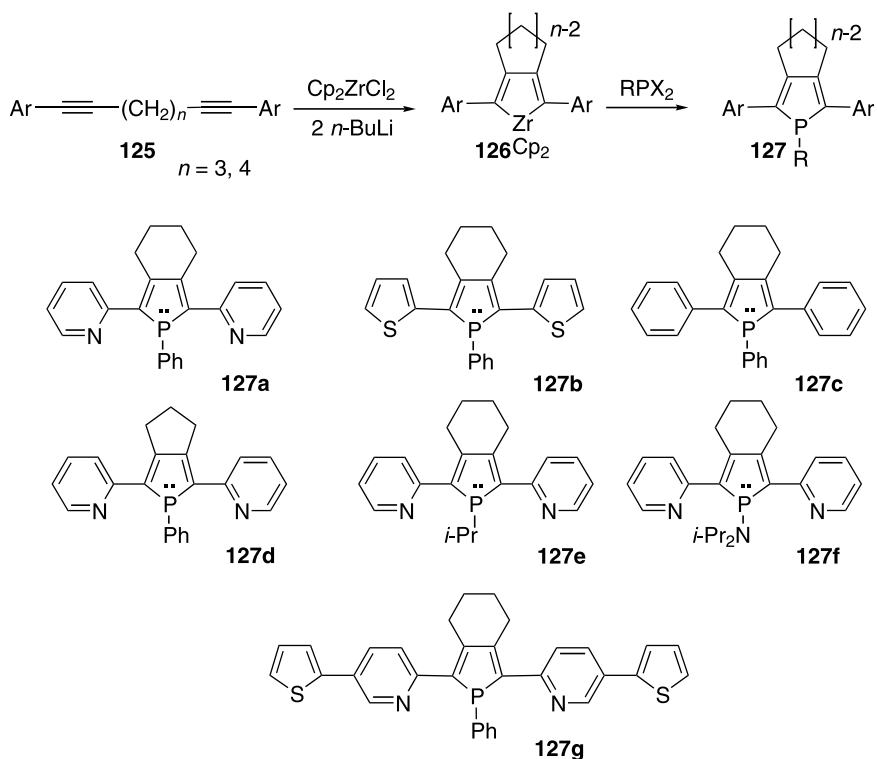

Scheme 34.
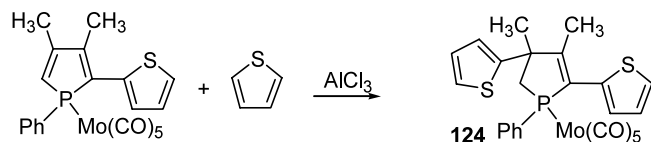
Scheme 35.

coupling of functionalised diynes **125** (Scheme 36), possessing a $(CH_2)_3$ or a $(CH_2)_4$ spacer in order to obtain the desired 2,5-substitution pattern, with 'zirconocenes' provides the corresponding zirconacyclopentadienes **126** which can be characterised by NMR spectroscopy [33]. These organometallic intermediates react with dihalogenophosphines to give the corresponding phospholes **127a–127g** in medium to good yields (Scheme 36). It is noteworthy that the stability of these phospholes is intimately related to the nature of the P-substituent. 1-Phenylphospholes (**127a–127d**) can be isolated, following flash column chromatography on basic alumina, as air-stable solids, yet 1-alkylphosphole (**127e**) and 1-amino (**127f**) are extremely air- and moisture-sensitive compounds.

σ^3,λ^3-Phospholes **127a** [136] and **127b** [137] bearing electron-deficient and electron-rich substituents, respectively, were characterised by X-ray diffraction studies. In spite of the different electronic nature of the two 2,5-substituents, these compounds share some important structural features in the solid state. The twist angles between two adjacent rings are rather small [**127a**, 7.0° and 25.6°; **127b**, 12.5° and 16.7°] and the phosphorus

atoms are strongly pyramidalised, as indicated by the sum of the CPC angles [**127a**, 299.3°; **127b**, 299.3°]. For both compounds, the lengths of the C–C linkages between the rings [1.436(6)–1.467(8) Å] are in the range expected for C sp²–C sp² single bonds. These metric data suggest a delocalisation of the π-system over the three heterocycles. It is amazing to note that these solid-state data are comparable to those recorded for the quaterphosphole **1** (Scheme 32) also based on σ^3,λ^3-phosphole units.

The presence of an extended π-conjugated system in phospholes **127a–127f** was confirmed by the observation of an absorption maximum in the visible region. The energy of these absorptions, attributed to π–π* transitions, depends dramatically on the nature of the 2,5-substituents of the phosphole ring (Table 12) [33,136,137]. The values of λ_{max} and the optical end absorption λ_{onset} (the solution optical "HOMO–LUMO" gap) [12b], become notably red-shifted on replacing the phenyl groups either by 2-pyridyl ($\Delta\lambda_{max} = 36$ nm) or 2-thienyl rings ($\Delta\lambda_{max} = 58$ nm). A rationalisation of the origins of these bathochromic shifts with respect to the reference 2,5-diphenylphosphole (**127c**) is not straightforward since the phenyl, pyridyl, and thienyl substituents each have a different degree of aromatic character and/or shape. However, a simplified analysis can be proposed on the basis that conjugated polymers built of alternating electron-deficient and electron-rich subunits exhibit a low HOMO–

Scheme 36.

Table 12
Photophysical and electrochemical[a] data for 2,5-diarylphospholes (127a–127e)

	λ_{max} (nm)	λ_{onset} (nm)	$\log \varepsilon$	λ_{em} (nm)	ϕ_f	E_{pa} (V)	E_{pc} (V)
127a	390	448	4.02	463	1.1×10^{-2}	+0.83	−2.45
127b	412	468	3.93	501	5.0×10^{-2}	+0.40	–
127c	354	430	4.20	466	14.3×10^{-2}	+0.69	−2.88
127d	395	442	3.96	480	–	–	–
127e	371	430	4.10	458	–	+0.79	−2.67

[a] Potentials are referenced to the ferrocene/ferrocenium couple.

LUMO gap due to charge transfer that favours the delocalisation of the π-system [35d,138]. Since the carbon atoms of the phosphole ring bear a significant negative charge [21], the observed bathochromic shift on going from 2,5-diphenylphosphole (127c) to 2,5-dipyridylphosphole (127a) can tentatively be attributed to the alternating electron-deficient/electron-rich ring structure of oligomer 127a [33]. At first glance, this hypothesis is in contradiction with the fact that the highest bathochromic shift was recorded for phosphole 127b that bears electron-rich thienyl substituents (Table 12). However, as indicated by theoretical calculations (see Section 2.3), phospholes possess low-lying LUMO levels and thus have a high electron affinity. Hence, charge-transfer from the thienyl substituents to the central phosphole may occur. This hypothesis is reinforced by the fact that the value of λ_{max} recorded for 2,5-dithienyl-phosphole (127b) (412 nm) approaches that of 2,5-dithienyl-siloles (420 nm) [97] and is considerably more red-shifted than those of related 2,5-dithienyl-heterocyclopentadienes featuring an electron-rich central Group 15 (1-methyl-pyrrole, 322 nm) or Group 16 (furan and thiophene, ca. 350–360 nm) ring [139].

Phospholes 127a–127d are fluorophores, emitting light in the visible region upon excitation at their λ_{max} (Table 12). A bluish-green emission is observed for diphenyl and di(2-pyridyl)phospholes 127a and 127c (463–466 nm) whereas the emission of di(2-thienyl)phosphole (127b) is red-shifted ($\Delta\lambda_{em} = 35$ nm). The quantum yields also depend on the 2,5-substitution pattern, the highest (14.3×10^{-2}) being observed for 2,5-diphenylphosphole (127c) (Table 12). Cyclic voltammetry (CV) performed at 200 mV s^{-1} revealed that the redox processes observed for all the σ³-phospholes 127 are irreversible and that their redox properties are related to the electronic properties of the phosphole substituents (Table 12). For example, derivative 127b featuring electron-rich thienyl substituents is more easily oxidised than compound 127a which possesses electron-deficient pyridyl substituents (Table 12) [33,137]. As observed for silole-based oligomers (Section 2.5), combining phosphole units with heteroaromatic rings that possess a significantly different electronic character is an effective way to control the properties of phosphole-based π-electron systems.

In contrast with the more common Group 14 and 15 heterocyclopentadienes (siloles, pyrroles), phospholes possess a reactive heteroatom that can be utilised as the parent to a family of π-conjugated systems starting from a single P-containing chromophore. Indeed, phospholes 127a and 127b have been the subject of very simple reactions [24,25] based on the nucleophilic behaviour of the σ³,λ³-phosphorus atom (Scheme 37) [33,136,137].

These chemical modifications have an impact on the optical properties of phospholes, the same transformation having different, and sometimes opposite, effects within the corresponding pyridyl- and the thienyl-phosphole series (Table 13). The highest bathochromic shift following modification of the environment at phosphorus, i.e. the most important reduction in the HOMO–LUMO gap, was observed for the 2,5-dithienylphosphole derivatives, hence only this series will be discussed in detail (Table 13). Upon oxidation of the P-atom, the phosphole ring becomes an electron-poor heterocycle. The electronic deficiency is gradually augmented on going from a neutral compound, possessing a polarised P$^{\delta+}$=Y$^{\delta-}$ bond (128b, 129b, and 130b), to the phospholium salt 131b. The observed lowering of the optical HOMO–LUMO gap is thus in line with the general trend that maximised π-conjugation is obtained with alternating electron-rich and electron-poor heterocycles [35c,35d,138]. Equally, the variation in the emission wavelengths following chemical modification of the P-atom is noteworthy. The chromophores based on 2,5-dithienylphospholes cover a range of 92 nm in their emission spectra (Table 13).

The electrochemical properties of these compounds are also affected by chemical modifications of the P-atom. All derivatives exhibit irreversible oxidation and reduction processes for which the potentials are clearly related to the electron density associated with the central phosphole rings (Table 13). σ⁴-Phospholes exhibit lower reduction and higher oxidation potentials than the corresponding σ³-phospholes (Table 13). For example, the phosphole 127b exhibits an E_{pa} at +0.40 V and E_{pc} at a potential less cathodic than −2.10 V, while for the phospholium salt 131b these peak potentials are recorded at +0.92 and −1.66 V, respectively. Compounds 128b–130b show similar electrochemical behaviour with

i : Me₃SiOOSiMe₃ ; ii : S₈ ; iii : Se; iv : CH₃OTf
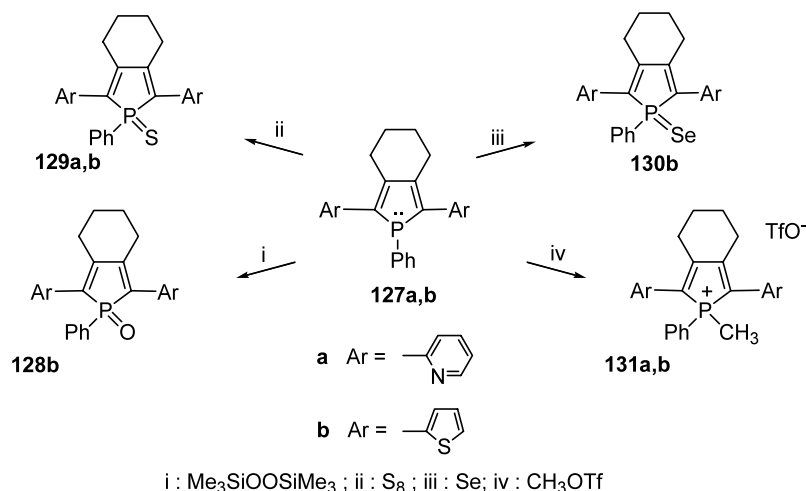
Scheme 37.

intermediate E_{pa} (+0.63 V/+0.68 V) and E_{pc} (−2.03 V/ −1.95 V) values. It is noteworthy that derivative **129a** exhibits a low reduction potential which is comparable to that observed for other highly electron-deficient systems [97,112]. This property is particularly important for the development of new electron-transporting (ET) materials suitable for the preparation of organic electroluminescent devices, since for greatest efficiency, a high electron affinity is required in order to decrease the energy barrier for electron injection [17a,17b].

Looking forward to the potential application of these phosphole π-electron systems in devices, the ability to tune the photophysical and electrochemical properties via chemical modification of the P-atoms is of significant importance. Furthermore, the drive to establish relationships between structure and photophysical properties has motivated the synthesis of heavier π-conjugated systems combining phospholes with thiophene and/or pyridine rings. Linear phosphole-thiophene derivatives appeared to be particularly interesting since the model 2,5-dithienyl-thioxophosphole **129b** exhibits a low optical HOMO–LUMO gap. Oligomers **132**, formally arising from an α,α-coupling of two **129b** units, was obtained using the Fagan–Nugent method (Scheme 38) [33]. The λ_{max} and λ_{onset} values of the resulting

oligomer **132** are considerably red-shifted compared to those of the monomer **129b** (Scheme 38). These data revealed no saturation of the conjugation and strongly motivated the synthesis of polymers based on motif **129b**.

As previously highlighted for oligophospholes, an important property of the corresponding phospholes is their ability to form coordination complexes. Indeed, σ^3,λ^3-phospholes (**127a**, **127b**, and **127g**) (Scheme 36) behave as classical two-electron donors towards transition metals. Compounds **133a**–**133c** (Scheme 39) have been investigated by X-ray diffraction [33,136]. Their important metric data (C–C inter-ring distances, P–C bond lengths, etc.) as well as their optical properties (λ_{max}, λ_{em}) are similar to those of the free derivatives.

The 2-(2-pyridyl)phospholes can act as tightly bonded 1,4-P,N chelates towards Pd(II) and Ru(II) centres, forming complexes **134**–**136** (Scheme 39) [140–142]. Note that the cationic version of complex **134** is an efficient catalyst for carbon monoxide-olefin copolymerisation [141] and that of complex **136** [140] is one of the very first examples of a phosphine exhibiting a symmetrically bridging mode of coordination [143].

The synthesis and photophysical properties of dinuclear transition metal complexes containing bridging

Table 13
Comparison of the photophysical and electrochemical[a] data for 2,5-diarylphospholes **116a** and **116b** and derivatives **128a**, **128b**, **131a**, and **131b**

|	λ_{max} (nm)	λ_{onset} (nm)	log ε	λ_{em} (nm)	ϕ_f	E_{pa} (V)	E_{pc} (V)
127a	390	448	4.02	463	1.1×10^{-2}	+0.83	−2.45
129a	364	444	3.94	470	0.004×10^{-2}	+1.43	−1.88
131a	394	458	3.98	510	6.8×10^{-2}	> +1.8	−1.29
127b	412	468	3.93	501	5.0×10^{-2}	+0.40	−2.10
128b	434	500	3.97	556	0.69×10^{-2}	+0.63	−2.03
129b	432	496	3.98	548	4.6×10^{-2}	+0.68	−1.95
130b	423	503	4.09	547	0.12×10^{-3}	+0.67	−1.96
131b	442	528	3.92	593	0.8×10^{-2}	+0.92	−1.66

[a] See Table 12.
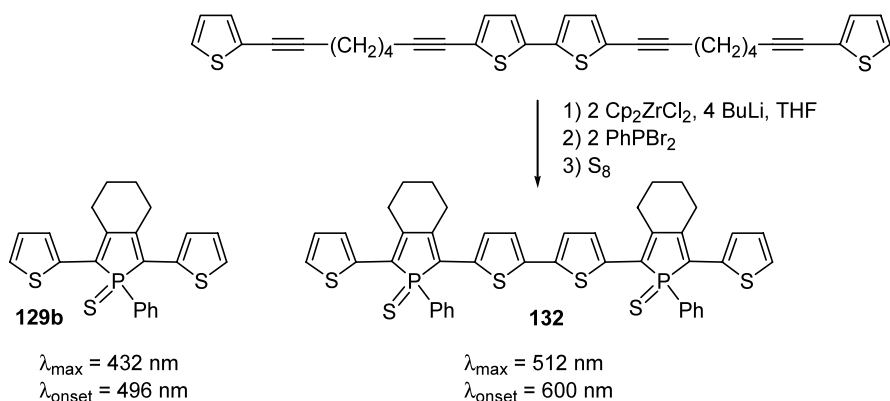
Scheme 38.

π-conjugated ligands as potentially novel molecular devices has received considerable attention [144]. The design of such ligands has led to important progress being made in the field of photo-induced electron- or energy-transfer processes. In this regard, derivative 137, featuring two terminal 2-pyridylphosphole moieties bridged by a thiophene ring, and the corresponding diruthenium complex 138 were recently investigated [142a] (Scheme 40). Derivative 137 exhibits a λ_{max} (480 nm) at a much longer wavelength than the corresponding 2-(2-pyridyl)-5-(thienyl)phosphole (396 nm). Coordination of chromophore 137 to ruthenium centres has been shown to have only a marginal influence on the π–π* transition of the extended conjugated system [142a].

Theoretical calculations have predicted that phosphole rings can be useful building blocks for the engineering of D-(π-bridge)-A derivatives with nonlinear optical (NLO) properties [30,34]. Phospholes 139a and 139b bearing an electron-deficient pyridine group and a classical electron-donor at the 2- and 5-positions, respectively, have been studied (Scheme 41)

[145]. Phospholes 139a and 139b exhibit moderate NLO activities, with $\beta_{1.9\,\mu m}$ values of 30×10^{-30} esu, which are consistent with the weak acceptor character of the pyridine group. 2-(2-Pyridyl)phospholes (139a and 139b) reacted with [Pd(CH₃CN)₄][BF₄]₂ giving rise to the corresponding complexes 140a and 140b (Scheme 41). In accordance with the *trans-effect*, heteroditopic P,N-dipoles 139a and 139b undergo a stereoselective coordination leading to a close parallel alignment of the dipoles on the square-planar d^8 palladium template. Thus, the *trans-effect* can overcome the natural antiparallel alignment tendency of 1D dipolar chromophores at the molecular level. Complexes 140b exhibit fairly high NLO activities with β-values reaching $(170-180) \times 10^{-30}$ esu, values that are much higher than the sum of the contributions of two sub-chromophores 128a and 128b. The enhancement of the NLO activity upon coordination was tentatively attributed to the onset of ligand-to-metal-to-ligand charge transfer that contributes coherently to the second harmonic generation [145].
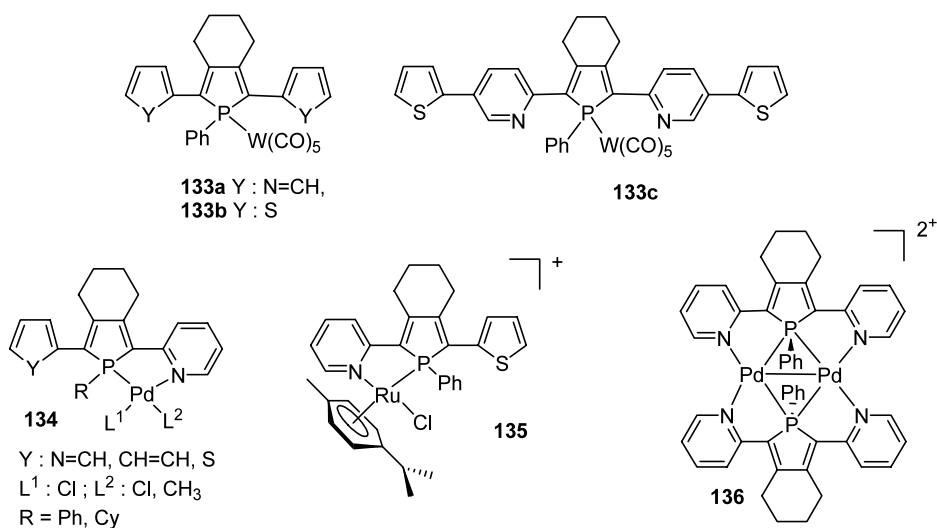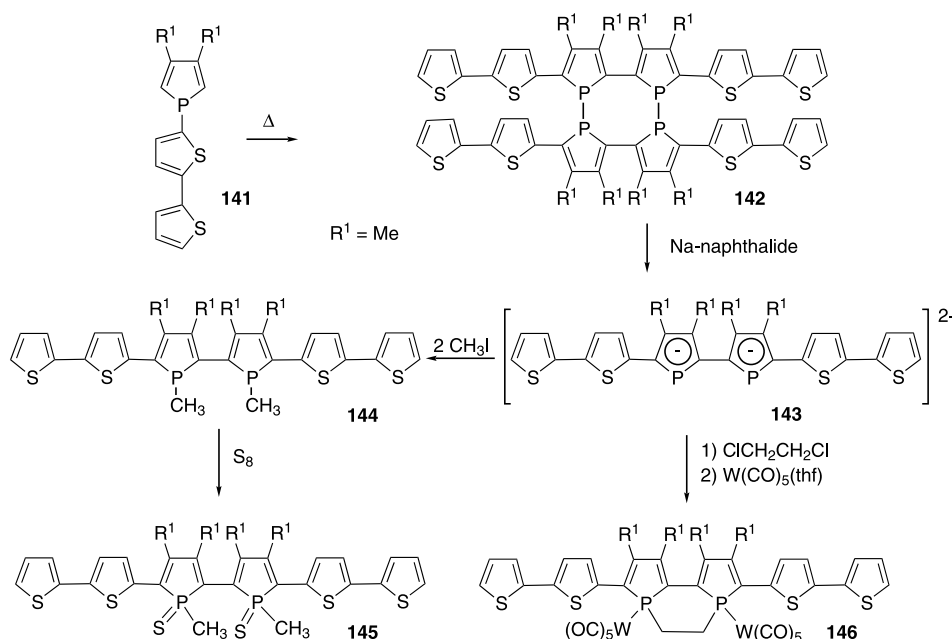

Scheme 39.
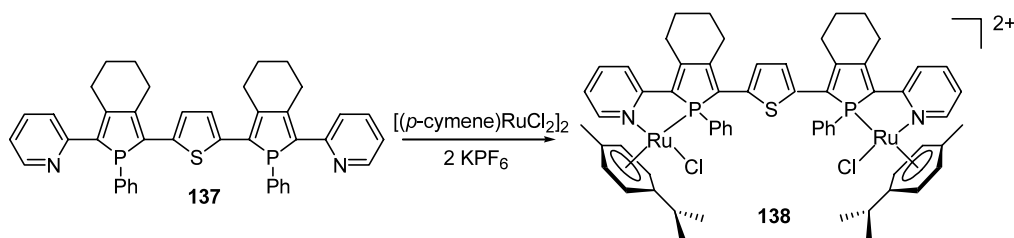
Scheme 40.
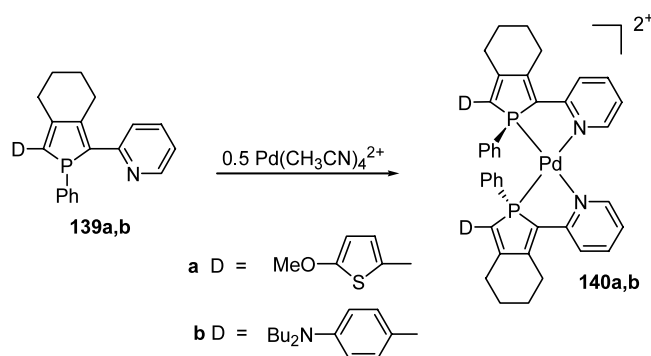
Scheme 41.

### 2.7.2. [Biphosphole]-[aromatic heterocycle] co-oligomers

Co-oligomers that alternate bithienyl and biphospho-lyl subunits were obtained according to the general strategy depicted in Scheme 29. The thermolysis of 1-(dithienyl)phosphole (**141**) afforded the cyclic tetra-phosphole **142** via a series of concerted 1,5-sigmatropic shifts and dihydrogen eliminations (Scheme 42) [146]. Subsequently, a quantitative reductive cleavage of the P–P bonds gave rise to dianion **143** which reacted with

iodomethane to afford the target derivative **144** in ca. 50% yield from **142**. This biphosphole was found to be reactive and, hence was isolated as a mixture of two diastereoisomers **145** after oxidation with elemental sulfur (Scheme 42). In the same way, derivative **146** (two P-atoms are linked by a carbon bridge) was obtained following addition of 1,2-dichloroethane and 2 equiv. of W(CO)$_5$(THF) to dianion **143** (Scheme 42). A related complex **147** possessing an inorganic bridge was obtained by heating **145** in the presence of molybdenum hexacarbonyl (Scheme 43).

Complexes **146** (Scheme 42) and **147** (Scheme 43) were obtained as single diastereoisomers and were studied by X-ray diffraction [146]. In both compounds, the bithie-nyl moieties are almost coplanar, the angles between the phosphole and the thiophene rings are rather small (15.2–24.3°), while the phosphole–phosphole interplane twist angles are somewhat larger [**146**, 66.26 ± 0.14°; **147**, 55.6 ± 0.3°]. These values are similar to those obtained for quaterphosphole **1** (Scheme 32). Most importantly, the lengths of the C–C links between the rings (1.42–1.47 Å) are in the range expected for C sp^2–C sp^2 single bonds. These data suggest a certain degree of delocalisa-


Scheme 42.
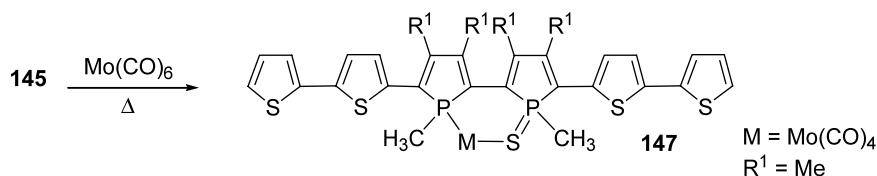
Scheme 43.

tion of the π-system over the six heterole rings for both compounds.

An electrochemical investigation of compound **145** (Scheme 42) and the related derivative **148** revealed that the two phosphole sulfide rings behave as a single redox centre and that the anion radicals **145⁻/148⁻** and dianions **145²⁻/148²⁻** exhibit relatively good stabilities [122c]. Furthermore, the nature of the 2,5-biphosphole substituents (phenyl versus bithienyl) was shown to have a profound influence on the electrochemical behaviour of these species. These data, as a whole, are clearly indicative of not only significant delocalisation between the two phosphole rings but also with their 2,5-substituents.
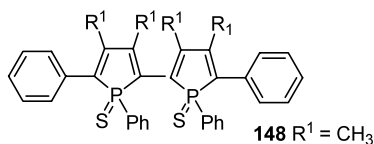

The synthesis and elucidation of structure–property relationships for π-conjugated co-oligomers incorporating phospholes is still in its infancy. However, the ability to be able to tune the electronic properties of such species via chemical modification of the P-atom com-

bined with the possibility to coordinate these chromophores to transition metals opens up a number of interesting avenues into potential device applications.

2.7.3. [Phosphole]-[ethenyl] or -[ethynyl] co-oligomers

Poly(*p*-phenylenevinylenes) are probably the most studied π-conjugated systems [17] although oligomers and polymers based on (thienylenevinylene) [12a,147] or (*p*-phenyleneethynylene) units [17c,17d] have, more recently, emerged as very promising molecular wires. In contrast, no poly(phospholylenevinylidene)s or poly(phospholyleneethynylene)s are yet known. However, oligomers that can be seen as models or potential building blocks for the synthesis of these latter polymers have been reported.

Initially, the synthesis of these types of P-containing co-oligomer was hampered as 2,5-dibromophosphole (**116**) and its iodo–bromo analogue **149** (Scheme 44) were found not to undergo Stille-type coupling with 1-stannyl-alkynes [148]. In contrast, Sonogashira coupling of 2-bromo-5-iodophosphole (**149**) with phenylacetylene afforded **150** (Scheme 44) albeit in a very poor yield (ca. 10%) [148]. The most efficient route to the target co-oligomers is based around the versatile 2-lithiophosp-
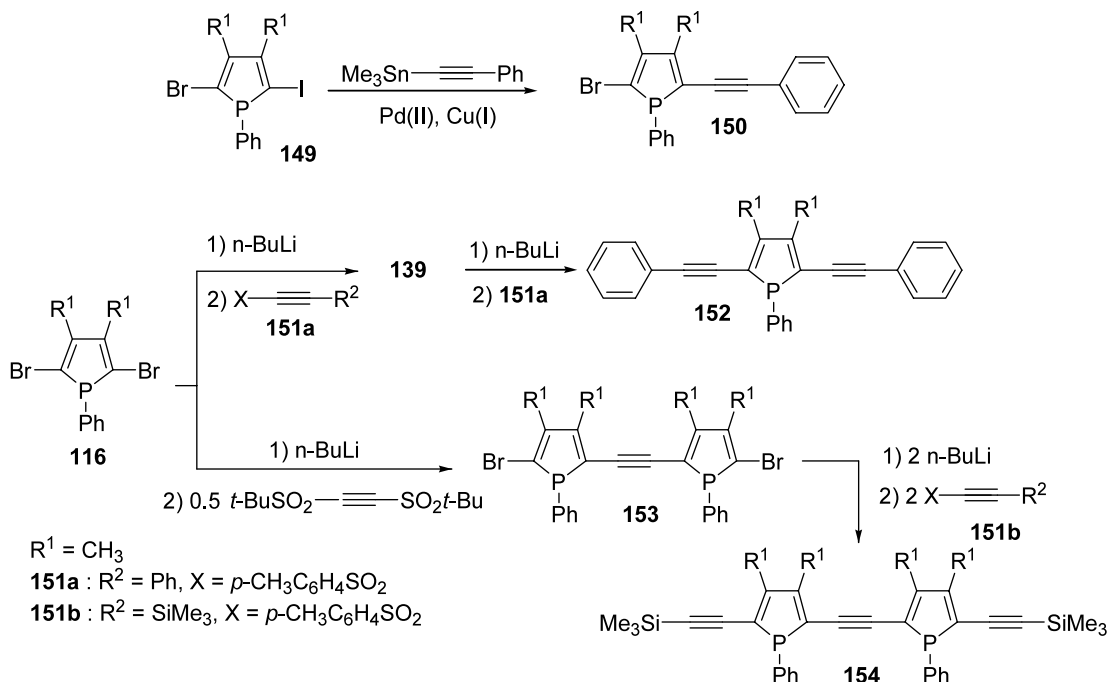
Scheme 44.
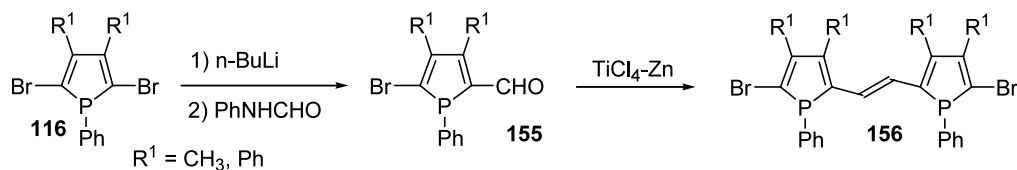
Scheme 45.

holes, which allow the direct functionalisation of the phosphole ring (see Scheme 32). Thus, treating the intermediate 2-lithio-5-bromophosphole with arylsulfonylacetylene (**151a**) gave rise to derivative **150** (25% isolated yield) which can be converted into α,α′-di(acetylenic)phosphole (**152**) according to the same general strategy as above (Scheme 44). Although the yields of these reaction sequences are rather modest (typically around 30%), this synthetic approach allows the stepwise preparation of derivatives **153** and **154** (Scheme 44) which are isolated as orange solids [148].

Analysis of **152** by X-ray diffraction revealed that the P-atom adopts a pyramidal geometry. The endocyclic P–C bond distances are typical for P–C single bonds [1.815(2)–1.821(2) Å] while the C–C linkages between the P-ring and the C≡C moieties are rather short [1.423(3)–1.416(3) Å] [148]. These data clearly show that the endocyclic dienic π-system of the phosphole is efficiently conjugated with the two acetylenic substituents. This model compound possesses an extended π-conjugated system as suggested by its orange colour.

The simplest oligo(phospholylenevinylidene), i.e. two phosphole rings linked by a ethenyl bridge have been recently prepared. The aldehydes **155** (Scheme 45), readily obtained from the corresponding 2-lithiophosphole, undergo McMurry coupling to afford the E-derivatives **156** in high yields [130a].

Derivatives **153**, **154**, and **156** are promising building blocks for the preparation of longer oligomers or polymers. However, the scope of these synthetic methods remains somewhat limited by their rather low yields. Further improvement in or discovery of new methods for coupling phospholes with vinylene or ethynylene fragments is needed.
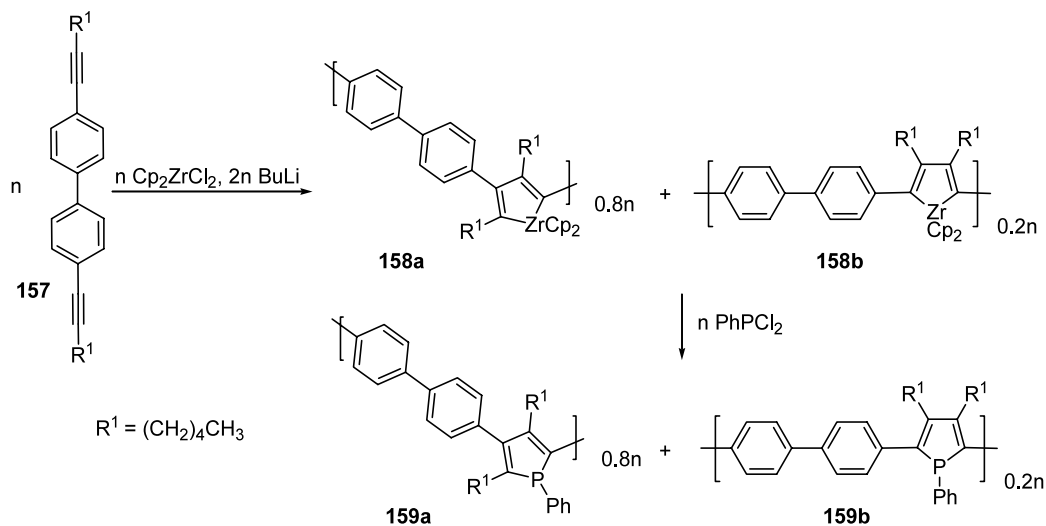
2.8. Polymers incorporating Group 15 elements

To date, no Homo-polymers based on Group 15 heteroles are known while only co-polymers incorporating phosphole rings have been described. Don Tilley and co-workers [149] prepared the first polymer of this type using a versatile organometallic approach. The zirconocene-coupling of rigid diynes **157** proceeded in a non-regioselective way affording an 80/20 isomeric mixture of 2,4- and 2,5-connected metallacycles **158a** and **158b**, respectively, in the polymer backbone (Scheme 46) [150]. The reactive zirconacyclopentadiene moieties can subsequently be converted to dienes, benzene rings and
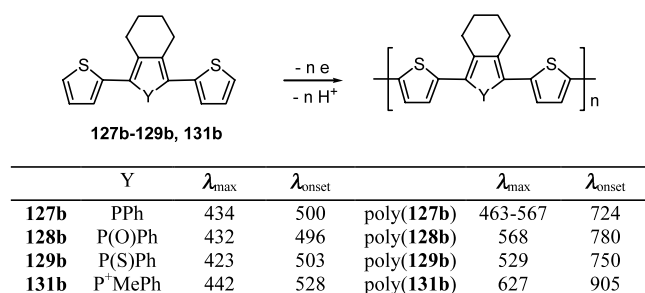
heterocyclopentadienes including phospholes [150]. Biphenyl-phospholyl polymers **159a** and **159b** are isolated as air-stable, soluble powders. They have been characterised by multinuclear NMR spectroscopy and their molecular weights were determined by GPC analysis ($M_w = 16\,000$; $M_n = 6200$). Although multinuclear NMR spectroscopy and elemental analysis support the proposed structures, the presence of a small number of diene units cannot be ruled out [150]. The polymer mixtures **159a** and **159b** exhibit a maxima absorption in its UV–Vis spectrum at 308 nm with a λ_{onset} of 400 nm. These values are consistent with a relatively high bandgap probably due to a preponderance of cross-conjugated segments [150]. Polymers **159a** and **159b** exhibit interesting photoluminescence properties. A marked Stokes shift was observed (162 nm) with a quantum yield reaching 9.2×10^{-2}.

The second type of phosphole-containing π-conjugated polymer was obtained by electropolymerisation of 2,5-dithienylphosphole derivatives (Scheme 47) [33,137]. Electropolymerisation of thienyl monomers via an oxidation process is a well-documented and straightforward route to polymers [2,40]. However, this method suffers from some important drawbacks. The electrochemically prepared polymers are often insoluble, preventing GPC analysis, and they often possess structural defects. The major process which occurs during the electropolymerisation of oligothiophenes is α,α′-coupling but the formation of some 2,4-linkages that disrupt the conjugation can also take place.

The films obtained on the working Pt electrodes are insoluble, electroactive materials [137]. The polymers were amenable to p- and n-doping processes with good reversibilities. Doping was observed to take place at potentials that depend on the nature of the phosphole monomer and occur at values lower than those for the corresponding monomers. Absorption spectra of the dedoped thin films showed that the optical data obtained from these materials were sensitive to the nature of the monomer and that the values of λ_{onset} were considerably red-shifted compared with those observed for the corresponding monomers (Scheme 47). These data suggest that the electroactive materials formed on the electrode possess rather long conjugation pathways. A remarkable feature is that the electrochemical and photophysical data associated with these materials obtained by electropolymerisation depend on

Scheme 46.

	Y	λ_{max}	λ_{onset}		λ_{max}	λ_{onset}
127b	PPh	434	500	poly(127b)	463–567	724
128b	P(O)Ph	432	496	poly(128b)	568	780
129b	P(S)Ph	423	503	poly(129b)	529	750
131b	P⁺MePh	442	528	poly(131b)	627	905

Scheme 47.

the nature of the phosphorus moiety, exactly as was observed for the P-containing monomers.

To date, all the known co-polymers that incorporate phosphole units suffer from having irregular structures, something due largely to the synthetic methods used for their preparation (e.g. via either a 'zirconocene route' or electropolymerisation). However, this deficiency is more than outweighed by their interesting optical and electrochemical properties, which can uniquely be fine-tuned through variation in the nature of the phosphorus moieties.

3. Linear π-conjugated systems incorporating heavy Group 15 elements

π-Conjugated polymers D_1 [151], D_2 [152], and D_3 [153] (Fig. 17) containing heteroatoms in their main chain have been widely investigated since their proper-
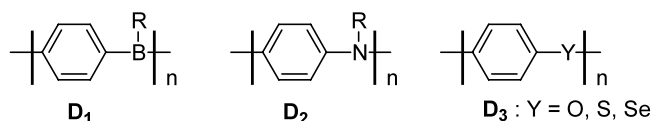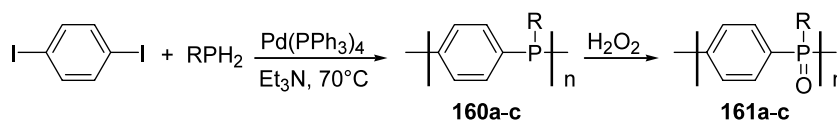

Fig. 17. Polymers based on aryle and heteroatomic moieties.

ties differ considerably from those of "all-carbon" analogues such as poly(p-phenylenevinyle)s. The heteroatoms participate in the π-conjugated system by virtue of their available vacant orbitals (polymers D_1) or lone pairs (polymers D_2 and D_3).

Polymers D_3 that feature heavy Group 16 elements (Y = S, Se, etc.) have been extensively studied. In contrast, P-analogues of the well-known polyanilines D_2 have only very recently been described. The palladium-catalysed cross-coupling of 1,4-diiodobenzene and aryl- and alkyl-phosphines afforded polymers 160a–160c (Scheme 48) [154]. These compounds are soluble in common organic solvents (THF, toluene, CHCl₃) allowing gel permeation chromatography (GPC) and multinuclear NMR spectroscopy to be performed. The average number of repeat units varies from 7 to 14 with polydispersity indices of ca. 1.4 ± 0.1. The ³¹P-NMR spectrum of polymer 160a consists of a broad singlet at −19.8 ppm while the UV–Vis spectra of polymers 160a–160c show λ_{max} between 276 and 291 nm that are attributed to π–π* transitions [154]. These rather low values are probably due to the fact that the P-atoms of polymers 160a–160c retain a tetrahedral geometry that prevents efficient conjugation of the phosphorus lone pair with the aryl groups. However, a certain degree of π-conjugation along the polymer chains is suggested by the bathochromic shift observed on going from triphenylphosphine ($\lambda_{max} = 263$ nm) to 1,4-diphenylphosphinobenzene ($\lambda_{max} = 275$ nm) and polymer 160b ($\lambda_{max} = 291$ nm).

Polymers 160a–160c can undergo two types of oxidation that dramatically modify their optical properties. Oxidation with FeCl₃ in the absence of oxygen afforded paramagnetic polymers characterised by UV–Vis absorptions that are considerably red-shifted in comparison with those of 160a–160c. The high value of λ_{onset} (ca. 800 nm) supports the presence of an
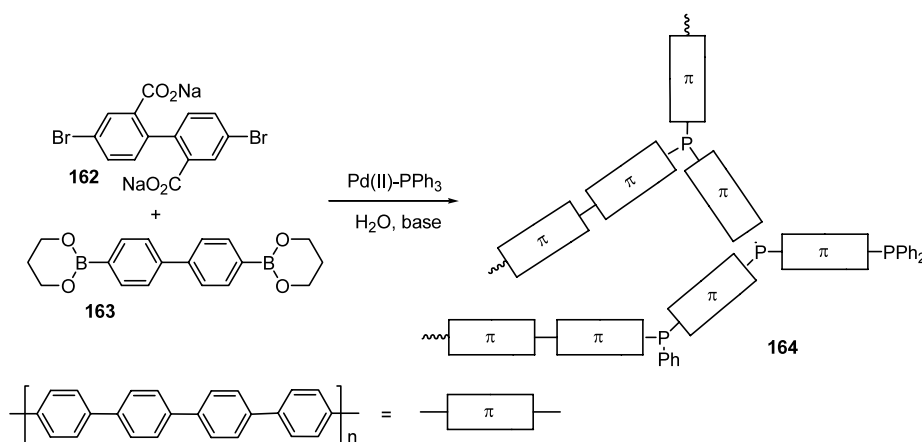
Scheme 48.

extension to the conjugation path through the P-atoms. Quantitative oxidation of the phosphorus centres of polymers **160a**–**160c** with hydrogen peroxide gave rise to derivatives **161a**–**161c** (Scheme 48). Chemical modification of the P-atoms induces dramatic changes in the UV–Vis spectra, although the origin of these changes is still not understood; further investigation of these interesting P-containing polymers is thus warranted [154].

Branched (*p*-phenylenes) incorporating phosphorus moieties were obtained during attempts to synthesise soluble linear (*p*-phenylenes) using Pd-catalysed Suzuki couplings [155a]. The coupling of derivatives **162** and **163** (Scheme 49) catalysed by palladium-tri(*o*-tolyl)phosphine systems led to the formation of linear poly(*p*-phenylene)s of high molecular weight [155a]. Using triphenylphosphine (TPP) as ligand, aryl–aryl interchange took place with the ArPd(TPP)$_2$I complexes [155b] leading to the formation of branched polymer **164** (Scheme 49), which incorporates phosphorus centres. Signals at +28.5 ppm due to phosphine oxide moieties were recorded in the ^{31}P-NMR spectra. It should be noted that although the concentration of phosphine defects is very low, they have an impact on the properties (molecular weight, viscosity, etc.) of the polymers. Despite the fact that compounds **164** represent a unique class of branched P-containing polymer, these derivatives are merely undesired by-products in the formation of well-defined linear poly(*p*-phenylene)s. It is noteworthy that a related exchange between phenyl groups of triphenylphosphine and iodophthalocyanines in the coordination sphere of Pd(II) leading to mono-, bis- and tris-(phthalocyanine)aryl phosphonium salts, has recently been reported [156].

Derivatives comprising alternating phosphorus moieties and ethynyl or diethynyl units represent another class of π-conjugated system. These compounds have mostly been prepared as building blocks for the synthesis of phosphapericyclynes and polyphosphacyclopolyynes, derivatives that are not covered by this review that focuses on linear systems.

Treatment of dihalogenophosphine (**165**) with an excess of ethynylmagnesium bromide gave rise to adducts **166** and **167** in 53 and 3% isolated yield, respectively (Scheme 50) [157]. These derivatives were subsequently transformed into triphospha[3]pericyclyne (**168**) and tetraphospha[4]pericyclyne (**169**) via a double deprotonation followed by addition of 1.5 equiv. of electrophile **165** (Scheme 50). Note that derivatives **168** and **169** exhibit strong absorption bands that extend out to nearly 300 nm showing that these heterocycles are
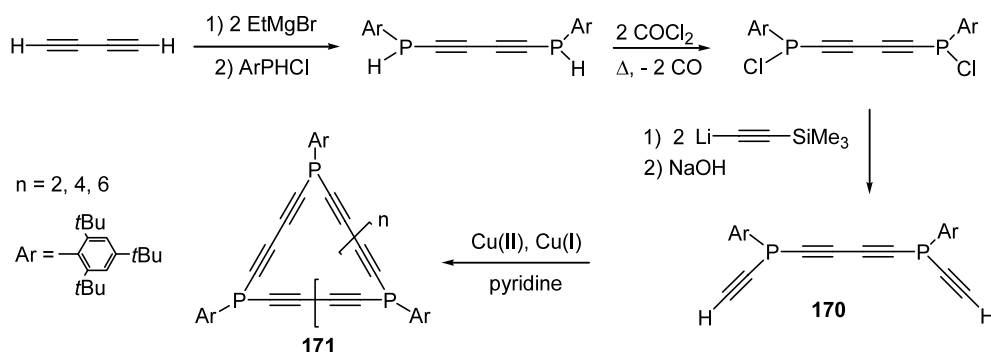

Scheme 49.
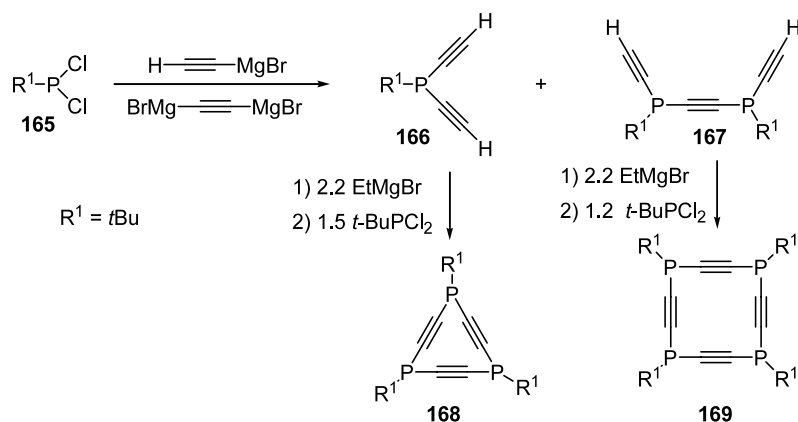
Scheme 50.

characterised by strong cyclic electronic interactions [157].

A variety of linear ethynylphosphines **170** (Scheme 51) and **172–175** (Scheme 52) have been prepared by Märkl et al. [158] as synthons for the synthesis of polyphosphacyclopolyynes of type **171** (Scheme 51). The ethynylphosphines are obtained either via a multi-step sequence depicted in Scheme 51, a Cadiot–Chodkiewicz coupling involving bis-copper salts or Eglinton coupling of terminal alkyne moieties (Scheme 52). An interaction between the phosphorus lone pairs and the organic π-systems is supported by the fact that the phosphorus atoms of mono- and di-silyl-capped analogues of derivative **170** exhibit an unusually low inversion barrier (65 kJ mol^{-1} versus 130–140 kJ mol^{-1} for classical alkyl or arylphosphanes) [158].

Polymers with transition metals in the main chain are attracting growing attention as a result of their interesting physical properties [159]. Ferrocene has been extensively used as a building block to prepare organometallic polymers and heteroatom-bridged poly(metallocenes) **K–M** (Scheme 53). These derivatives have been the focus of numerous investigations since the nature of the bridging atom has key implications for the properties of the polymers [160]. Although such derivatives are at the very limit of the scope of this review, the chemistry of the P-containing derivatives will be described briefly.

The first attempts to prepare P-containing derivatives **M** date back to 1967. Lewis acid-catalysed condensation of ferrocene with dihalogenophenylphosphines at high temperatures followed by oxidation with hydrogen peroxide afforded mixtures of oligomeric materials with different ferrocenylene linkages [161]. The breakthrough came about in 1982 with the synthesis of well-defined oligomers and polymers using phosphorus-bridged [1]ferrocenophane monomers [162]. The nucleophilic attack of phenyllithium at the strained P-bridged centre of **176** yielded the lithium species **177** [162a], which can attack the starting material **176** to give a mixture of oligomers **178** containing mainly the dimer and the trimer (Scheme 54) [162b]. These compounds are air-stable and quite soluble in organic solvents. Their ^{31}P{^{1}H} spectra indicated that they are obtained as a mixture of diastereoisomers due to the presence of chiral P-atoms.

Polymers **180** containing ferrocene units (R^1 = H) were obtained by reacting 1,1′-dilithioferrocene-tetramethylethylenediamine (**179**) with dichlorophenylphosphine (Scheme 55) [162b]. Their molecular weights varied from 8900 to 161 000 depending on the solvent, the mode of addition, and the reaction temperature. The highest molecular weights were observed using diethylether at 25 °C. Oligomers **178** and related polymers **180** feature reactive σ^3,λ^3-P moieties which can coordinate to transition metal centres [163]. Their good thermal
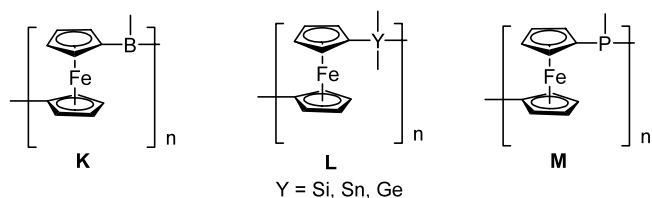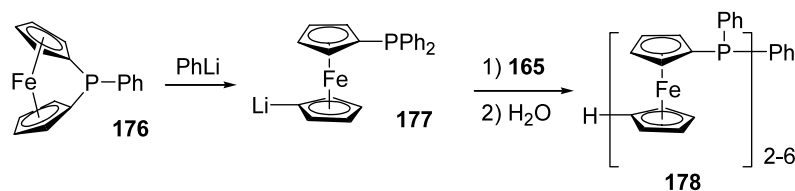

Scheme 51.
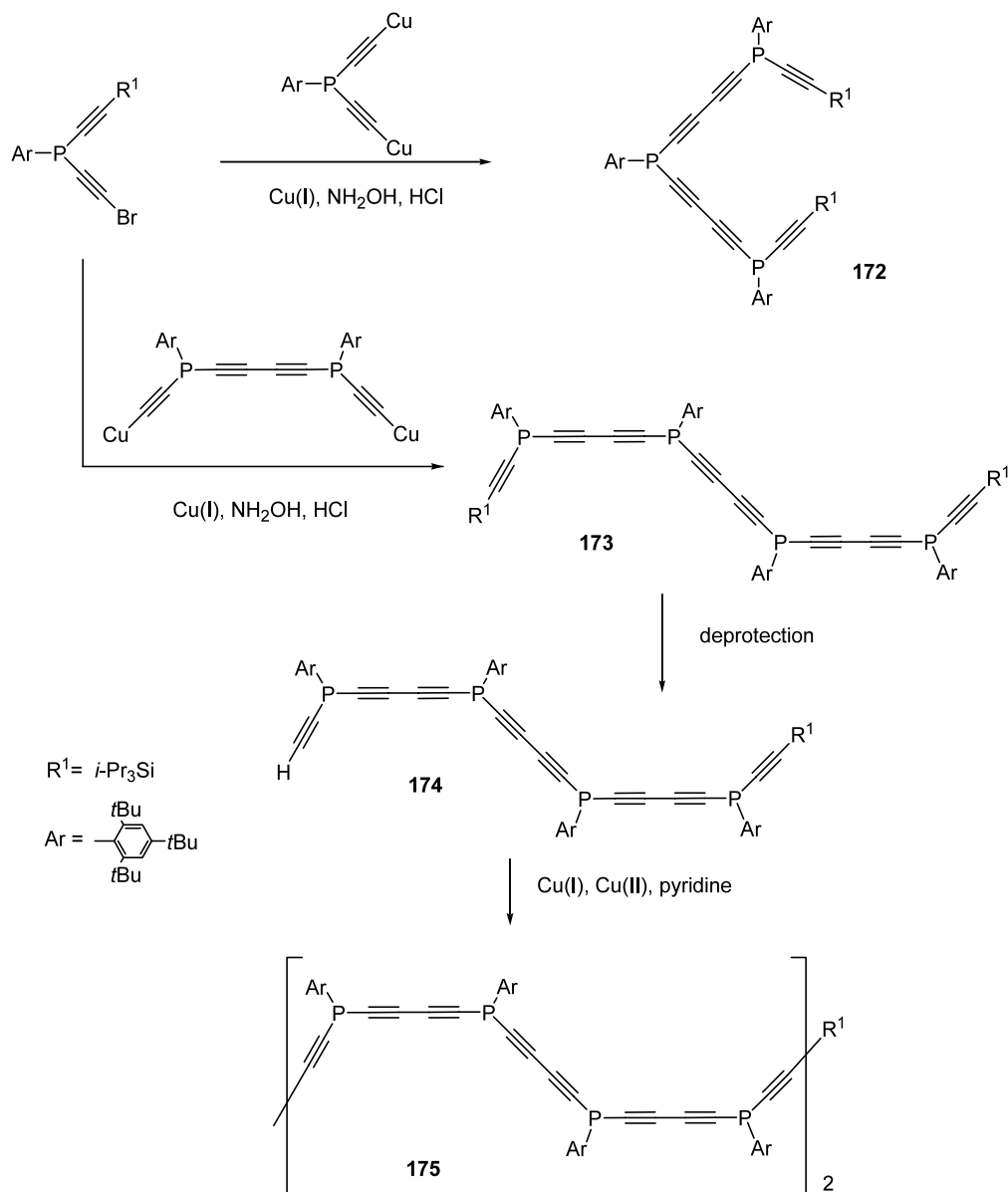
Scheme 52.

stability makes them attractive supports for catalysts in high reaction temperature applications such as the Co-catalysed hydroformylation of olefins. Oligomers **178** act as tridentate ligands toward Co(CO)$_2$ fragment, the same coordination behaviour being observed for polymers **180** at low Co loadings [163]. These supported species were used to catalyse the hydroformylation of 1-

hexene at high temperature (170–190 °C). Quantitative conversion of olefin was observed and, interestingly, the rate of the reduction of the aldehydes into the corresponding alcohols is lowered relative to the homogeneous Co-catalytic system [163].

It has been proposed that the reaction of **179** with PhPCl$_2$ does not give polymer **180** via a polycondensation but through the ring-opening polymerisation (ROP) of [1]-phosphaferrocenophane (**176**) generated in situ (Scheme 56) [164,165]. In fact, the living ROP of derivative **176** can be achieved by adding various amounts of BuLi in THF at 25 °C [165a,165b]. GPC analysis of the thiooxoderivatives **181** showed that the molecular weights of the polymers can be controlled from $M_n = 2.4 \times 10^3$ to 3.6×10^4 by varying the BuLi/**176** ratio. Narrow polydispersities ranging from 1.08 to

Scheme 53.

Scheme 54.
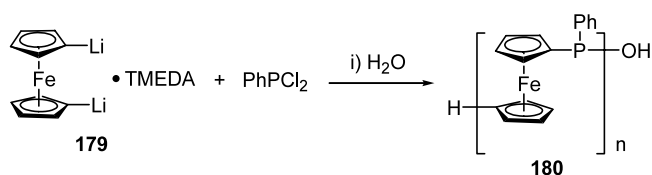
Scheme 55.

1.25 were observed. Note that the living nature of the process allows block copolymers to be obtained with either poly(dimethylsiloxane) or poly(ferrocenylsilane) segments [165a,165b]. The phosphorus centres of the copolymer coordinate to transition metals [Pd(II), Fe(0)] and the overall loading of metallated sites is quite low (ca. 20%) [165b].
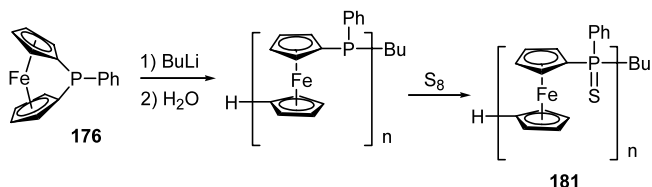
The ring strain inherent in phosphorus-bridged [1]ferrocenophane (176) is a key factor in the observed ring-opening polymerisation, a process that can also be induced thermally [166]. Thermolysis of derivatives 182 afforded poly(ferrocenylphosphines) (183) (Scheme 57) which can readily be converted into the corresponding sulfides (184). These compounds have been characterised by NMR spectroscopy and GPC analysis. The average molecular weight of these materials varies from $M_w = 18\,000$ to $66\,000$ with rather high polydispersities (1.52–2.26). Note that the ROP of [2]ferrocenophane with C–P bridges has recently been reported (Scheme 57) [167].

These mixed phosphorus-organometallic polymers exhibit novel structures. The role of the σ^3,λ^3-P atom as a possible conjugated spacer has not been investigated [168]; however, the possibility to perform chemical transformations at these reactive centres opens promising avenues for future research.

4. Concluding remarks

Linear organic π-conjugated systems featuring the heavy Group 14 and 15 elements exhibit novel proper-

ties that are profoundly different to those of their well-studied "all-carbon", thiophene- or pyrrole-based analogues. The study of the electronic behaviour of these new π-conjugated systems is interesting from a fundamental point of view, posing intriguing questions about the influence of the heavy heteroatoms. Oligomers and polymers with low HOMO–LUMO bandgaps have been prepared using silole- or phosphole-based building blocks and some of these new systems are showing great promise for future use in nonlinear optical or optoelectronic applications. The use of silole-based materials for the optimisation of organic LEDs is particularly noteworthy. However, it is still too early to assess the full potential of these comparatively young π-conjugated systems featuring the heavy Group 14 and 15 elements in the context of materials for micro-electronic applications. Further research toward π-conjugated systems that can be altered at the molecular level in order to tune the electronic and optical properties can be expected since the underlying heteroatomic building blocks as well as methodologies to construct such macromolecules are now available. Thus, it seems extremely likely that optoelectronic devices built around these main-group containing materials are going to have an impact in this domain.

4.1. Postscript: poly(p-phenylenephosphaalkene)

Very recently, the gamut of potential π-conjugated polymeric materials possessing heavier Group 15 elements in their backbone has expanded dramatically with the synthesis and characterisation of the first poly(p-phenylenephosphaalkene) (187) by Wright and Gates [169]. Indeed, polymer 187 may be regarded as the first phosphorus analogue of the now well-known poly(p-phenylenevinylenes) {PPVs} **C** (Fig. 1) [121]. The synthesis of the solid yellow polymer 187 (35% isolated

Scheme 56.

R^1 = R^2 = H, R^3 = Ph
R^1 = H, R^2 = Bu, R^3 = Ph
R^1 = R^2 = SiMe$_3$, R^3 = Ph
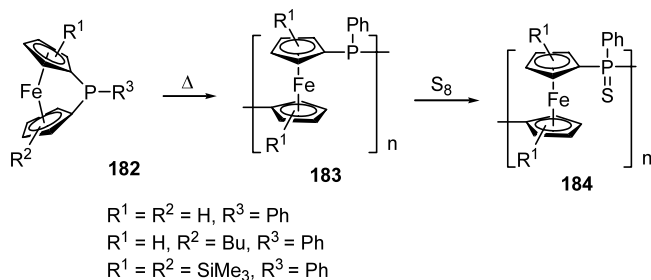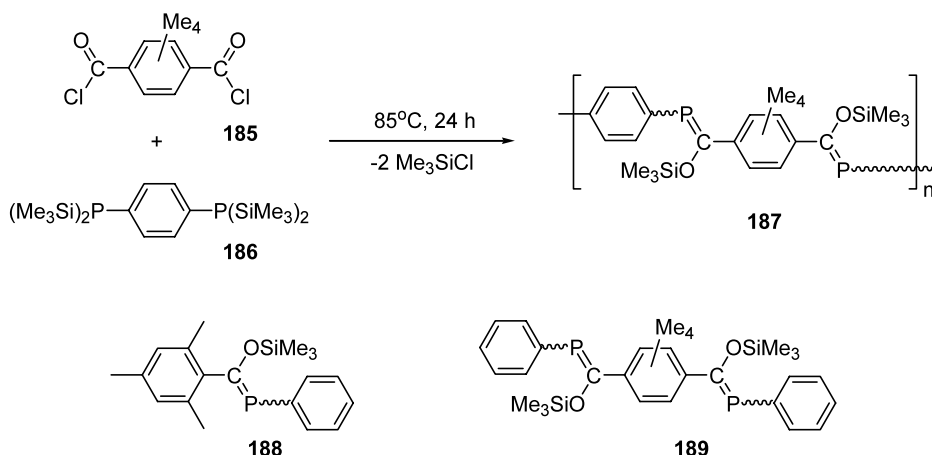
Scheme 57.

Scheme 58.

yield) was achieved through a thermally induced poly-condensation reaction between the two bifunctional monomers **185** and **186** (Scheme 58) followed by reprecipitation from THF (heating the polymerisation mixture for ca. 48 h lead to the formation of what is believed to be a partially cross-linked material). The ^{31}P-NMR spectrum of **187** exhibited broad overlapping resonances corresponding to E and Z isomers ($Z/E \approx$ 1.1) of the backbone P=C units and the polymer end groups, $-P(SiMe_3)_2$. An estimate of the molecular weight (M_n) of several samples of **187** was obtained from the relative integration of the two sets of ^{31}P signals since its air and moisture sensitivity precluded GPC analysis. The analysis revealed a moderate degree of polymerisation ($n = 5–21$), consistent with a step-growth polymerisation.

The electronic structure of polymer **187** has been investigated together with those for the monomeric analogues **188** and **189** by UV–Vis spectroscopy (solutions in THF). Broad absorbances were observed for the latter two model compounds, $\lambda_{max} = 310$ and 314 nm, respectively, while analysis of the polymer revealed a broad absorbance ($\lambda_{max} = 328–338$ nm) that possessed a tail stretching into the visible region. This bathochromic shift has been taken as being indicative of some degree of π-conjugation through the phenylene and P=C units. It is interesting to note that the red-shift of the phosphorus-containing polymer system is significantly less than that for *trans*-PPV compared with *trans*-stilbene (ca. 426 versus 294/307 nm). This has been attributed to the presence of non-planarity in the polymer backbone, caused by the bulky C_6Me_4 groups (something observed previously for substituted PPVs [170]), and by the mixture of E and Z isomers present.

The preparation of **187** represents a milestone in the history of π-conjugated polymers incorporating phosphorus moieties, opening the way for the preparation of a wide range of fundamentally new materials.

References

[1] (a) H. Shirakawa, E.J. Lewis, A.G. MacDiarmid, C.K. Chiang, A.J. Heeger, J. Chem. Soc. Chem. Comm. (1977) 578;
(b) C.K. Chiang, C.R. Fincher, Y.W. Park, A.J. Heeger, A.J. Shirakawa, E.J. Louis, S.C. Gau, A.G. MacDiarmid, Phys. Rev. Lett. 39 (1977) 1098.

[2] T.A. Skotheim, R.L. Elsenbaumer, J.R. Reynolds (Eds.), Handbook of Conducting Polymers, Marcel Dekker, New York, 1998.

[3] H. Shirakawa, A. McDiarmid, A. Heeger, Chem. Commun. (2003) 1.

[4] J.F. Lennard-Jones, Proc. R. Soc. London A 158 (1937) 280.

[5] G. Natta, G. Mazzanti, P. Corrandini, Rend. Accad. Naz. Lincei CI Sc. Fis. Mat. e. Nat. 25 (1958) 3.

[6] D.J. Berets, D.S. Smith, Trans. Faraday Soc. (1968) 823.

[7] Electrical conductivity σ (S cm^{-1}) is a function of the number of charge carrying species i (n_i) and is defined by the relationship $\sigma = \Sigma \mu_i n_i \varepsilon_i$ where ε_I is the charge on each carrier and μ_i is the carrier mobility.

[8] (a) H. Shirakawa, S. Ikeda, Polym. J. 2 (1971) 231;
(b) H. Shirakawa, S. Ikeda, J. Polym. Sci. Polym. Chem. Ed. 12 (1973) 929;
(c) T. Ito, H. Shirakawa, S. Ikeda, J. Polym. Sci. Polym. Chem. Ed. 13 (1974) 11.

[9] N. Basescu, Z. Liu, D. Moses, A.J. Heeger, H. Naarmann, N. Theophilou, Nature 327 (1987) 403.

[10] N.C. Billingham, P.D. Calvert, Adv. Polym. Sci. 90 (1989) 1.

[11] J.G. Verkade, J. Chem. Ed. 68 (1991) 739.

[12] (a) J. Roncali, Chem. Rev. 97 (1997) 173;
(b) R.E. Martin, F. Diederich, Angew. Chem. Int. Ed. Engl. 38 (1999) 1350;
(c) K. Susumu, M.J. Therien, J. Am. Chem. Soc. 124 (2002) 8550.

[13] E. Hückel, Z. Für. Phys. 70 (1931) 204.

[14] O. Wennerström, Macromolecules 18 (1985) 1977.

[15] D.O. Cowan, F.M. Wiygul, Chem. Eng. News 64 (1986) 28.

[16] R.E. Peierls, Quantum Theory of Solids, OUP, London, 1956.

[17] (a) A. Kraft, A.C. Grimsdale, A.B. Holmes, Angew. Chem. Int. Ed. Engl. 37 (1998) 403;
(b) U. Mitschke, P. Bäuerle, J. Mater. Chem. 10 (2000) 1471;
(c) U.H.F. Bunz, Chem. Rev. 110 (2000) 1605;
(d) J.M. Tour, Acc. Chem. Res. 33 (2000) 791.

[18] (a) E.H. Bray, W. Hübel, Chem. Ind. (London) (1959) 1250.;
(b) E.H. Bray, W. Hübel, I. Caplier, J. Am. Chem. Soc. 83 (1961) 4406.

[19] (a) F.C. Leavitt, T.A. Manuel, F. Johnson, J. Am. Chem. Soc. 81 (1959) 3163;

(b) F.C. Leavitt, T.A. Manuel, F. Johnson, L.U. Matternas, D.S. Lehman, J. Am. Chem. Soc. 82 (1960) 5099.

[20] S. Yamaguchi, K. Tamao, J. Chem. Soc. Dalton Trans. (1998) 3693.

[21] L. Nyulaszi, Chem. Rev. 101 (2001) 1229.

[22] S. Yamaguchi, Y. Itami, K. Tamao, Organometallics 17 (1998) 4910.

[23] (a) J. Dubac, A. Laporterie, G. Manuel, Chem. Rev. 90 (1990) 215;
(b) E. Colomer, R.J.P. Corriu, M. Lheureux, Chem. Rev. 90 (1990) 265.

[24] F. Mathey, Chem. Rev. 88 (1988) 429.

[25] L.D. Quin, in: A.R. Katritzky (Ed.), Comprehensive Heterocyclic Chemistry, Pergamon Press, Oxford, 1996, p. 757.

[26] P. von Ragué Schleyer, P.K. Freeman, H. Jiao, B. Goldfuss, Angew. Chem. Int. Ed. Engl. 34 (1995) 337.

[27] P. von Ragué Schleyer, C. Maerker, A. Dransfeld, H. Jiao, N.J.R. van Eikema Hommes, J. Am. Chem. Soc. 118 (1996) 6317.

[28] W. Schäfer, A. Schweig, F. Mathey, J. Am. Chem. Soc. 28 (1975) 407.

[29] E. Mattmann, F. Mathey, A. Sevin, G. Frison, J. Org. Chem. 67 (2002) 1208.

[30] D. Delaere, A. Dransfeld, M.N. Nguyen, L.G. Vanquickenborne, J. Org. Chem. 65 (2000) 2631.

[31] (a) G. Keglevich, Z. Böcskei, G.M. Keseru, K. Ujszaszy, L.D. Quin, J. Am. Chem. Soc. 119 (1997) 5095;
(b) L. Nyulaszi, G. Keglevich, L.D. Quin, J. Org. Chem. 61 (1996) 7808.

[32] E. Mattmann, D. Simonutti, L. Ricard, F. Mercier, F. Mathey, J. Org. Chem. 66 (2001) 755.

[33] C. Hay, M. Hissler, C. Fischmeister, J. Rault-Berthelot, L. Toupet, L. Nyulaszi, R. Réau, Chem. Eur. J. 7 (2001) 4222.

[34] I. Albert, T. Marks, M. Ratner, J. Am. Chem. Soc. 119 (1997) 6575.

[35] (a) P. Audebert, J.-M. Catel, G. Le Coustumer, V. Duchenet, P. Hapiot, J. Phys. Chem. B 102 (1998) 8661;
(b) P. Audebert, J.-M. Catel, V. Duchenet, L. Guyard, P. Hapiot, G. Le Coustumer, Synth. Met. 101 (1999) 642;
(c) Z. Zhou, T. Maruyama, T. Kanbara, T. Ikeda, K. Ichimura, T. Yamamoto, K. Tokuda, Chem. Commun. (1991) 1210;
(d) T. Yamamoto, Z.-H. Zhou, T. Kanbara, M. Shimura, K. Kizu, T. Maruyama, Y. Nakamura, T. Fukuda, B.L. Lee, N. Ooba, S. Tomura, T. Kurihara, T. Kaino, K. Kubota, S. Sasaki, J. Am. Chem. Soc. 118 (1996) 10389.

[36] (a) J. Shinar, S. Ijadi-Maghsoodi, Q.-X. Ni, Y. Pang, T.J. Barton, Synth. Met. 28 (1989) C593;
(b) S. Grigoras, G.C. Lie, T.J. Barton, S. Ijadi-Maghsoodi, Y. Pang, J. Shinar, Z.V. Vardeny, K.S. Wong, S.G. Han, Synth. Met. 49–50 (1992) 293;
(c) S.Y. Hong, S.J. Kwon, S.C. Kim, D.S. Marynick, Synth. Met. 69 (1995) 701;
(d) S.Y. Hong, S.J. Kwon, S.C. Kim, J. Chem. Phys. 103 (1995) 1871.

[37] U. Salzner, J.B. Lagowski, P.G. Pickup, R.A. Poirier, Synth. Met. 96 (1998) 177.

[38] J. Ma, S. Li, Y. Jiang, Macromolecules 35 (2002) 1109.

[39] D. Delaire, M.T. Nguyen, L.G. Vanquickenborne, J. Organomet. Chem. 643 (2002) 194.

[40] D. Fichou (Ed.), Handbook of Oligo- and Poly-thiophene, Wiley–VCH, Weinheim, 1999.

[41] M. Karelson, M.C. Zerner, Chem. Phys. Lett. 224 (1994) 213.

[42] (a) M. Gouygou, O. Tissot, J.-C. Daran, G.G.A. Balavoine, Organometallics 16 (1997) 1008;
(b) O. Tissot, M. Gouygou, F. Dallemer, J.-C. Daran, G.G.A. Balavoine, Angew. Chem. Int. Ed. Engl. 40 (2001) 1076.

[43] E. Deschamps, L. Ricard, F. Mathey, Angew. Chem. Int. Ed. Engl. 33 (1994) 1158.

[44] (a) H.S. Nalwa, S. Miyata, Non-linear Optics of Organic Molecules and Polymers, CRC Press, Boca Raton, FL, 1997;
(b) G. Wagnière, Linear and Non-linear Optical Properties of Molecules, VCH, Weinheim, Germany, 1993.

[45] A. Julg, P. François, Theoret. Chim. Acta 7 (1967) 249.

[46] (a) R.D. Miller, J. Michl, Chem. Rev. 89 (1989) 1359;
(b) K. Tamao, S. Yamaguchi, J. Organomet. Chem. 611 (2000) 5.

[47] V.N. Khabashesku, V. Balaji, S.E. Boganov, O.M. Nefedov, J. Michl, J. Am. Chem. Soc. 116 (1994) 320.

[48] S. Yamaguchi, K. Tamao, Bull. Chem. Soc. Jpn. 69 (1996) 2327.

[49] Y. Yamaguchi, Synth. Met. 82 (1996) 149.

[50] S. Yamaguchi, K. Tamao, in: Z. Rappoport, Y. Apeloig (Eds.), The Chemistry of Organic Silicon Compounds, vol. 3, Wiley, New York, 2001, pp. 647–694.

[51] J. Dubac, C. Guerin, P. Meunier, in: Z. Rappoport, Y. Apeloig (Eds.), The Chemistry of Organic Silicon Compounds, vol. 2 (Chapter 34), Wiley, New York, 1999, p. 34 (Chapter 34).

[52] D.A. Armitage, in: A.R. Katritzky (Ed.), Comprehensive Heterocyclic Chemistry, Pergamon Press, Oxford, 1996, p. 903.

[53] P. Jutzi, A. Karl, J. Organomet. Chem. 214 (1981) 289.

[54] U. Losehund, N.W. Mitzel, J. Chem. Soc. Dalton Trans. (2000) 1049.

[55] T.J. Barton, J. Organomet. Chem. 179 (1975) C17.

[56] J. Dubac, Organometallics 5 (1986) 1742.

[57] K. Tamao, S. Yamaguchi, M. Shiro, J. Am. Chem. Soc. 116 (1994) 11715.

[58] N.E. Schore, in: B.M. Trost, I. Fleming (Eds.), Comprehensive Organic Synthesis, vol. 5, Pergamon Press, Oxford, 1991, p. 1129 See for example:

[59] S. Yamaguchi, R.-Z. Jin, K. Tamao, M. Shiro, Organometallics 16 (1997) 2230.

[60] T. Hiiro, N. Kambe, A. Ogawa, N. Miyoshi, S. Murai, N. Sonoda, Angew. Chem. Int. Ed. Engl. 26 (1987) 1187 (and references therein).

[61] M. Katkevics, S. Yamaguchi, A. Toshimitsu, K. Tamao, Organometallics 17 (1998) 5796.

[62] S. Yamaguchi, R.-Z. Jin, S. Ohno, K. Tamao, Organometallics 17 (1998) 5133.

[63] S. Yamaguchi, R.-Z. Jin, K. Tamao, F. Sato, J. Org. Chem. 63 (1998) 10060.

[64] See for examples: (a) A.J. Ashe, III, J.W. Kampf, S.M. Al-Taweel, J. Am. Chem. Soc., 114 (1992) 372;
(b) E. Negishi, S.J. Holmes, J.M. Tour, J.A. Miller, F.E. Cederbaum, D.R. Swanson, T. Takahashi, J. Am. Chem. Soc. 111 (1989) 3336 (and references therein).

[65] K.-I. Kanno, M. Kira, Chem. Lett. (1999) 1127.

[66] (a) P.J. Fagan, W.A. Nugent, J. Am. Chem. Soc. 110 (1988) 2310;
(b) P.J. Fagan, W.A. Nugent, J.C. Calabrese, J. Am. Chem. Soc. 116 (1994) 1880.

[67] Y. Ura, Y. Li, Z. Xi, T. Takahashi, Tetrahedron Lett. 39 (1998) 2787.

[68] B. Lucht, M. Buretea, T. Don Tilley, Organometallics 19 (2000) 3469.

[69] W.P. Freeman, T.D. Tilley, L.M. Liable-Sands, A.L. Rheingold, J. Am. Chem. Soc. 118 (1996) 10457.

[70] K. Tamao, S. Yamaguchi, M. Shiozaki, Y. Nakagawa, Y. Ito, J. Am. Chem. Soc. 114 (1992) 5867.

[71] H. Sohn, R. Huddleston, D.R. Powell, R. West, J. Am. Chem. Soc. 121 (1999) 2935.

[72] S. Yamaguchi, R.-Z. Jin, K. Tamao, M. Shiro, Organometallics 16 (1997) 2486.

[73] K. Kanno, M. Ichinohe, C. Kabuto, M. Kira, Chem. Lett. (1998) 99.

[74] J.H. Burroughs, D.D.C. Bradley, A.R. Brown, R.N. Marks, K. Mackay, P.L. Burns, A.B. Holmes, Nature 347 (1990) 539.

[75] (a) J.-S. Yang, T.M. Swager, J. Am. Chem. Soc. 120 (1998) 5321;
(b) J.-S. Yang, T.M. Swager, J. Am. Chem. Soc. 120 (1998) 11864.

[76] S. Content, W.C. Trogler, M.J. Sailor, Chem. Eur. J. 6 (2000) 2205.

[77] H. Sohn, R. Calhoun, M.J. Sailor, W.C. Trogler, Angew. Chem. Int. Ed. 40 (2001) 2104.

[78] W.P. Freeman, T. Don Tilley, G.P.A. Yap, A.L. Rheingold, Angew. Chem. Int. Ed. Engl. 35 (1996) 882.

[79] J.-H. Hong, P. Boudjouk, S. Castellino, Organometallics 13 (1994) 3387.

[80] J.-H. Hong, Y. Pan, P. Boudjouk, Angew. Chem. Int. Ed. Engl. 35 (1996) 186.

[81] S. Yamaguchi, R.-Z. Jin, K. Tamao, J. Am. Chem. Soc. 121 (1999) 2937.

[82] S. Yamaguchi, R.-Z. Jin, K. Tamao, ICR Annu. Rep. 4 (1997) 34.

[83] S. Yamaguchi, R.-Z. Jin, Y. Itami, T. Goto, K. Tamao, J. Am. Chem. Soc. 121 (1999) 10420.

[84] (a) K. Tamao, S. Yamaguchi, Pure Appl. Chem. 68 (1996) 139;
(b) S. Yamaguchi, K. Tamao, J. Syn. Org. Chem. Jpn. 56 (1998) 500.

[85] R.J.P. Corriu, W.E. Douglas, Z.-X. Yang, J. Organomet. Chem. 456 (1993) 35 (and references therein).

[86] E. Toyada, A. Kunai, M. Ishikawa, Organometallics 14 (1995) 1089.

[87] T.J. Barton, S. Ijadi-Maghsoodi, Y. Pang, Macromolecules 24 (1991) 1257.

[88] (a) B. Wrackmeyer, J. Chem. Soc. Chem. Comm. (1986) 397;
(b) B. Wrackmeyer, G. Kehr, J. Süß, Chem. Ber. 126 (1993) 2221.

[89] S. Yamaguchi, K. Tamao, Tetrahedron Lett. 37 (1996) 2983.

[90] J. Ferman, J.P. Kakareka, W.T. Kloster, J.L. Mullin, J. Quattrucci, J.S. Ricci, H.J. Tracy, W.J. Vining, S. Wallace, Inorg. Chem. 38 (1999) 2465.

[91] K. Tamao, M. Asahara, A. Kawachi, J. Organomet. Chem. 521 (1996) 325.

[92] L. Párkányi, J. Organomet. Chem. 216 (1981) 9.

[93] H. Gilman, S.G. Cottis, W.H. Atwell, J. Am. Chem. Soc. 86 (1964) 1596.

[94] B.Z. Tang, X. Zhan, G. Yu, P.P.S. Lee, Y. Liu, D. Zhu, J. Mater. Chem. 11 (2001) 2974.

[95] A. Adachi, H. Yasuda, T. Sanji, H. Sakurai, H. Okita, J. Luminol. 87–89 (2000) 1174.

[96] K. Tamao, M. Uchida, T. Izumizawa, K. Furukawa, S. Yamaguchi, J. Am. Chem. Soc. 118 (1996) 11974.

[97] S. Yamaguchi, M. Endo, M. Uchida, T. Izumizawa, K. Furukawa, K. Tamao, Chem. Eur. J. 6 (2000) 1683.

[98] J. Luo, Z. Xie, J.W.Y. Lam, L. Cheng, H. Chen, C. Qiu, H.S. Kwok, X. Zhan, Y. Liu, D. Zhu, B.Z. Tang, Chem. Commun. 18 (2001) 1740.

[99] B.L. Lucht, M.A. Buretea, T. Don Tilley, Organometallics 19 (2000) 3469.

[100] G. Froyer, Y. Pelous, G. Ollivier, Springer Ser. Solid State Sci. 76 (1988) 303.

[101] For a review, see: R.H. Baughman, J.L. Bredas, R.R. Chance, R.L. Elsenbauer, L.W. Shacklette, Chem. Rev., 88 (1982) 209

[102] K. Tamao, S. Yamaguchi, Y. Ito, Y. Matsuzaki, T. Yamabe, M. Fukushima, S. Mori, Macromolecules 28 (1995) 8668.

[103] S. Yamaguchi, K. Tamao, J. Organomet. Chem. 653 (2002) 223.

[104] S. Yamaguchi, T. Goto, K. Tamao, Angew. Chem. Int. Ed. 39 (2000) 1695.

[105] For a review of cross-coupling reactions for the synthesis of π-conjugated polymers see: T. Yamamoto, J. Organomet. Chem., 653 (2002) 195

[106] S.Y. Hong, J.M. Song, Synth. Met. 85 (1997) 1113.

[107] S. Yamaguchi, K. Tamao, J. Organomet. Chem. 653 (2002) 223.

[108] (a) J.W. Sease, L. Zechmeister, J. Am. Chem. Soc. 69 (1947) 3674;
(b) R.D. McCullough, R.D. Lowe, M. Jayaramam, D.L. Anderson, J. Org. Chem. 58 (1993) 904.

[109] (a) Y. Lee, S. Sadki, B. Tsuie, P. Schottland, J.R. Reynolds, Synth. Met. 119 (2001) 77;
(b) Y. Lee, S. Sadki, B. Tsuie, J.R. Reynolds, Chem. Mater. 13 (2001) 2234.

[110] K. Tamao, S. Ohno, S. Yamaguchi, Chem. Commun. (1996) 1873.

[111] T. Kauffmann, L. Hexy, Chem. Ber. 114 (1981) 3674.

[112] T. Yamamoto, K. Sugiyama, T. Kushida, T. Inoue, T. Kanbara, J. Am. Chem. Soc. 118 (1996) 3930.

[113] (a) H. Murata, G.G. Malliaras, M. Uchida, Y. Shen, Z.H. Kafafi, Chem. Phys. Lett. 339 (2001) 161;
(b) M. Uchida, T. Izumizawa, T. Nakano, S. Yamaghushi, K. Tamao, K. Furukawa, Chem. Mater. 13 (2001) 2680;
(c) H. Murata, Z.H. Zakia, Z.H. Kafafi, M. Uchida, Appl. Phys. Lett. 80 (2002) 189.

[114] S. Yamagushi, T. Endo, M. Uchida, T. Izumizawa, K. Furukawa, K. Tamao, Chem. Lett. (2001) 98.

[115] S. Yamaguchi, K. Iimura, K. Tamao, Chem. Lett. (1998) 89.

[116] W. Chen, S. Ijadi-Maghshoodi, T.J. Barton, Polym. Prepr. (Am. Chem. Soc. Div. Polym. Chem.) 38 (1997) 189.

[117] M. Moroni, J.L. Moigne, T.A. Pham, J.-Y. Bigot, Macromolecules 30 (1997) 1964.

[118] E. Toyada, A. Kunai, M. Ishikawa, Organometallics 14 (1995) 1089.

[119] J. Oshita, T. Hamaguchi, E. Toyoda, A. Kunai, K. Komagushi, M. Shiotani, M. Ishikawa, A. Naka, Organometallics 18 (1999) 1717.

[120] (a) R.J.P. Corriu, P. Gerbier, C. Guérin, B.J.L. Henner, A. Jean, P.H. Mutin, Organometallics 11 (1992) 2507;
(b) R.J.P. Corriu, W.E. Douglas, Z.-X. Yang, J. Organomet. Chem. 456 (1993) 35.

[121] K.B. Dillon, F. Mathey, J.F. Nixon, Phosphorus: The Carbon Copy, Wiley, Chichester, UK, 1998.

[122] (a) F. Mathey, F. Mercier, F. Nief, J. Fischer, A. Mitschler, J. Am. Chem. Soc. 104 (1982) 2077;
(b) F. Laporte, F. Mercier, L. Ricard, F. Mathey, J. Am. Chem. Soc. 116 (1994) 3306;
(c) M.O. Bevierre, F. Mercier, F. Mathey, A. Jutand, C. Amatore, New J. Chem. 15 (1991) 545.

[123] (a) F. Mercier, F. Mathey, J. Fischer, J.H. Nelson, Inorg. Chem. 24 (1985) 4141;
(b) F. Mercier, F. Mathey, J. Fischer, J.H. Nelson, J. Am. Chem. Soc. 106 (1984) 425.

[124] F. Mercier, S. Holand, F. Mathey, J. Organomet. Chem. 316 (1986) 271.

[125] O. Tissot, J. Hydrio, M. Gouygou, F. Dallemer, J.-C. Daran, G.G.A. Balavoine, Tetrahedron 56 (2000) 85.

[126] O. Tissot, M. Gouygou, J.-C. Daran, G.G.A. Balavoine, Chem. Commun (1996) 2287.

[127] (a) O. Tissot, M. Gouygou, J.-C. Daran, G.G.A. Balavoine, Organometallics 17 (1998) 5927;
(b) O. Tissot, M. Gouygou, F. Dallemer, J.-C. Daran, G.G.A. Balavoine, Eur. J. Inorg. Chem. (2001) 2385.;
(c) T. Kojima, K. Saeki, K. Ono, Y. Matsuda, Bull. Chem. Soc. Jpn. 71 (1998) 2885.

[128] O. Tissot, M. Gouygou, J.-C. Daran, G.G.A. Balavoine, Acta Crystallogr. Sect. C 54 (1998) 676.

[129] E. Deschamps, F. Mathey, Bull. Soc. Chim. Fr. 129 (1992) 486.

[130] (a) T.-A. Niemi, P.L. Coe, S.J. Till, J. Chem. Soc. Perkin Trans. 1 (2000) 1519;

(b) J. Hydrio, M. Gouygou, F. Dallemer, G.G.A. Balavoine, J.-C. Daran, Eur. J. Org. Chem. (2002) 675.

[131] I.G.M. Campbell, R.C. Cookson, M.B. Hocking, A.N. Hughes, J. Chem. Soc. (1965) 2184.

[132] Z. Raciszewski, E.H. Braye, Photochem. Photobiol. 12 (1970) 429.

[133] W.P. Ozbirn, R.A. Jacobson, J.C. Clardy, J. Chem. Soc. Chem. Comm. (1971) 1062.

[134] E. Deschamps, L. Ricard, F. Mathey, Heteroatom. Chem. 2 (1991) 377.

[135] E. Deschamps, F. Mathey, J. Org. Chem. 55 (1990) 2494.

[136] D. Le Vilain, C. Hay, V. Deborde, L. Toupet, R. Réau, Chem. Commun. (1999) 345.

[137] C. Hay, C. Fischmeister, M. Hissler, L. Toupet, R. Réau, Angew. Chem. Int. Ed. Engl. 10 (2000) 1812.

[138] Q.T. Zhang, J.T. Tour, J. Am. Chem. Soc. 120 (1998) 5355.

[139] (a) A. Hucke, M.P. Cava, J. Org. Chem. 63 (1998) 7413;
(b) P.E. Niziurski, C.C. Scordilis-Kelley, T.L. Liu, M.P. Cava, R.T. Carlin, J.P. Ferraris, J. Am. Chem. Soc. 115 (1993) 887;
(c) J.P. Ferraris, R.G. Andrus, D.C. Hrncir, J. Chem. Soc. Chem. Commun. (1989) 1318.

[140] M. Sauthier, B. Le Guennic, V. Deborde, L. Toupet, J.-F. Halet, R. Réau, Angew. Chem. Int. Ed. 40 (2001) 228.

[141] M. Sauthier, F. Leca, L. Toupet, R. Réau, Organometallics 21 (2002) 1591.

[142] (a) C. Hay, M. Sauthier, V. Deborde, M. Hissler, L. Toupet, R. Réau, J. Organomet. Chem. 643–644 (2002) 494;
(b) M. Sauthier, L. Toupet, R. Réau, J. Organomet. Chem. 643–644 (2002) 494.

[143] (a) T. Pechmann, C.D. Brandt, H. Werner, Angew. Chem. Int. Ed. 39 (2000) 3909;
(b) P. Braunstein, N.M. Boag, Angew. Chem. Int. Ed. 40 (2001) 2427.

[144] (a) V. Balzani, A. Juris, M. Venturi, S. Campagna, S. Serroni, Chem. Rev. 96 (1996) 759;
(b) R. Ziessel, M. Hissler, A. El-Ghayoury, A. Harriman, Coord. Chem. Rev. 178–180 (1998) 1251;
(c) J.M. Lehn, Supramolecular Chemistry, VCH, Weinheim, 1995;
(d) R. Dembinski, T. Bartik, B. Bartik, M. Jaeger, J.A. Gladysz, J. Am. Chem. Soc. 122 (2000) 810;
(e) F. Barigelletti, L. Flamigni, V. Balzani, J.-P. Colin, J.-P. Sauvage, A. Sour, E.C. Constable, A.M.W. Cargill-Thompson, J. Am. Chem. Soc. 104 (1994) 7692;
(f) F. Paul, C. Lapinte, Coord. Chem. Rev. 178–180 (1998) 431;
(g) C. Rovira, D. Ruiz-Molina, O. Elsner, J. Vidal-Gancedo, J. Bonvoisin, J.-P. Launay, J. Veciana, Chem. Eur. J. 7 (2001) 240;
(h) V. Wing-Wah Yam, Chem. Commun. (2001) 789.

[145] C. Fave, M. Hissler, K. Sénéchal, I. Ledoux, J. Zyss, R. Réau, Chem. Commun. (2002) 1674.

[146] M.O. Bevierre, F. Mercier, L. Ricard, F. Mathey, Angew. Chem. Int. Ed. 29 (1990) 655.

[147] J.J. Apperloo, J.-M. Raimundo, P. Frère, J. Roncali, R.A.J. Janssen, Chem. Eur. J. 9 (2000) 1698.

[148] S. Holand, F. Gandolfo, L. Ricard, F. Mathey, Bull. Soc. Chem. Fr. 33 (1996) 133.

[149] (a) B.L. Lucht, S.S.H. Mao, T. Don Tilley, J. Am. Chem. Soc. 120 (1998) 4354;
(b) B.L. Lucht, T.D. Tilley, Chem. Commun (1998) 1645.

[150] S.S.H. Mao, T. Don Tilley, Macromolecules 30 (1997) 5566.

[151] (a) N. Matsumi, K. Naka, Y. Chujo, J. Am. Chem. Soc. 120 (1998) 10776;
(b) N. Matsumi, K. Naka, Y. Chujo, J. Am. Chem. Soc. 120 (1998) 5112.

[152] (a) A.G. MacDiarmid, J.C. Chiang, A.J. Epstein, Synth. Met. 18 (1987) 285;

(b) F. Wudl, R.O. Angus, Jr., F.L. Lu, P.M. Allemand, D.F. Vachon, M. Novak, Z.X. Liu, A.J. Heeger, J. Am. Chem. Soc. 109 (1987) 3677;
(c) F. Lux, Polymer 14 (1994) 2915;
(d) A.G. MacDiarmid, A.J. Epstein, Faraday Discuss. Chem. Soc. 31 (1989) 31 and 317;
(e) T.A. Skotheim (Ed.), Handbook of Conducting Polymers, Vols. I and II, Marcel Dekker, New York, 1986.

[153] (a) S.A. Hay, Adv. Polym. Sci. 4 (1967) 496;
(b) S.A. Hay, Polym. Eng. Sci. 16 (1967) 1;
(c) S.A. Hay, G.F. Endres, J. Polym. Sci. Polym. Lett. Ed. 3 (1965) 887;
(d) S.A. Hay, Macromolecules 2 (1969) 107;
(e) C.G. Overberger, Macromolecular Synthesis, vol. 1, Wiley, New York, 1963, p. 75 and 345;
(f) R.H. Baughman, J.L. Bredas, R.R. Chance, R.L. Elsenbaumer, L.W. Shacklette, Chem. Rev. 82 (1982) 209;
(g) E. Tsuchida, K. Yamamoto, H. Nishide, S. Yoshida, Macromolecules 20 (1987) 2030;
(h) L. Freund, W. Heitz, Makromol. Chem. 191 (1990) 815;
(i) E. Tsuchida, K. Yamamoto, M. Jikei, H. Nishide, Macromolecules 23 (1990) 930;
(j) K. Yamamoto, M. Jikei, H. Nishide, E. Tsuchida, J. Chem. Soc. Chem. Commun. (1991) 596;
(k) E. Tsuchida, M. Jikei, K. Miyatake, K. Yamamoto, H. Nishide, Macromolecules 26 (1993) 4732.

[154] B.L. Lucht, N.O. St Onge, Chem. Commun. (2000) 2097.

[155] (a) F.E. Goodson, T.I. Wallow, B.M. Novak, Macromolecules 31 (1998) 2047;
(b) F.E. Goodson, T.I. Wallow, B.M. Novak, J. Am. Chem. Soc. 119 (1997) 12441.

[156] G. de la Torre, A. Gouloumis, P. Vazquez, T. Torres, Angew. Chem. Int. Ed. 40 (2001) 2895.

[157] L.T. Scott, M. Unno, J. Am. Chem. Soc. 112 (1990) 7823.

[158] G. Märkl, T. Zollitsch, P. Kreitmeier, M. Prinzhorn, S. Reithinger, E. Eibler, Chem. Eur. J. 6 (2000) 3806.

[159] M.H. Chisholm, Acc. Chem. Res. 33 (2000) 53.

[160] (a) P. Nguyen, P. Gomez-Elipe, I. Manners, Chem. Rev. 99 (1999) 1515;
(b) E.W. Neuse, J.G. Chris, J. Macromol. Sci. Chem. A 1 (1967) 371;
(c) C.U. Pittman, J. Polym. Sci. A1 5 (1967) 2927.

[161] (a) E.W. Neuse, J.G. Chris, J. Macromol. Sci. Chem. A 1 (1967) 371;
(b) C.U. Pittman, J. Polym. Sci. A 5 (1967) 2927.

[162] (a) H.P. Withers, D. Seyferth, Organometallics 1 (1982) 1275;
(b) H.P. Withers, D. Seyferth, J.D. Fellmann, P.E. Garrou, S. Martin, Organometallics 1 (1982) 1283.

[163] J.D. Fellmann, P.E. Garrou, H.P. Withers, D. Seyferth, D. Traficante, Organometallics 2 (1983) 818.

[164] C.H. Honeyman, T.J. Peckham, J.A. Massey, I. Manners, Chem. Commun. (1996) 2589.

[165] (a) I. Manners, Adv. Organomet. Chem. 37 (1995) 131;
(b) T.J. Peckham, J.A. Massey, C.H. Honeyman, I. Manners, Macromolecules 32 (1999) 2830.

[166] C.H. Honeyman, D.A. Foucher, F.Y. Dahmen, R. Rulkens, A.J. Lough, I. Manners, Organometallics 14 (1995) 5503.

[167] R. Resendes, J.M. Nelson, A. Fischer, F. Jäkle, A. Bartole, A.J. Lough, I. Manners, J. Am. Chem. Soc. 123 (2001) 2116.

[168] P. Nguyen, P. Gomez-Elipe, I. Manners, Chem. Rev. 99 (1999) 1515.

[169] V.A. Wright, D.P. Gates, Angew. Chem. Int. Ed. 41 (2002) 2389.

[170] S. Chung, D.W. Lee, D. Oh, C.E. Lee, J. Jin, Acta Polym. 50 (1999) 298.